Feasibility of building an Optical Phase–Lock Loop Using Semiconductor Lasers

A thesis submitted to
the Faculty of Engineering of the
University of Glasgow for the Degree of
Doctor of Philosophy

by

Michael Joseph Fletcher

May 1993

ACKNOWLEDGEMENTS

I wish to express my thanks to Professor John Lamb for the use of the facilities of the Department of Electronic Engineering during the duration of this project.

My thanks go also to Dr P. Hlawiczka for his supervision of the project and to Professor Richard De La Rue, Dr John Arnold and Dr Charlie Ironside for the support they have given to me to complete this thesis.

I must also thank Dr Craig Michie and Dr Mike Grant who as colleagues offered not only support and friendship but also offered advice and suggestions which assisted me greatly in clarifying my thoughts. I also thank Dr. Joe Isaac and Mr Ian McIntyre for their friendship and support.

The assistance of the technical staff within the department is also gratefully acknowledged. I thank Mr R. Hutchins, Mr T. Wright, Mr H Anderson and their supporting staff.

Finally, my special thanks go to my parents and my wife for their love and support as well as their encouragement over many years to complete this thesis.

Contents

Executive Summary

This thesis reports on the work carried out in designing and attempting to build an optical heterodyne phase-lock loop using semiconductor lasers as the local oscillator and as the transmitter.

It is shown that homodyne detection of PSK is the most sensitive modulation/demodulation format a communication system can use. Receiver sensitivities for various schemes are evaluated. Performance improvements of more than 10dB are realisible in a coherent scheme. In a coherent system it is also possible to send thousands of signals simultaneously down one piece of fibre providing they are separated in frequency by a set amount, say 5GHz. This use of the bandwidth is called frequency division multiplexing and in monomode fibre could result in increasing channel capacity by more than 10,000 fold.

Design guidelines are determined for building optical phase lock loops. Laser phase noise, shot noise and loop propagation delay are determined to be the main criteria which must be taken into account when designing a coherent reciever.

Specifically if a receiver is to operate with a 10^{-9} bit error rate and suffer no more than 1dB power penalty as a result of phase noise degradation then the bit rate to laser linewidth ratio must be in excess of 2000. In addition to this the absolute stability requirement for a phase lock loop is

$$\omega_n \tau_d \leq 0.736$$

where ω_n is the bandwith of the loop and τ_d is the loop propagation delay. In reality if $\omega_n \tau_d$ is greater than 0.2 or 0.3 then severe penalties are incurred.

The Hitachi HLP1400 laser diode which was used in this project is fully characterised. It is shown that it is not suitable as the optical source for a phase-lock loop as it has too large a linewidth, greater than 5MHz, and it does not have a broad continuously tunable tuning range.

Several techniques are presented which can be used to enhance the

operation of laser diodes. In particular compound cavity and external cavity laser modules were designed and built up around HLP1400 diodes. These modules had some vastly improved characteristics with the external cavity having a linewidth of less than 100kHz and a tuning range in excess of 10nm. The compound cavity although it had a reduced linewidth was extremely sensitive to any alteration in current, temperature or optics.Results are quoted for the performance of other semiconductor laser devices incorporating different structures such as Distributed Feedback and Distributed Bragg Reflector diodes.

The results of the experimental programme including the design and build of the laser modules and the attempts at phase locking two devices are presented. Phase lock was not observed during the experimental programme. The main reason for this was that small amplitude, 1 – 10nm, low frequency vibrations of the external cavity of the laser module resulted in low frequency fluctuations of magnitude 10 – 100MHz. The loop could not cope with such frequency variations. This was partly due to the loop bandwidth being restricted to less than 50MHz because of the size of propagation delay and partly due to the frequency tuning control of the external cavity diode.

The experimental programme terminated when it was found that the spectral properties of the lasers being used deteriorated to the point where they were useless. Upon close inspection it was found that the lasers spectral profile had dramatically altered. Under free running conditions it displayed a spectrum similar to that which might be expected from a compound cavity structure.

Subsequent to the termination of the experimental programme other groups worldwide have designed and built phase–lock loops using semiconductor lasers. These loops operate in the manner predicted by the design criteria developed during this project.

CHAPTER 1

1.1 INTRODUCTION

Mankind's ability to communicate not only with those around him but also with those in other countries and those in future generations, firstly through drawings and paintings, then through books, films and tapes has enabled him to accelerate the rate of his development. Although the speed at which he can transmit, receive and process information is not as important as is his ability to read and write, developments in "Real Time Communications" have also accelerated and influenced the development of mankind.

During the last two hundred years man has advanced from sending letters which, although they can contain much information, take days to deliver and longer to reply to, through telegraph and telephone to radio and satellite links. The main incentives in developing each of these new technologies arose from reducing the cost of the overall system and in increasing both its speed and information carrying capacity. The communications requirements of today's Information Technology Industry, where huge amounts of data are repeatedly transferred to and fro between computers, demand that continual improvements be made.

One area of communications technology where potential exists for major improvements over current system performance and future reductions in cost are likely is coherent optical fibre communication.

1.2 COHERENT OPTICAL COMMUNICATION SYSTEMS

For the purpose of this thesis a coherent communication system will be defined as one which uses either heterodyne or homodyne detection and depends upon the relative stability of the carrier frequency of the signal source when compared to the modulation rate.

An essential part of a coherent system is the transmitter, which must have a relatively monochromatic signal when compared to both the bandwidth of the proposed receiver and the proposed modulation rate.

It has, therefore, only become feasible to build a coherent optical system since the invention of the laser in the 1950's[1]. Since then many scientists and engineers around the world have explored the possibility of building free-space optical communication systems[2,3], with work still on going in this area, eg, for inter satellite links[4,5]. Perhaps not quite such an important development as the laser itself, but nonetheless a very important commercial as well as technical development, was the invention in the 1960's of the semiconductor laser[6,7]. These small, highly-reliable, coherent sources which are now manufactured using fairly mature technologies have made the prospect of revolutionising communications seem both very attractive and possible. To a certain extent this is already the case.

The other advance which stimulated most of today's interest in coherent optical communications was the invention of optical fibres[8]. Today after years of development these low loss (less than 0.2dB/km) and high bandwidth (greater than 50,000GHz at 1.5μm[8]) fibres are being installed all over the world, replacing much more expensive co-axial cables.

Currently most commercially operated optical communication systems have one basic format. They use digital intensity modulation and direct detection. In its simplest form this consists of turning on and of the laser to transmit either a one or a zero and then detecting the power at the other end. This works well but it suffers from thermal noise and it does not exploit the bandwidth available in optical fibre. Instead of sending thousands of signals spaced several GHz apart down one piece of fibre, only one signal is transmitted at a time.

Yamamoto[9] predicted that coherent systems would offer improvements of upto 20dB in receiver sensitivities over practical IM/DD systems. Improvements such as these promise the reduction and possible removal of the current requirement for remote booster/repeater stations in trans-Oceanic or trans -continental hardwire communications.

As a result of Yammamoto's paper[9], much work has been carried out over the past decade. Indeed it was his paper which was the prime motivation for starting the work at Glasgow. Many systems experiments

have been performed, which verified the predicted improvements of coherent systems over direct detection systems[10,11,12,13]. These experiments have invariably used either gas lasers, or have been of a self homo/heterodyne type, when attempting to investigate the most sensitive type of receiver, the optical phase–locked loop. The main reason for this has been the inadequacy of the spectral purity/stabilty of the semiconductor laser as an optical source and the requirements this inadequacy places upon the receiver design. Much effort has also been placed upon improving the spectral qualities of semiconductor lasers.

The main reasons behind research into coherent systems can be summarised as the potential to exploit the bandwidth of optical fibre together with substantial improvements in receiver sensitivity. It must however be noted that in recent years much effort has been diverted back towards intensity modulation and direct detection. The reason for this has been the advent of in fibre, erbium doped, optical amplifiers combined with the use of narrow bandwidth optical filters. The key attraction of fibre amplifiers are that they have high gain, high saturation output power, are polarisation independent, and have low insertion losses. Which technology will prove to offer the most cost effective solution in the longer term is a matter for debate. Coherent systems are more complicated but can space channels close together and truly exploit the bandwidth of the fibre. Perhaps the most important aspect however will be the ease of monolithic integration[13a,b,c].

Many researchers have investigated, both experimentally and theoretically, the problems behind building an optical phase–locked loop[14,15,16,17,18,19,20]. These workers have, however, invariably failed to incorporate the effect of signal propagation delay around the loop. In optical systems where laser linewidths on the order of 1 – 10MHz or greater may have to be tolerated, large receiver bandwidths, in excess of 100MHz have to be used. In such a receiver the effect of time delays on the order of 1ns can have an extremely undesirable effect upon the system sensitivity. In this thesis these effects are quantified and design guidelines drawn up. Two design examples are included in chapter 3.

1.3 OUTLINE OF THESIS

The research carried out by the author and reported upon in this thesis was focussed on building a coherent optical transmission system using semiconductor lasers as both the transmitter and as local oscillator in an optical phase–locked loop reciever. The work was all carried out at 0.85μm, as the only monomode semiconductor lasers commercially available at the start of this project operated at this wavelength.

The reasons for attempting to build such a system are that a phase–locked loop using phase modulation is the most sensitive communication format known and that, if such systems as those mentioned previously are ever to be used commercially, they will most probably use semiconductor lasers. The work presented here also builds upon the work of R.C. Steele and M.A. Grant both of whom worked previously in the same department as the author. The author also acknowledges the research carried out by W.C. Michie and the contribution made by him on similar systems.

Chapter two begins by defining much of the terminology used in analysing communications systems before proceeding on to present the theory behind and to compare the performance predictions of present day IM/DD systems with various coherent systems. In doing this the reader is shown how to analyse a communications system in terms of its receiver sensitivity and how to incorporate the effect of laser phase noise upon such a system.

In chapter 3 the theory of operation of an optical phase–locked loop is presented. Loop performance is analysed in terms of phase error variance, a measure of the effect upon the system of both receiver shot noise and laser phase noise. It is shown in this analysis that it is possible to design an optical phase–locked loop so that the phase error variance is minimised. Two design examples are given to show how the optimum loop bandwidth is estimated.

In the latter part of chapter 3 it is shown that for real systems it is

essential that loop propagation time be fully incorporated into the loop analysis. This is the case as the required bandwidth of the receiver can be of comparable magnitude to the reciprocal of the propagation time. It turns out that this is so if the laser phase noise is large, ie the spectral bandwidth of the laser signal is greater than 100kHz, as is the case with semiconductor lasers. The chapter concludes by quantifying some design criteria for building an OPLL.

The purpose of chapter 4 is to summarise the theory of oscillation in semiconductor lasers and to document fully the operating characteristics of the Hitachi HLP1400 laser diode. Special attention is given to those properties which are of importance in a coherent system, such as modal stability and spectral purity. A description of the experimental techniques used to measure the various properties such as, linewidth, modulation sensitivity and modal stability is also presented. Some elementary theory of oscillation in semiconductor lasers is given to assist in the understanding of how these properties arise. There is also an abbreviated analysis of the work by Henry[24] which explains how laser phase noise arises and how it manifests itself in laser spectra. The chapter concludes by summarising the strengths and weaknesses of "free running" laser diodes in relation to coherent communication systems.

In chapter five, various approaches for improving the modal stability and reducing the laser linewidth of semiconductor lasers are examined. The theory behind the operation of compound cavity, weak optical feedback, and external cavity, strong optical feedback, structures is given, as are experimental results detailing their relative suitability as signal sources for coherent systems. Experimental results characterising the operation of other laser structures such as Distributed Feedback, Distributed Bragg, Integrated Passive cavity and Cleaved Coupled Cavity diodes are quoted.

Chapter six reports on the experimental attempts which were made throughout the course of the project to build an optical phase–locked loop using line narrowed semiconductor lasers, both with external and with compound cavity structures. The loops were designed using the theory and results presented in the previous chapters. Although

extremely good beat spectra, less than 100kHz wide, were obtained on a reproducible basis, solid phase lock was never achieved. The chapter concludes by identifying inadequate modal stability, caused by low frequency vibrations of the external reflector, as the main reason why the loops did not lock. An alternative design for an external cavity or an improved laser would probably resolve the situation.

The final chapter reviews the work presented within the thesis noting that subsequent successful OPLL[25] have been built in agreement with the design criteria presented throughout this thesis. The thesis concludes by offering some suggestions for future research and development in the broad area of coherent optical communications.

REFERENCES

1. A.L. Schalow & C.H. Townes "Infrared and Optical Masers" Physical Review vol.112(6) Dec. 1958. pp1940–1949

2. F.E. Goodwin " A 3.19μm Infrared Optical Heterodyne Communication System" IEE J. Quant. Elect. vol. QE–3(11) 1967. pp524 – 531

3. T.A. Nussmeier, F.E. Goodwin, J.E. Zavin "A 10.6μm Terrestrial Communication Link" IEEE J. Quant> Elect. vol. QE–10(2) 1974. pp230 – 235

4. W.R. Leeb, H.K. Philipp, A.L. Sholtz & E. Bonek "Frequency Synchronization and Phase Locking of CO_2 Lasers" Appl. Phys. Lett. 41(7) 1982. pp592 – 594

5. H.K. Philipp, A.L. Sholtz, E. Bonek & W.R Leeb "Costas Loop Experiment for a 10.6μm Communications Receiver" IEEE Trans. Commun. vol. COM–31(8) Aug. 1983. pp1000–1002

6. R.N. Hall, G.E. Fenner, J.D. Kingsley, T.J. Soltys & R.O. Carlson "Coherent Light Emission from GaAs Junctions" Phys. Rev. Lett. vol. 9 1962 pp366

7. M.I. Nathan, W.P. Dumke, G.Burns, F.H.Dills & G. Lasher "Stimulated Emmision of Radiation from GaAs PN Junctions" Appl. Phys. Lett. vol. 1 1962. pp62

8. K.C. Kao & G.A. Hockham "Dielectric Fibre Surface Waveguides for Optical Frequencies" Proc. IEE 113 1966 pp115 – 1158

9. Y. Yammamoto "Receiver Performance Evaluation of Various DigitalOptical Modulation–Demodulation Systems in the 0.5 – 10μm Region" IEEE J. Quant. Elect vol. QE–16(11) 1980 pp1251 – 1259

10. K. Kikuchi, T. Okoshi, J. Kitano "Measurement of BER of Heterodyne Type Optical Communication System – A Simulation Experiment" IEEE J. Quant. Elect. vol QE–17(2) 1981 pp2266 – 2267

11. T.G. Hodgkinson, R. Wyatt, D.W. Smith "Experimental Assessment of a 140MBit/s Coherent Optical Receiver at 1.52μm" Elect. Lett. vol 18(12) 1982 pp523 – 525

12. S. Saito, Y. Yamamoto, T. Kimura "S/N and Error Rate Evaluation for an Optical FSK Heterodyne Detection System using Semiconductor Lasers" IEEE J. Quant. Elect. vol QE–19(2) 1983 pp180 – 193

13. D.J. Malyon et al "PSK Homodyne Receiver Sensitivity Measurements at 1.5μm" Elect. Lett. vol 19 1983 pp144 – 146

13a. S. Wen, S. Chi "Characteristics of the gain and signal to noise ratio of a distributed Erbium Doped Optical Amplifier" IEEE Journal of Lightwave Technology No. 12 Dec. 1992 pp1869 – 1878

13b B. Pedersen et al "The design of Erbium Doped Fiber Amplifiers" J.L.T. vol 9 September
1991 pp 1105 – 1112

13c B. Pedersen et al"Evaluation of the 800nm pump based Erbium Doped Fibre Amplifier" J.L.T. Vol 10 No. 6 August 1992 pp 1041 – 1049

14. J.B. Armor, S.R. Robinson "Phaselock Control Considerations for Coherently Combined Lasers" Appl. Opt. vol 18(18) 1979 pp3165 – 3175

15. L.G. Kazovsky "Decision Driven Phase Locked Loop for optical Homodyne Receivers: Performance Analysis and Laser Linewidth Requirements" J. Lightwave Tech. vo LT–3(6) 1985 pp1238 – 1247

16. L.G. Kazovsky "Balanced Phase Locked Loops for Optical Homodyne Receivers: Performance Analysis, Design Consideration and Laser Linewidth Requirements" J. Lightwave Tech. vol LT−4(2) 1986 pp 182 − 194

17. L.G. Kazovsky "Performance Analysis and Laser LInewidth Requirements for Optical PSK Heterodyne Communication Systems" IEE J. Lightwave Tech. vol LT−4(4) 1986 pp415 − 425

18. T.G. Hodgkinson "Phase Locked Loop Analysis for Pilot Carrier Coherent Optical Receivers" Elect. Lett. vol 21 1985 pp1202 − 1203

19. T.G. Hodgkinson "Costas Loop Analysis for Optical Receivers" Elect. Lett. vol22(7) 1986 pp394 − 396

20. W.R. Leeb, H.K. Philipp, A.L. Sholtz, E Bonek "Frequency Synchronisation and Phase Locking of CO_2 Lasers" Appl. Phys. Lett. 1982 pp592 − 594

21. R.C. Steele PhD Thesis University of Glasgow 1984

22. M.A. Grant "Design Considerations for an Optical PSK Homodyne Receiver" PhD Thesis University of Glsagow Oct. 1986

23. W.C. Michie "Carrier Phase Recovery for Coherent Optical Transmission Systems" PhD. Thesis Lasgow University 1989

24. C.H. Henry, Theory of Linewidth of Semiconductor Lasers, IEEE J. Quantum Electronics, vol QE−18(2) 1982 pp259−264

25. R.T. Ramos, A.J. Seeds "Fast Heterodyne Optical Phase Lock Loop Using Double Quantum Well Laser Diodes" Elect Lett. vol 28(1) 1992 pp82−83

CHAPTER 2

2.1 INTRODUCTION

Most optical communication systems in use today use an intensity modulation / direct detection format, IM/DD. This technique is both simple and cheap but it does not fully exploit the huge bandwidth available in optical fibre, 50,000 GHz[1] at a wavelength of 0.85 μm. In a coherent system, using different modulation/demodulation formats, it would be possible to transmit thousands of signals simultaneously down one piece of monomode fibre by separating each of them in frequency by a set amount, say 5GHz. This approach is called frequency division multiplexing and it would be possible to increase the channel capacity 10,000 fold. This huge increase in channel capacity and the prospect of shot noise limited detection thus allowing signals to be transmitted over greater distances and hence reducing the number of repeater stations required are the two main attractions of coherent optical systems.

It should be stressed at this point that there are some very serious technical problems which have to be overcome before coherent optical transmission sytems supercede IM/DD systems. The major area for concern relates to the suitability of the chosen optical source, the semiconductor laser. This area will be addressed in chapters 4 and 5.

It is the aim of this chapter to state the case for coherent fibre optical systems in general by pointing out the benefits, in terms of improved system sensitivities and in terms of exploiting the available bandwidth, that may be gained by implementing such a system. The chapter will analyse both non coherent and coherent systems in terms of the noise sources at their receivers. Bit error rate calculations will be evaluated for IM/DD, coherent Amplitude Shift Keyed (ASK), coherent Frequency Shift Keyed (FSK) and coherent Phase Shift Keyed (PSK) systems. Finally the effect of phase noise on coherent systems will be incorporated into the analysis. Comparisons between the various systems will be made in terms of the receiver sensitivities of the different schemes. Most of this work can be found in references 2 through to 9, while reference 10 is an excellent introduction to many

of the general techniques mentioned throughout the chapter.

The receiver sensitivity of a communication system will be defined as the minimum power required to achieve a specified bit error rate, BER.

2.2 NOISE IN AN OPTICAL COMMUNICATIONS RECEIVER

Figure 2.1a shows a diagram of a typical receiver which could be used for detecting an IM signal. The receiver consists of either an avalanche or a PIN photodiode, an amplifier, equalisation and filtering equipment as well as some decision circuitry.

Figure 2.1b shows a typical coherent receiver. This differs from 2.1a in that a coherent receiver requires a local signal generator which is part of a control loop that is used to track the frequency or phase of the incoming signal.

2.2.1 SHOT NOISE

One feature of optical communications is that the receiver noise contains a component which is proportional to the received optical power. This is the shot noise that is characteristic of the quantum–limited photodetection process. Noise of this type is generated by all the light that falls on a photodetector. There is also some additional shot noise generated by dark current, as the noise is dependent upon the current flow in the diode. Shot noise is also dependent upon the bandwidth of the receiver. The various components of the shot noise photocurrent can be represented by the following expressions, which give mean square variances:

$$\overline{i^2}_s = 2eRP_s\langle M\rangle^{(2+x)}.B$$

$$\overline{i^2}_b = 2eRP_s\langle M\rangle^{(2+x)}.B \qquad 2.2.1$$

$$\overline{i^2}_{LO} = 2eRP_{LO}\langle M\rangle^{(2+x)}.B$$

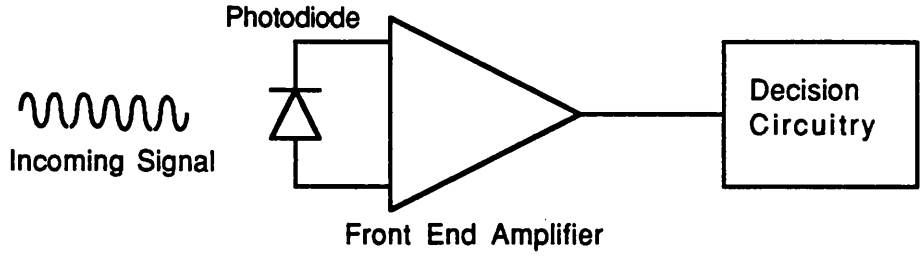

a) IM/DD Receiver

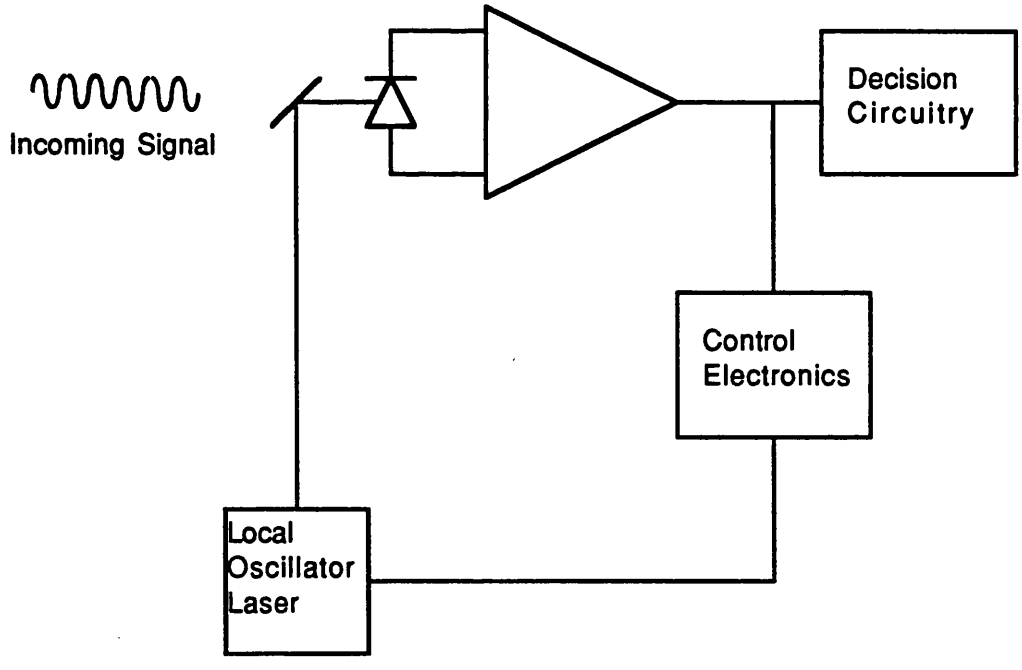

b) Coherent Receiver

Figure 2.1 Schematic diagrams of a) IM/DD Receiver
b) Coherent Receiver

$$\overline{i^2_d} = 2e(I_m + I_n)B$$

where s denotes signal power
LO denotes local oscillator
d denotes dark current
b denotes background light
B is the bandwidth of the receiver
e is the electronic charge
R is the responsivity of the diode
P is optical power
M is the gain of the APD
x is the excess noise factor
I_m is the multiplied part of the dark current
I_n is the non multiplied part of the dark current

2.2.2 CIRCUIT NOISE

In any system, dissipative elements give rise to noise. In an electronic circuit all resistors give rise to Johnson Noise as a result of the random thermal motion of the charge carriers. The noise introduced into a receiver using a high impedance front stage FET amplifier is given by [1]

$$\overline{i_c}^2 = \left[\frac{4kT}{R_L}\left[\ 1 + \frac{\Gamma}{g_m R_L}\right] + 2qI_{gate}\ \right]B + 4kT\Gamma\frac{(2\pi C_T)^2}{g_m}B^3 \quad 2.2.2$$

where k is Boltzmann's constant
R_L is the load resistance
I_{gate} is gate leakage current
Γ is a numerical factor determined by the choice of FET material, 1.2 for silicon and 0.7 for GaAs
g_m is the transconductance of the FET.

As can be seen from this equation Johnson noise is dependent upon bandwidth which for the purpose of this chapter will be assumed to be equal to be 1/2 the bit rate.

2.3 EVALUATION OF BER IN OPTICAL COMMUNICATION SYSTEMS

All the modulation formats which will be discussed in this chapter are binary systems. In a binary system the probability of making a mistake in deciding what has been transmitted is given by

PE = (probability of regenerating 0 when 1 is sent)
× (probability of sending 1) +
(probability of regenerating 1 when 0 is sent)
× (probability of sending 0) 2.3.1

Using probability notation[11] this can be written as

$$PE = P(0|1)P(1) + P(1|0)P(0) \qquad 2.3.2$$

When 0's and 1's are sent in equal numbers, P(0) = P(1) = 1/2, so that:

$$PE = 1/2[P(0|1) + P(1|0)] \qquad 2.3.3$$

The problem of calculating error probability has now been reduced to determining P(0|1) and P(1|0).

2.3.1 IM/DD

In an IM/DD system, ones and zeros may correspond to the power on and power off states, dependant upon the coding used. If a mark, power on, is sent the total noise power at the receiver is proportional to the sum of all the variances of the individual noise sources.

$$\sigma_m^2 = \overline{i_S}^2 + \overline{i_D}^2 + \overline{i_b}^2 + \overline{i_c}^2 \qquad 2.3.4$$

When a space, power off, is transmitted the total noise variance is

$$\sigma_s^2 = \overline{i_D}^2 + \overline{i_b}^2 + \overline{i_c}^2 \qquad 2.3.5$$

Strictly speaking, shot noise is a discrete process and so it is governed by Poisson statistics. If however the number of events taking place is large, one can use Gaussian statistics and this is the procedure followed here.[10]

For ease of calculation we assume that the multiplication factor of the avalanche photodiode (APD) used equals 1 then the received signal current I_m in the presence of a mark is given by:

$$I_m = P_s R = P_s \frac{\eta e}{h\nu} \qquad 2.3.6$$

where P_s is the received signal power, R is the responsivity of the diode and η is its quantum efficiency. The probability density function $P_m(x)$ for reception of a mark, power on, is given by:

$$P_m(x) = \frac{1}{(2\pi\sigma_m^2)^{1/2}} \exp -((I_m-x)^2/2\sigma_m^2) \qquad 2.3.7$$

For a space, power off, the function $P_s(x)$is given by:

$$P_s(x) = \frac{1}{(2\pi\sigma_s^2)^{1/2}} \exp -(x^2/2\sigma_s^2) \qquad 2.3.8$$

where σ_s^2 is the noise variance when a space is sent. These functions are plotted in figure 2. D, which is the decision level derived from the overlap of the two functions, is evaluated below.

P(1|0) is the area of the probability distribution $P_s(x)$ which falls above the decision level D. Similarly P(0|1) is the area of $P_m(x)$ which falls below D.

$$P(1|0) = \frac{1}{(2.\pi.\sigma_s^2)^{1/2}} \int_D^\infty \exp -(x^2/2\sigma_s^2)dx \qquad 2.3.9$$

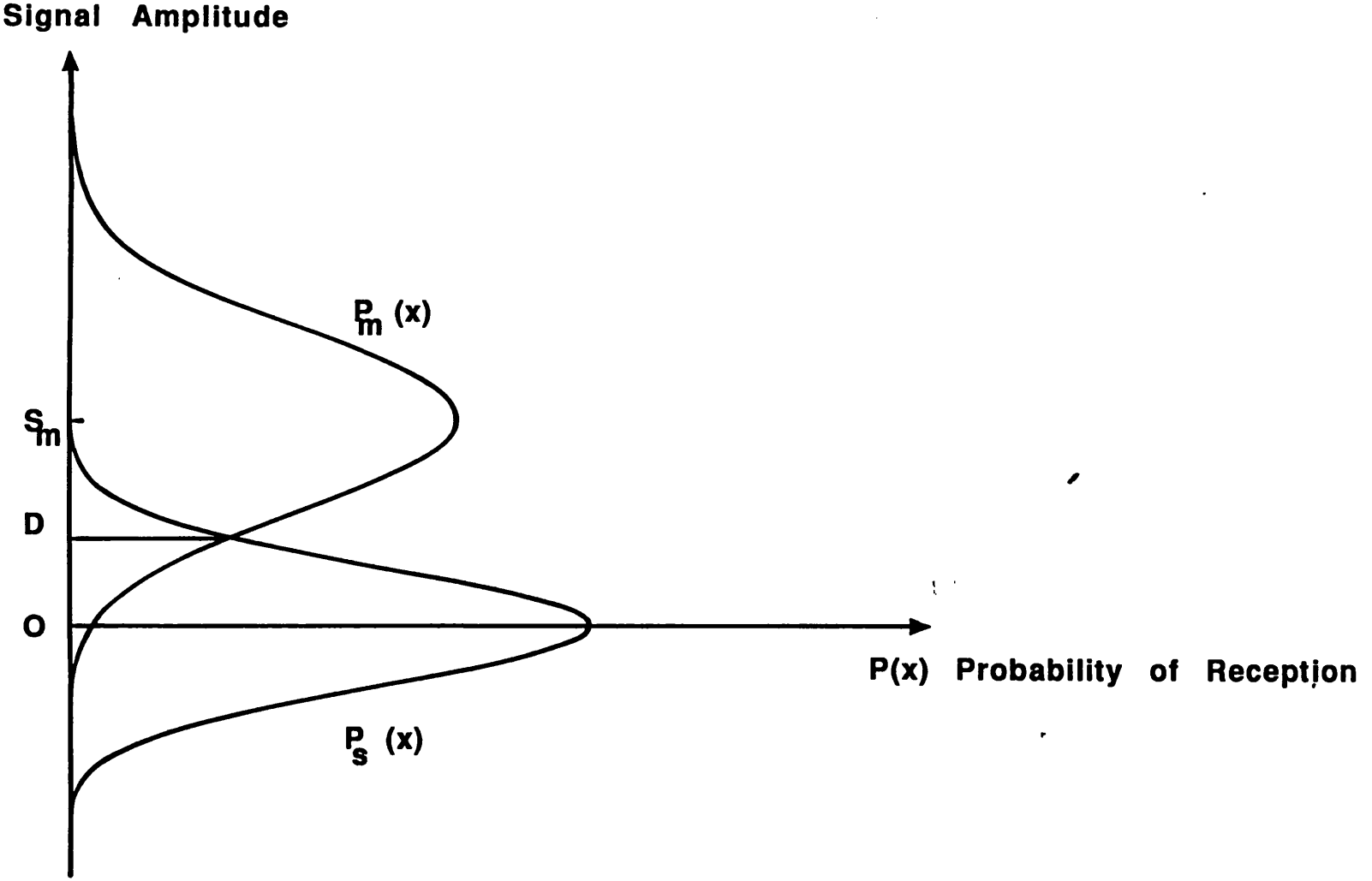

Figure 2.2 Probability Density Function for a Direct Detection System

$$P(0|1) = \frac{1}{(2.\pi.\sigma_m^2)^{1/2}}\int_{-\infty}^{D} \exp -((I_m-x)^2/2\sigma_m^2)dx \qquad 2.3.10$$

$$PE = \frac{1}{2}\left[\frac{1}{(2.\pi.\sigma_s^2)^{1/2}}\int_{D}^{\infty} \exp -(x^2/2\sigma_s^2)dx + \right.$$

$$\left.\frac{1}{(2.\pi.\sigma_m^2)^{1/2}}\int_{-\infty}^{D} \exp -((I_m-x)^2/2\sigma_m^2)dx\right] \qquad 2.3.11$$

Introducing the standard change of variable, $t = (I_m - x)/\sigma_m$ in $P(0|1)$ and $t = x^2/\sigma_s$ in $P(1|0)$ gives

$$PE = \frac{1}{2}\left[\frac{1}{(2.\pi)^{1/2}}\int_{D/\sigma_s}^{\infty} \exp -t^2/2\ dt + \right.$$

$$\left.\frac{1}{(2.\pi)^{1/2}}\int_{(I_m-D)/\sigma_M}^{\infty} \exp -t^2/2\ dt\right] \qquad 2.3.13$$

Assuming that the probability of error in detecting a mark or space is equal, the decision level D can be optimised:

$$D_{opt}/\sigma_s = (I_m - D_{opt})/\sigma_m \qquad 2.3.14$$

$$D_{opt} = \frac{\sigma_s I_m}{\sigma_m + \sigma_s} \qquad 2.3.15$$

Substituting 2.3.15 into 2.3.13 gives the BER in terms of the complementary error function.

$$BER = \frac{1}{(2\pi)^{1/2}}\int_{Q}^{\infty} \exp -t^2/2\ dt \qquad 2.3.16$$

where $Q = I_M/(\sigma_M + \sigma_S)$

Q^2 is the input signal–to–noise ratio, SNR, at the detector. The BER of this system is thus given by

$$BER = erfc(Q) = erfc[(S/N)^{1/2}] \qquad 2.3.17$$

This function is shown graphically in figure 2.3. It can be seen from this that for a 10^{-9} BER the required SNR is 15.56dB.[10]

2.4 QUANTUM LIMIT

In an ideal binary system the only noise present would be shot noise generated as a result of the quantum nature of the light and of the randomness of charge transport. There would be no noise present when a space is sent as no power would be received. The only circumstances in which errors would arise would be when the power being sent as a mark did not generate any carriers at all. Therefore using these assumptions the quantum limit can be calculated:–

$$Q = I_m/\sigma_m \qquad 2.4.1$$

$$Q = \frac{\eta e P_m/h\nu}{(2e^2 B\eta P_m/h\nu)^{1/2}} \qquad 2.4.2$$

$$Q^2 = \eta P_m/(h\nu f_B) \qquad 2.4.3$$

where f_B is the bit rate and is defined as twice the bandwidth.

In an ideal system $\eta = 1$. The number of photons incident on the diode per second is given by $P_m/h\nu$ and so the number of photons/bit required for a 10^{-9} BER is 36. The average number of photons/bit is half this value = 18.

The minimum received power required for a 10^{-9} BER can be evaluated, given the parameters of the system. For a system operating at 830nm, with a responsivity of 0.85 and a bit rate of 565Mbit/s, the minimum power required is −57.2dBm.

2.4.1 PRACTICAL LIMITATIONS

In practice this limit is not achievable in an IM/DD system. The

Figure 2.3 BER Versus Signal to Noise Ratio

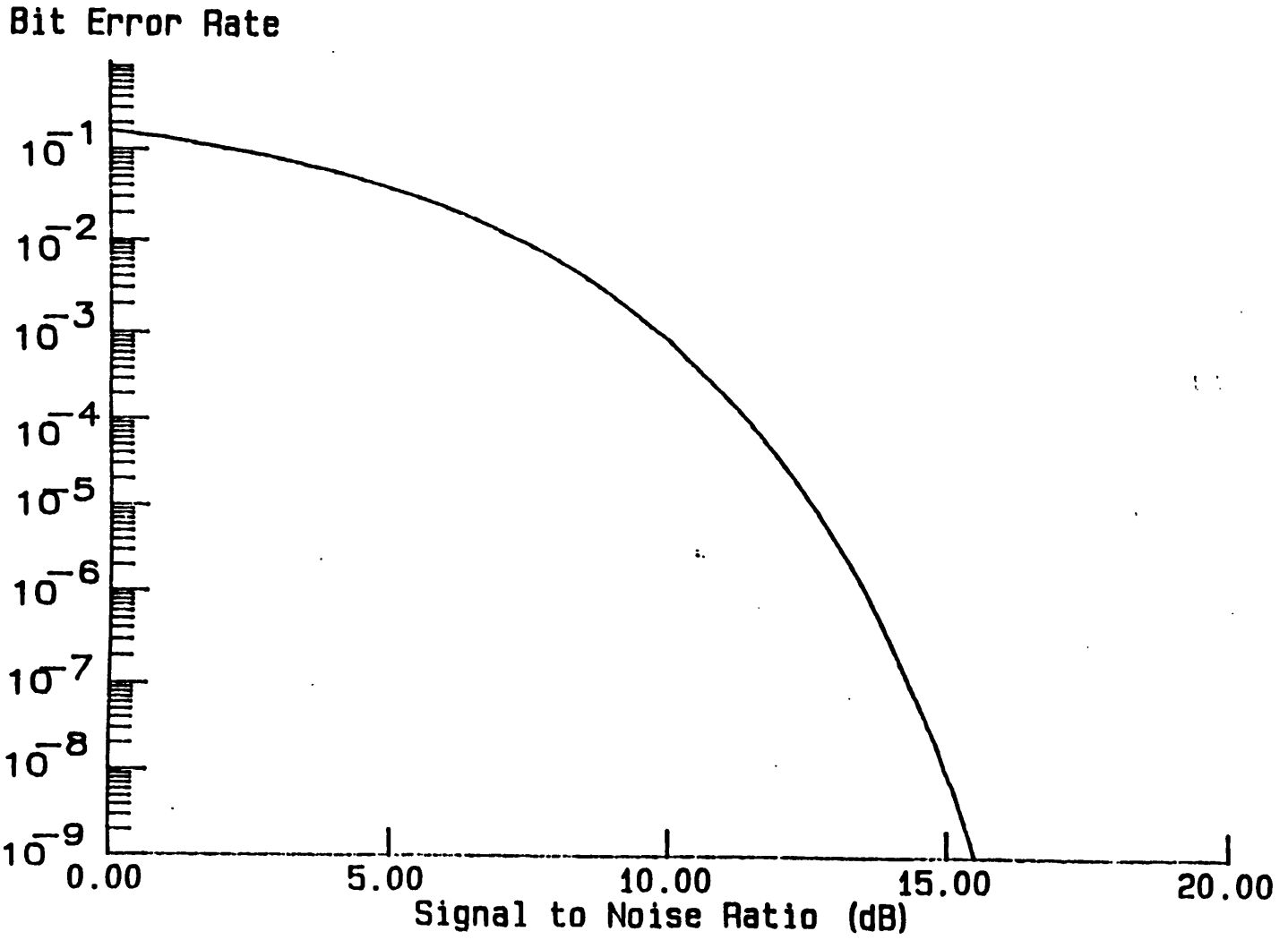

dominant noise source is invariably the thermal noise at the front end of the receiver. This fact results in practical systems being some 7 to 15dB less sensitive than the quantum limit [3,5,6].

2.5 COHERENT SYSTEMS

Figure 4 shows a diagram of a typical coherent receiver. This differs significantly from that used for IM/DD systems in that this receiver has extra components and a feedback control loop.

In a coherent receiver the incoming signal is mixed with a locally generated signal of known frequency and phase to produce an intermediate frequency signal. The transmitted information can then be read straight off from the IF signal. The extra components in the receiver are the mixer, a photodiode in optical systems which is used to compare the local signal with the incoming one, a local oscillator and finally some feedback electronics to control the local oscillator so that it has a definite phase relationship with the incoming signal.

2.5.1 HETERODYNE VERSUS HOMODYNE DETECTION

In the following analysis no consideration is made of phase noise in the optical signals. This problem will be dealt with in section 2.6. The optical signals will be treated as pure sinusoids.

In a coherent system, waves from a local source are mixed with the incoming modulated waves from a transmitter. Provided that the signals are mutually coherent and that they maintain their coherence over the area of the photodiode, then the output current from the photodiode will have a component which varies at the difference frequency between the two lasers.

Consider a photodiode which is simultaneously illuminated by both an incoming signal and by a local signal. To understand what happens it is important to note that the instantaneous rate of carrier regeneration is proportional to the square of the electric field amplitude. Let the electric field components of the transmitted signal and that of the local signal be represented by $E_T(t)$ and $E_{LO}(t)$ respectively. Then

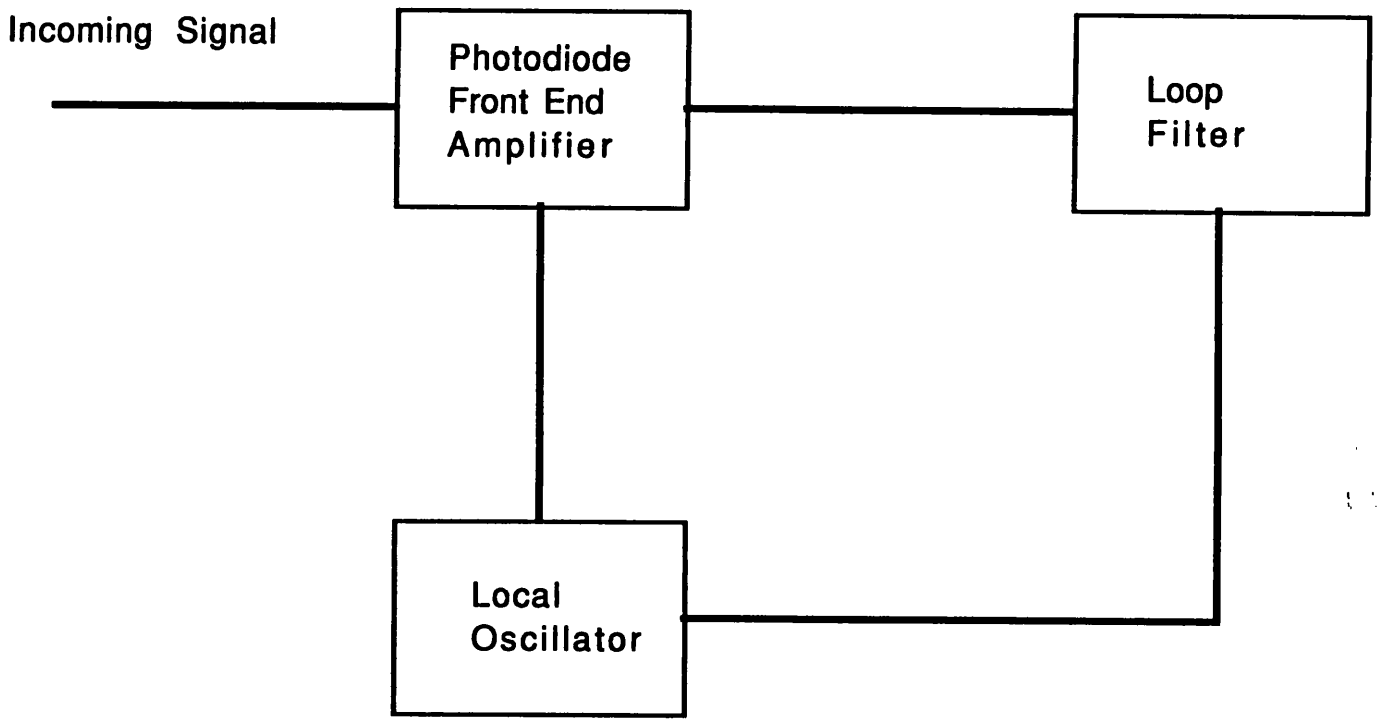

Figure 2.4 Generalised Coherent Receiver

assuming perfect alignment of phase fronts

$$E_T(t) = \mathrm{Re}[(2P_TZ)^{1/2}\exp(i(\omega_T t + \varphi_T))]$$

$$= (2P_TZ)^{1/2}\cos(\omega_T t + \varphi_T) \qquad 2.5.1$$

and

$$E_{LO}(t) = \mathrm{Re}[(2P_{LO}Z)^{1/2}\exp(i(\omega_{LO} t + \varphi_{LO}))]$$

$$= (2P_{LO}Z)^{1/2}\cos(\omega_{LO} t + \varphi_{LO}) \qquad 2.5.2$$

where Z is the local space impedance (in vacuum Z = 377Ω), P_{LO} and P_T are the optical power densities, ω is the mean angular frequency and φ is the phase of the respective waveforms. Using the above two equations, one can obtain an expression for the time varying photocurrent by integrating over the area,A, of detection.

$$i(t) = R.A.[E_T(t) + E_{LO}(t)]^2/Z$$

$$= R.A.[P_T + P_{LO} + 2(P_TP_{LO})^{1/2}*$$

$$\cos(\omega_T t + \varphi_T)\cos(\omega_{LO} t + \varphi_{LO})] \qquad 2.5.3$$

Since the photodiode has no electrical response at $(\omega_T + \omega_{LO})$, the above expression may be rewritten as

$$i(t) = R.A.[P_T + P_{LO} + 2(P_TP_{LO})^{1/2}$$

$$\cos((\omega_T - \omega_{LO})t + (\varphi_T - \varphi_{LO}))] \qquad 2.5.4$$

The third term in this equation is the desired signal component. This term is the difference frequency of the beat between the local and transmitted signals. $(\varphi_T - \varphi_{LO})$ is the phase difference between the two signals. This component is proportional to $(P_TP_{LO})^{1/2}$ and so it is possible to amplify the incoming signal directly by increasing the local oscillator power. This is the main advantage of coherent systems over IM/DD.

In a frequency locked–loop, only the difference frequency, ω_{IF}, is used to feed back information to the local source. In a phase locked–loop it is the phase difference that is important. If the loop

works with a finite frequency difference then it is a heterodyne system. If the loop locks with $\omega_{IF} = 0$ then it is a homodyne system.

In the remainder of this thesis the impedance of the transmission medium and the area of detection have been normalised to one. This is done to simplify the analysis.

2.5.2 COHERENT ASK

In coherent systems there is additional shot noise generated by the LO. The extra shot noise photocurrent is

$$\overline{i_{LO}^2} = 2eRP_{LO}B \qquad 2.5.5$$

It is this term which makes the noise in coherent systems different from IM/DD. The total noise variance of the receiver is now given by

$$\sigma^2 = \overline{i_s^2} + \overline{i_b^2} + \overline{i_D^2} + \overline{i_c^2} + \overline{i_{LO}^2} \qquad 2.5.6$$

As a result of the proximity of the LO to the photodiode it is quite simple to increase the local power until the LO shot noise dominates all other noise sources. When this occurs, the receiver is shot noise limited. Since $P_{LO} >> P_T$ the noise variance for both on and off states may be equated.

$$\sigma_M^2 = \sigma_s^2 = \sigma^2 \qquad 2.5.7$$

Using this approximation the optimum decision level is given by

$$D_{OPT} = \frac{I_M}{2} \qquad 2.5.8$$

The BER can now be evaluated by repeating the procedure used in section 2.3. The result is

$$BER = erfc\left[\frac{I_M}{2\sigma}\right] \qquad 2.5.9$$

Now using the same parameters as for IM/DD the receiver sensitivity can be evaluated for a 10^{-9} BER. The minimum required power for such an ASK coherent on/off system is -51.2dBm.

2.5.3 COHERENT FSK

In this system it is assumed that two different frequencies are transmitted, f_1(mark) and f_2(space). The signal is received by two receivers tuned to f_1 and f_2 respectively. The receiver is shown in figure 5.

It is possible to analyse this system by considering what happens only in the time slot when a mark is transmitted. We shall denote the voltages generated at the output of each receiver as v_1 and v_2. The probability density functions of the output voltages are

$$p(v_1) = \frac{1}{(2\pi)^{1/2}\sigma_m}\exp\left[-\frac{(I_m - v_1)^2}{2\sigma_m^2}\right] \qquad 2.5.10$$

$$p(v_2) = \frac{1}{(2\pi)^{1/2}\sigma_s}\exp\left[-\frac{-v_2^2}{2\sigma_s^2}\right] \qquad 2.5.11$$

These probability distributions are shown in figure 6. An error occurs in this state only if $v_2 > v_1$. Therefore the probability of error when a mark is transmitted is given by

$$\begin{aligned} P_e &= \text{prob}((v_2 - v_1) > 0) \\ &= \int_{-\infty}^{0} \frac{1}{(2\pi(\sigma_m^2 + \sigma_s^2))^{1/2}} * \\ &\qquad \exp\left[-\frac{(w - I_m)^2}{2(\sigma_m^2+\sigma_s^2)}\right] dw \end{aligned} \qquad 2.5.12$$

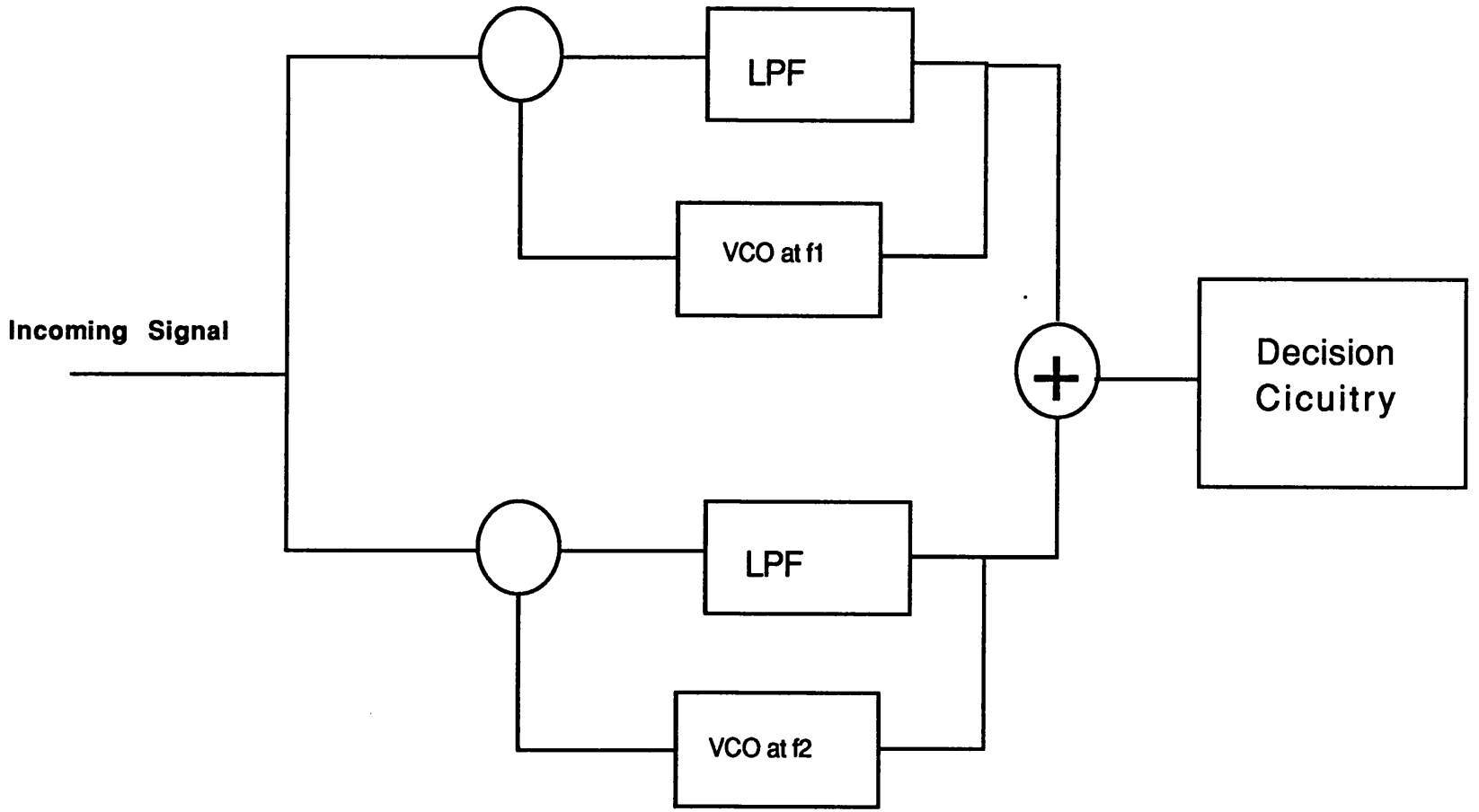

Figure 2.5 Schematic of an FSK Receiver

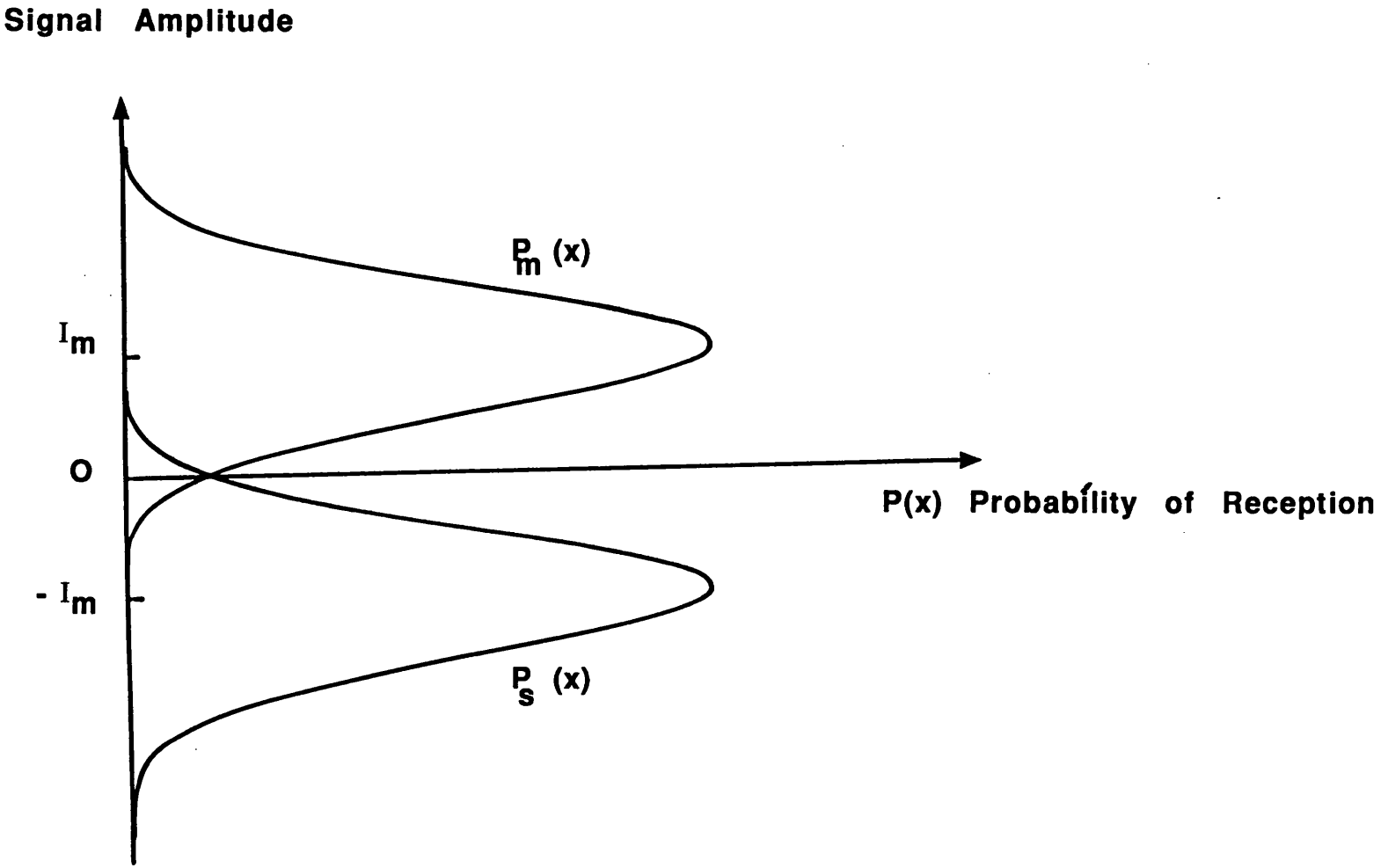

Figure 2.6 Probability Density Function of FSK Detection System

Using $\sigma_m = \sigma_s = \sigma$ and substituting

$$u = \frac{(w - I_m)}{2^{1/2}\sigma} \qquad 2.5.13$$

$$P_e = \frac{1}{(2\pi)^{1/2}} \int_{I_m/(2^{1/2}\sigma)}^{\infty} \exp -(u^2/2)du$$

$$= \text{erfc}\left[\frac{I_m}{2^{1/2}\sigma}\right] \qquad 2.5.14$$

The probability of error when a space is transmitted is the same as that for a mark and so, assuming that both are transmitted with equal probability, the BER for an FSK coherent system is

$$\text{BER} = \text{erfc}\left[\frac{I_m}{2^{1/2}\sigma}\right] \qquad 2.5.15$$

Thus for a 10^{-9} BER operating at 830nm and at a bit rate of 565Mbit/s the minimum required received power is -54.2dBm. This is a 3dB improvement on the ASK system but it should be noted that in the ASK format power is only transmitted half of the time. The average power required is therefore the same for both cases.

2.5.4 COHERENT PSK

It can be shown[6] that the most sensitive type of binary modulation format is one which employs antipodal signalling, ie the two signals denoting the two possible information symbols have exactly the same shape but are of opposite polarity. Binary phase shift keying, BPSK, is a constant carrier mode which can employ such a modulation. A typical BPSK signal can be represented by

$$E(t) = E\cos[\omega t + \Delta\theta p(t)] \qquad 2.5.16$$

where $\Delta\theta$ is the phase shift and p(t) is a binary switching function

with two possible states ±1. At this point it is useful to define a modulation index m for BPSK as:

$$m = \cos\Delta\theta \qquad 0 \leqslant m \leqslant 1 \qquad 2.5.17$$

Substituting 2.5.17 into 2.5.16 and then expanding it is possible to rewrite 2.5.16 as

$$E(t) = m.E.\sin(\omega t) + p(t)(1-m^2)^{1/2}E.\cos(\omega t) \qquad 2.5.18$$

The first term in this equation is the carrier component and the second term is the modulation component of the received signal. The average power in each component is given by $m^2A^2/2$ and $(1-m^2)A^2/2$ respectively. It follows from this that the carrier will be totally suppressed for $\Delta\theta = \pi/2$.

The BER will now be evaluated. The received signal generates a photocurrent

$$I_m = I\sin\Delta\theta \qquad 2.5.19a$$

for a mark and

$$I_s = -I\sin\Delta\theta \qquad 2.5.19b$$

for a space, where $I = 2R(P_TP_{LO})^{1/2}$. The probability distributions of the two states in an antipodal PSK system are shown in figure 7.

The probability of error when a mark is transmitted is given by

$$PE = \frac{1}{(2\pi)^{1/2}\sigma_m}\int_{\infty}^{0} \exp - \frac{(I\sin\Delta\theta - x)^2}{2\sigma_m^2}\,dx$$

$$= \operatorname{erfc}\left[\frac{I.\sin\Delta\theta}{\sigma_m}\right] \qquad 2.5.20$$

But since the probability of error when a space is transmitted is the same as that for a mark, and assuming both are transmitted with

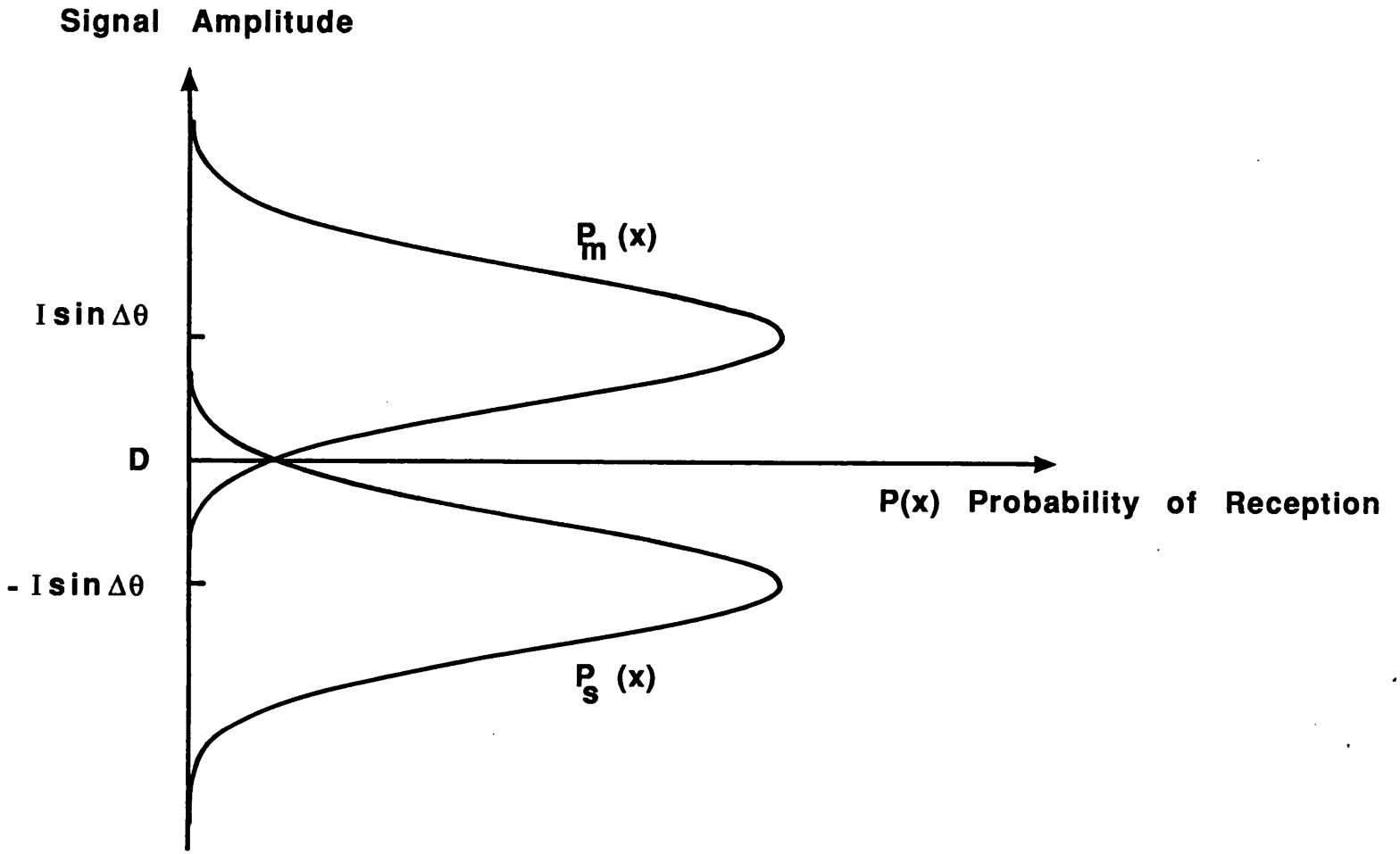

Figure 2.7 Probability Density Function of PSK Detection System

equal probability, the BER is:

$$BER = erfc\left[\frac{I.\sin\Delta\theta}{\sigma}\right] \qquad 2.5.21$$

If the system has m = 0 then equation 2.5.21 states that a PSK system gives a 3dB improvement over a heterodyne FSK. Using the parameters stated earlier the receiver sensitivity can be calculated. The receiver requires -57.2dBm for a 10^{-9} BER. This is only true for m = 0.

If $m \neq 0$ a power penalty has to be paid. The receiver sensitivity is reduced by $10\log_{10}(1-m^2)$ dB. The extra power is required for a carrier so that carrier synchronisation can be achieved. Otherwise a Costas loop or some other form of carrier regeneration would have to be employed at the receiver. A 1dB power penalty is incurred if $\Delta\theta$ is reduced from 90^0 to 63^0 and the required power at the receiver will be -56.2dBm.

2.5.5 HOMODYNE DETECTION

Up to this point all calculations have been based upon a heterodyne receiver. If a homodyne receiver were used instead, there would be an immediate improvement of 3dB in the receiver sensitivity. This improvement arises because homodyne detectors only require half the bandwidth of a heterodyne receiver[4] for a given bit rate. This improvement is only obtainable in ASK and PSK systems.

2.6 EFFECT OF LASER PHASE NOISE ON A COHERENT SYSTEM

So far in this chapter no account has been taken of the effect of laser phase noise on an optical communication channel. The laser signal has so far been modelled as a perfect sinusoid. Unfortunately lasers do not emit perfectly monochromatic signals and it is the purpose of this section to detail the effect of laser phase noise upon the BER of a PSK system. Section 4.6 explains the origin and describes the manifestations of laser phase noise.

2.6.1 STATISTICAL REPRESENTATION OF LASER PHASE NOISE

The optical field emitted, far above threshold, from a monomode laser diode can be modelled as an amplitude stabilised field undergoing phase fluctuations[9]

$$E(t) = E.\exp\, i[\omega t + \varphi(t)] \qquad 2.6.1$$

where $\varphi(t)$ is a stochastic process representing the random phase fluctuations which lead to a broadening of the laser spectrum. Amplitude noise is ignored far above threshold as its contribution to the laser spectrum is negligible by comparison.

In analysing a coherent system it is is not the absolute phase of the laser which is of interest but rather the phase jitter $\Delta\varphi(t,T)$. This is defined as

$$\Delta\varphi(t,T) = \varphi(t + T) - \varphi(t) \qquad 2.6.2$$

The phase fluctuations of a laser output show, in a first order approximation, the same statistical properties as brownian motion of free particles. In this instance, first–order approximation means that the phase fluctuations lead to a Lorentzian Lineshape. Thus the phase jitter is assumed to be a zero mean stationary random Gaussian process with the following probability distribution function [9]

$$p(\Delta\varphi(T)) = \frac{1}{[2\pi<\Delta\varphi^2(T)>]^{1/2}} \exp\left[-\frac{\Delta\varphi^2(T)}{2<\Delta\varphi^2(T)>}\right] \qquad 2.6.3$$

where $<\Delta\varphi^2(T)>$ is the mean square phase jitter of the laser field.

2.6.2 EFFECT OF PHASE NOISE ON BER

The system which will be analysed in this section is a Phase Locked–Loop, ie one form of phase sensitive detection. Laser phase noise can be treated simply as phase jitter in carrier recovery or as a random phase modulation. Therefore its effect on a coherent system can be analysed using standard techniques.

The photocurrent is modified when phase noise is included and can be written as:

$$i(t) = I\cos[\Phi_E(t) + \Delta\varphi_n(t)] + n(t) \qquad 2.6.4$$

where $I = 2.R.(P_R P_{LO})^{1/2}$, $\Phi_E(t) = \Phi_R - \Phi_{LO}$ and n(t) is a term representing the receiver shot noise. n(t) is assumed to be a zero mean Gaussian function with variance given by $\sigma_n^2 = e.R.P_{LO}.B$.

When a mark or a space are transmitted the received signals are now given by

$$i_m(t) = I\cos(\Delta\varphi_n(t)) + n(t) \qquad 2.6.5$$

$$i_s(t) = -I\cos(\Delta\varphi_n(t)) + n(t) \qquad 2.6.6$$

respectively. Making the same assumptions as before, that marks and spaces are transmitted with equal probability and that the signal is antipodal BPSK the probability of error is given by

$$PE = \text{erfc}\left[\frac{I\cos(\Delta\varphi_n(t))}{\sigma}\right] \qquad 2.6.7$$

The average bit error rate is evaluated by integrating the above equation over the probability distribution of $\Delta\varphi_n(t)$. It should be stated that the variance of $\Delta\varphi_n$ is a function of both the probability distribution of the intrinsic phase noise of the laser and also of the bandwidth of the tracking circuit.

$$BER = \frac{1}{2}\int_{-\infty}^{\infty} \text{erfc}\left[\frac{I\cos(\Delta\varphi_n(t))}{\sigma}\right] p(\varphi)d\varphi \qquad 2.6.8$$

In evaluating the above expresion it is assumed that $\cos(\Delta\varphi_n(t))$ is quasi-constant over the bit period. The justification for this assumption is given in section 3.3, where it is shown that the linewidth-to-bit-rate ratio must be around 0.05% or less if the system is to suffer no more than a 1dB power penalty, 0.5 dB due to carrier generation and 0.5dB to compensate for the laser linewidth.[5,8]

This equation was evaluated by Prabhu[9] for two different probability

distributions, Gaussian and Tikhonov. The BER curves are shown in figure 8.

A Tikhonov distribution is a more accurate representation of the phase noise probability distribution in a phase locked–loop. In practice it is very much more difficult to work with than the Gaussian approximation and the final results are similar[9].

It can be seen from figure 8 that in the case of a Tikhonov distribution the system suffers a 0.5dB power penalty for $\sigma_\varphi = 10^\circ$ if a BER of 10^{-9} is to be achieved. It is also shown that a 10^{-9}BER cannot be acheived if $\sigma_\varphi = 12.5°$. If the Gaussian analysis is used then the severity of the power penalty is increased.

2.7 CONCLUSIONS

In this chapter the case for attempting to implement a coherent optical communication system has been presented. It was stated at the start of the chapter that the major attraction of such a system was that the bandwidth of the optical fibre could be more efficiently exploited. It was then shown that it is possible to attain shot noise limited detection in a coherent system where as practically this has never been achieved in an IM/DD system. BER have been calculated for different systems using the same parameters and it was shown that the most sensitive modulation/demodulation format employs homodyne detection of an antipodal PSK signal. The results of the BER calculations are summarised in figure 9. It should also be noted that, although no mention has been made of more complicated modulation formats such as multi –level systems, it is possible to achieve performance improvements at the cost of added complexity.[12]

Finally it was stated that if the phase error variance of the noise in the receiver is larger than 12.5°, a 10^{-9}BER cannot be achieved. It was also shown that when coherent detection is employed the performance of the system is corrupted by the intrinsic phase noise of the laser. The final phase error variance is a function of both the linewidth of the laser sources and the bandwidth of the receiver.

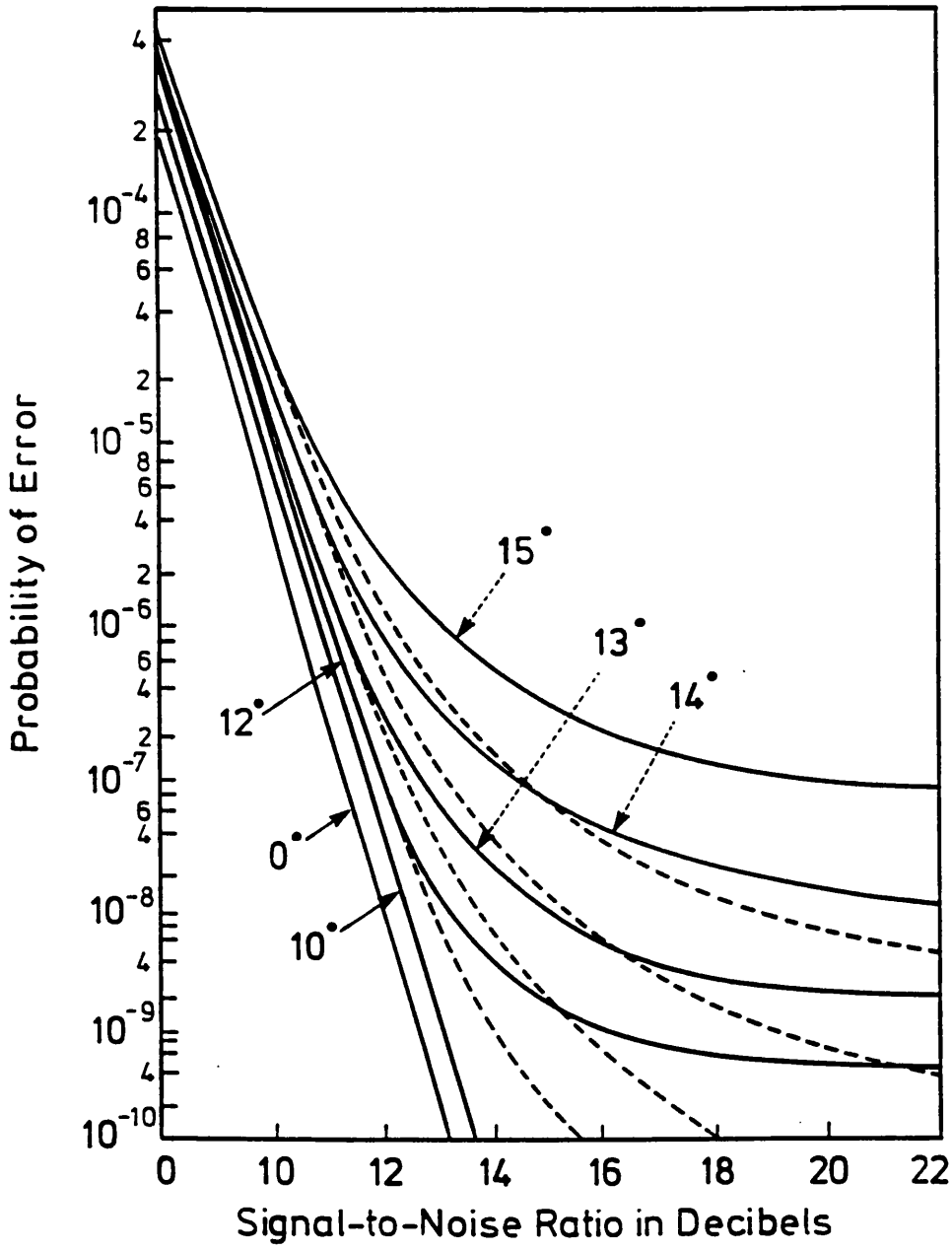

Figure 2.8 Probability of Error for Binary PSK Transmission

Solid Lines denote Tikhonov Distribution
Dashed Lines denote Gaussian Distribution
Legends denote values of σ_ϕ

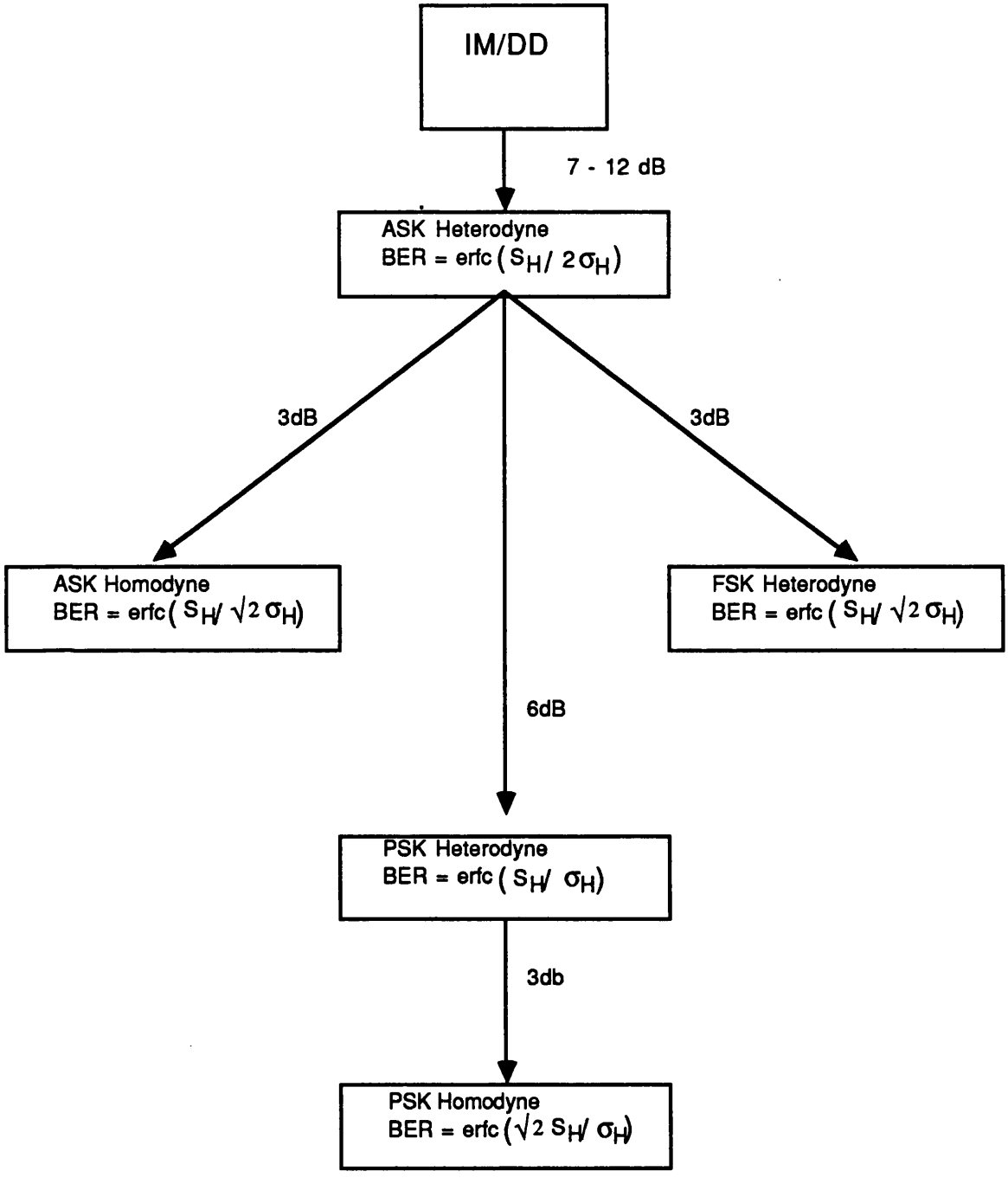

Figure 2.9 Relative Performance of Various Optical Detection Schemes

References

1. T.G. Hodgkinson, et al "Coherent Optical Fibre Transmission Systems." British Telecom Technology Journal Volume 3 No 3 July 1985.

2. T. Okoshi et al "Computation of the Bit Error Rate of Various Heterodyne and Coherent Type Optical Communication Schemes." Journal of Optical Communication Vol. 2(3) 1983. pp89– 96

3. Y. Yammamoto "Receiver Performance Evaluation of Various Digital Optical Modulation – Demodulation Systems in the 0.5 – 10μm Wavelength Region." IEEE J. Quant. Elec. 16(11) 1980 pp1251 – 1259

4. S. Saito et al "S/N and Error Rate Evaluation for anOptical FSK Heterodyne Detection System using Semiconductor Lasers." IEEE J. Quant. Elec. 19(2) 1983 PP 180 –193

5. L.G. Kazovsky "Optical Heterodyning vs Optical Homodyning: A Comparison." J. Opt. Comm. vol 6(1985) No 1 pp 18 –24

6. K. Kikuchi et al "Degradation of Bit Error Rate in Coherent Optical Communications Due to the Spectral Spread of the Transmitter and the Local Oscillator." J. Lightwave Tech. 2(6), 1984 pp 1024 – 1033

7. J. Franze "Evaluation of the Probability Density Function and Bit Error Rate in Coherent Optical Transmission Systems Including Laser Phase Noise and Gaussian Additive Noise." J. Opt. Comm. 6(2) 1985 pp51 – 57

8. B.Glance "Performance of Homodyne Detection of Binary PSK Optical Signals." J. Lightwave Tech. 4(2) 1986 pp228 – 235

9. V.K.Prabhu "PSK Performance with Imperfect Carrier Phase Recovery" IEEE Transactions on Aero and Elect. Syst. vol AES 12(2) 1976 pp275 – 286

10. F.G. Stremmler "Introduction to Communication Systems" 2nd ed Addison – Wesely Inc. 1982

11. J. Gowar "Optical Communication Systems" 1st ed Prentice Hall 1984.

12. W.C. Michie "Carrier Phase Recovery for Coherent Optical Transmission Systems" Phd Thesis Dept of Elec. Eng. Glasgow University 1989

CHAPTER 3

3.1 INTRODUCTION

From chapter 2 it should be clear that the most sensitive optical binary modulation/demodulation scheme is one which employs bipolar PSK homodyne detection. Such a receiver has many important advantages but unfortunately is extremely difficult to implement. The major difficulty is that a homodyne receiver must incorporate a local oscillator which is phase locked to the received signal. The best way to achieve phase locking from a communications viewpoint is to use a phase–locked loop.

It is the purpose of this chapter to describe the operation of an Optical Phase Lock Loop. The loop performance will be discussed in terms of its phase error variance, $\sigma_{\Delta\varphi}{}^2$. An expression for $\sigma_{\Delta\varphi}{}^2$ will be derived in terms of the loop parameters and the noise sources– : phase noise and shot noise. It will be shown that the two types of noise are processed in different ways by the loop and that an optimum loop bandwidth exists, at which the effect of the noise is minimised. It will also be pointed out that if the received carrier power SNR is large, around 10dB, then $\sigma_{\Delta\phi}{}^2$ is proportional to $1/\omega_n$ where ω_n is the loop natural frequency.

Consideration will then be given to the design of a particular system and it will be shown that if the loop is to suffer no more than 1dB power penalty (0.5dB from carrier generation and 0.5dB resulting from the size of $\sigma_{\Delta\phi}{}^2$) and operate with a BER of 10^{-9}, the bit–rate–to–linewidth ratio must be at least 2000. The total system power penalty will also be calculated for the same set of parameters as used in chapter 2.

In the latter half of this chapter, consideration will be given to the effect of loop propagation delay upon loop operation. This is not a problem in microwave or electrical loops where the bandwidths are relatively small, but does become a problem in optical systems where $1/\omega_n$ is comparable to τ_D (ω_n is the loop bandwidth and τ_D is the time delay). The limits of stability are calculated in terms of $\omega_n\tau_D$

and it is shown that inclusion of τ_D in the loop analysis is necessary if the loop is to be properly understood.

3.2 OPTICAL PHASE–LOCKED LOOP

In this section the basic equations describing the operation of an optical phase–locked loop (OPLL) will be derived and then used to analyse a particular system, a pilot carrier loop. Experimental problems in implementing such a loop, eg laser mode hopping, will not be covered in this chapter. Chapter 6 will deal with experimental systems.

Figure 3.1 shows a diagram of an OPLL complete with noise sources. There are three main components in the loop– : the phase detector; the loop filter and the local oscillator. In optical systems there are no direct detectors of the laser field E(t). All detectors detect optical power, $|E(t)|^2$, thus losing all phase information. To circumvent this problem the signals from the transmitter laser and the local oscillator are superimposed before reaching the photodiode. The output of the photodiode then includes a component with a phase equal to the difference of the laser phases. The loop filter is a low pass filter which is included in the feedback arm to control the transient and dynamic behaviour of the loop. The third component is the local oscillator. In this project only semiconductor laser diodes were used as local oscillators. These devices, if biased well above threshold, can be modelled as amplitude stabilised current controlled oscillators. The frequency of the laser light changes when the bias current is changed.

There is phase noise associated with the laser signal as a result of quantum fluctuations within the diode cavity. These fluctuations are included in the model as random noise terms in the phase of the laser signal. The origin and manifestation of the phase noise is described in sections 4.6,4.7 and 4.8 in chapter 4.

3.2.1 MATHEMATICAL ANALYSIS

The analysis of loop operation is based on standard PLL theory[1,2,3].

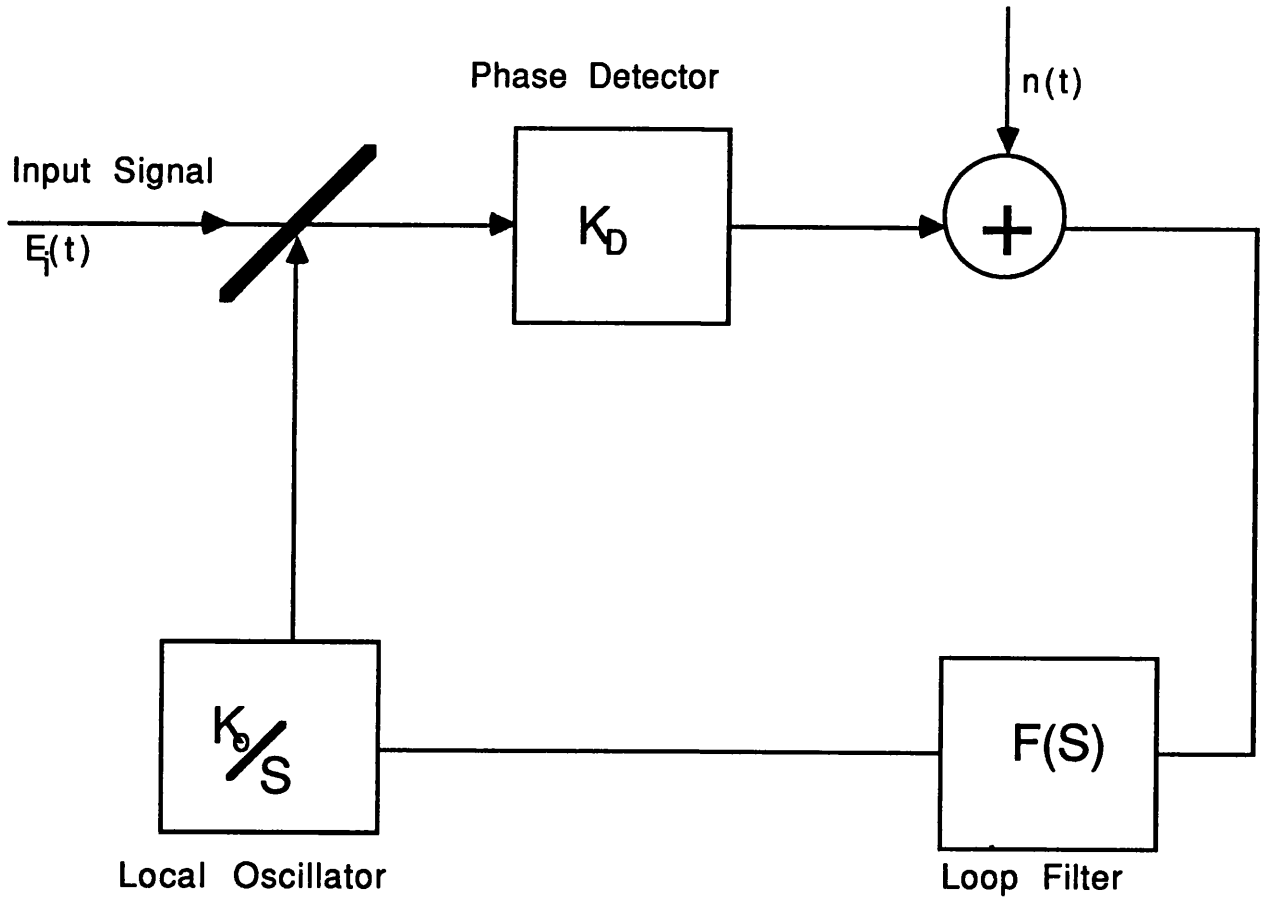

Figure 3.1. Schematic Diagram of an Optical Phase Lock Loop

The received and local oscillator signals may be written as

$$E_R(t) = E_R \exp\, i(\varphi_R(t)) \qquad 3.2.1$$

$$E_{lo}(t) = E_{lo} \exp\, i(\varphi_{lo}(t)) \qquad 3.2.2$$

where E_R and E_{lo} are the amplitudes of the received and local oscillator signals and φ_R and φ_{lo} are the phases of the respective signals. They may be expressed as:

$$\varphi_R(t) = 2\pi f_R t + \varphi_R + \varphi_{Rn}(t) \qquad 3.2.3$$

$$\varphi_{lo}(t) = 2\pi f_{lo} t + \varphi_{lo} + \varphi_{lon}(t) \qquad 3.2.4$$

where f represents frequency, φ_R and φ_{lo} are the steady state phase terms and $\varphi_{Rn}(t)$ and $\varphi_{lon}(t)$ are terms representing the laser phase noise.

The output from the phase detector, which in an OPLL is a photodiode, contains a term which depends upon the phase/frequency difference between the two signals. It is assumed in this analysis that the loop is locked and so the signals are at the same frequency. The output of the phase detector is then given by

$$i_D(t) = K_D \sin[\varphi_E(t)] + n(t) \qquad 3.2.5$$

where $K_D = 2R(P_{lo}P_t)^{1/2}$ is the gain of the photodiode, n(t) is the shot noise term and $\varphi_E(t)$ is the phase error

$$\varphi_E(t) = \varphi_R(t) - \varphi_{lo}(t) \qquad 3.2.6$$

If the loop is locked then one can linearise equation 3.2.5 using the small angle approximation $\varphi_E \simeq \sin(\varphi_E)$ for small φ_E.

The rate of change of the local oscillator phase is

$$\dot{\varphi}_{lo}(t) = 2\pi(f_{lo} + K_{lo} v_f(t)) + \varphi_{lon}(t) \qquad 3.2.7$$

where K_{lo} (HzA^{-1})is the gain of the local oscillator and $i_f(t)$ is the feedback control signal given by

$$i_f(t) = i_D(t) \oplus f(t) \qquad 3.2.8$$

where f(t) is the impulse response of the loop filter and $\oplus$ is the symbol representing the convolution product.

The rate of change of the phase error can be expressed as:

$$\dot{\varphi}_E(t) = -2\pi K_{1o} i_f(t) + \dot{\varphi}_{En}(t) \qquad 3.2.9$$

where $\varphi_{En}(t)$ is the sum of the phase noise terms.

At this point in the analysis it is convenient to transfer to the Laplace domain. The last equation may now be rewritten as:

$$s\varphi_E(s) = 2\pi K_{1o} I_f(s) + s\varphi_{En}(s)$$

$$= 2\pi K_{1o} F(s)(K_D \varphi_E(s) + N(s)) + s\varphi_{En}(s) \qquad 3.2.10$$

where s is equivalent to $j\omega$ in the frequency domain. φ_E may now be written as

$$\varphi_E(s) = \frac{1}{K_D} \frac{2\pi K_{1o} K_D F(s)}{(s + 2\pi K_{1o} K_D F(s))} N(S) + \frac{s}{s + 2\pi K_{1o} K_D F(s)} \varphi_{En}(s) \qquad 3.2.11$$

which can be rewritten as

$$\varphi_E(s) = \frac{1}{K_D} H(s) N(s) + (1 - H(s)) \varphi_{En}(s) \qquad 3.2.12$$

where H(s) is defined as the loop transfer function for the complete PLL system.

3.2.2 STATISTICAL REPRESENTATION OF THE NOISE SOURCES

Before an expression for the loop phase error variance is derived it is necessary to specify the statistical nature of the noise sources involved. It has been shown experimentally that, to a first approximation, the laser frequency noise is typically of the form shown in Figure 3.2.

There are three distinct regions. The first is the low frequency region where frequency fluctuations are primarily due to thermal effects. The resulting effect of this noise is ignored in this analysis, as its effect turns out to be small in comparison to the dominant source of phase noise, spontaneous emission[7].

The second region is spectrally flat and is caused by spontaneous

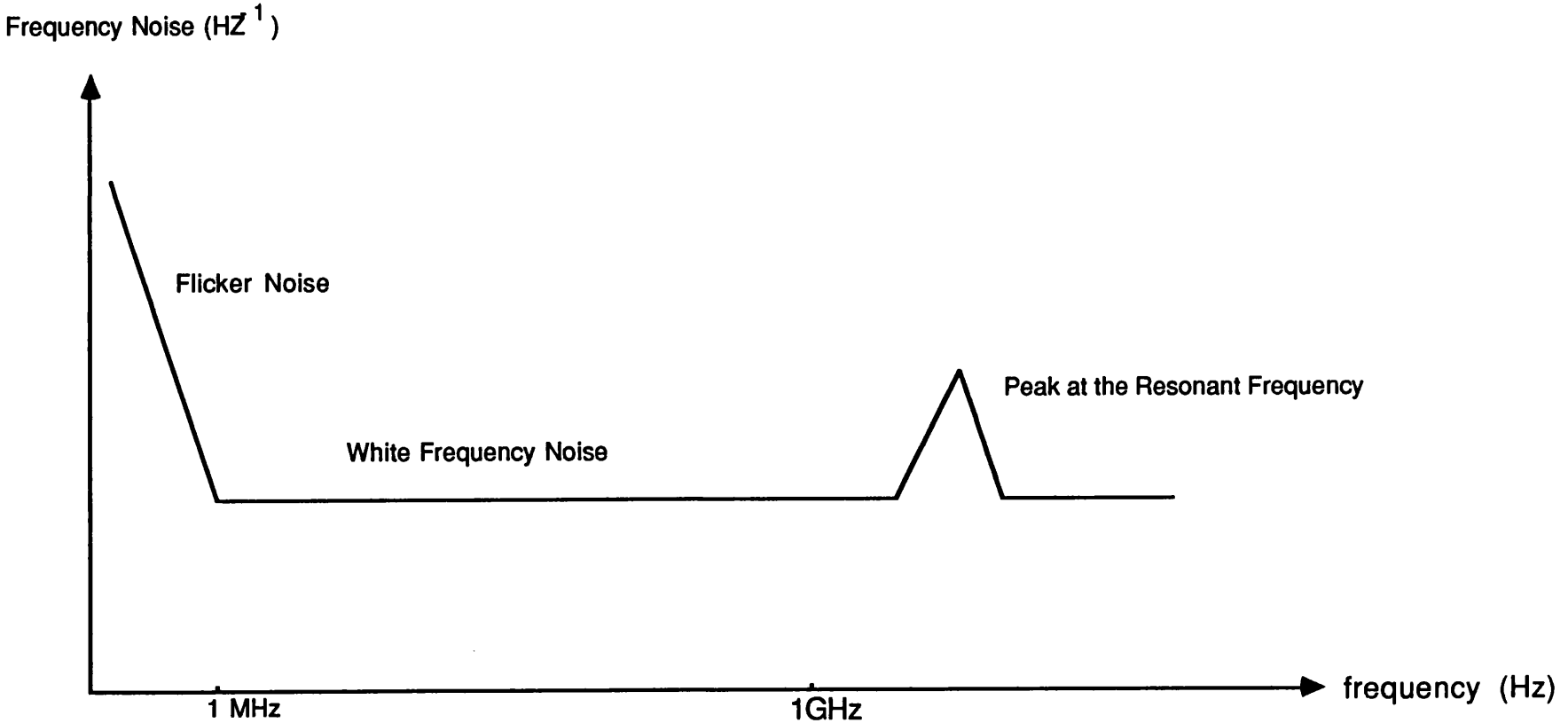

Figure 3.2. Laser Frequency Noise Spectrum

emission events. The origin and manifestation of this noise is discussed in chapter 4. It is also shown there that it is these spontaneous emission events which give rise to the Lorentzian lineshape of the laser

The third part of the frequency noise spectrum is the high frequency peak. This peak is a result of relaxation oscillations within the laser cavity. In a well designed system the frequency of this oscillation is always much greater than the bandwidth of the receiver and so it can be ignored.

The phase noise of the laser is related to the frequency noise by the following identity[6,8,9].

$$S_{\Delta\varphi\tau}(f) = \frac{S_{\varphi}}{2\pi f^2} \qquad 3.2.13$$

where S_{φ} is the power spectral density of the frequency noise. For a laser with a Lorentzian lineshape, and hence a flat frequency noise spectrum, the magnitude of S_{φ} is equal to the FWHM of the power spectrum of the laser diode.

The current spectral density of the shot noise is[7,8,9]

$$S_{sh}(f) = eRP_{lo} \qquad 3.2.14$$

where e is the electron charge
R is the responsivity of the diode
P_{lo} is the local oscillator power

The noise sources are assumed to be statistically independent. Under this and previous assumptions it is possible to evaluate the phase error variance of the OPLL. The phase error variance is the Fourier Transform of the power spectral density of the phase error, that is the Fourier Transform of φ_E as given by equation 3.2.12.

$$\sigma_{\Phi}^2 = \frac{1}{K_D}2\int_{-\infty}^{\infty}|H(s)|^2 S_{sh}df + \int_{-\infty}^{\infty}|1 - H(s)|^2 S_{\varphi}df \qquad 3.2.15$$

where S_N and S_{φ} are the power spectral densities of the shot noise

and phase noise processes.

3.2.2 CHOICE OF LOOP FILTER

The loop transfer function H(s) is dependent upon the choice of the loop filter. The most common choice of filter in microwave systems is the lead lag filter

$$F(s) = \frac{1 + \tau_2 s}{\tau_1 s} \qquad 3.2.16$$

where τ_1 and τ_2 are the time constants of the filter shown in Figure 3.3. Substituting F(s) as given by 3.2.16 into the expression for H(s) gives

$$H(s) = \frac{\omega_n^2 + 2\zeta\omega_n s}{s^2 + 2\zeta\omega_n s + \omega_n^2} \qquad 3.2.17$$

where ω_n is the loop natural frequency and ζ is the loop damping term given respectively by

$$\omega_n = \left[\frac{K_D K_{1o}}{\tau_1}\right]^{1/2} \qquad 3.2.18$$

$$\zeta = \frac{\tau_2}{2}\left[\frac{K_D K_{1o}}{\tau_1}\right] \qquad 3.2.19$$

This particular filter response was chosen as it allows ω_n, ζ and the loop gain to be varied independently. Other filters may be used[3,4].

3.2.3 CALCULATION OF $\sigma_{\Delta\varphi}^2$

Equation 3.2.15 may be solved analytically for the particular case where the loop filter transfer function is that given in equation 3.2.16, using the standard integrals given in Table 3.1.

$$\sigma_\Phi^2 = \frac{(\Delta f_R + \Delta f_{1o})\pi}{2\zeta\omega_n} + \frac{(4\zeta^2 + 1)\omega_n e}{16\zeta R P_C} \qquad 3.2.20$$

P_C in Eq 3.2.20 is the carrier power which is used for phase tracking. From this expression it is clear that the loop processes the phase

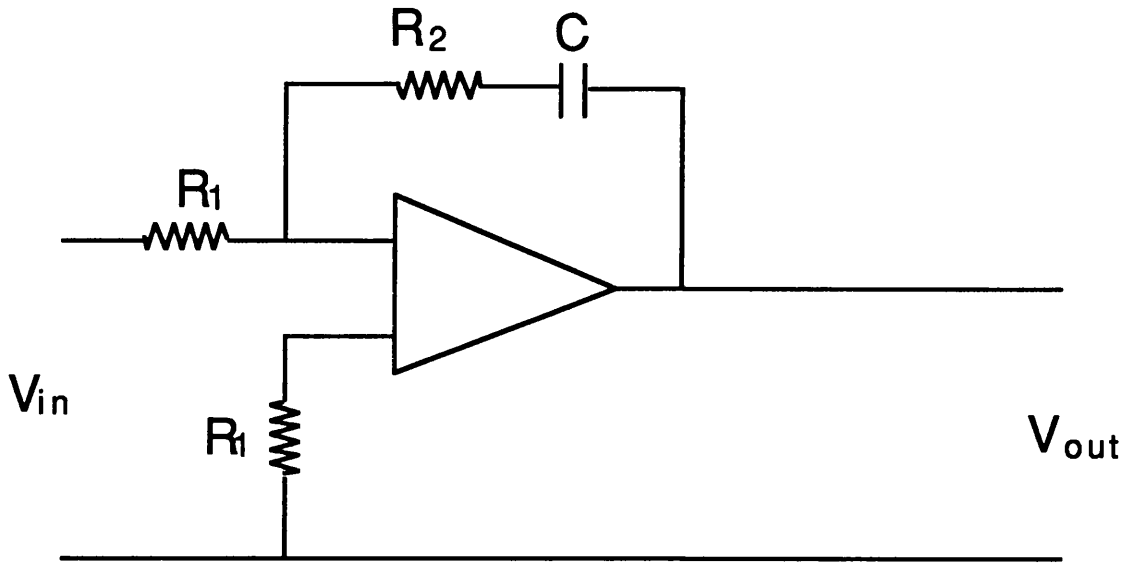

$$F = \frac{1 + S\,\tau_2}{S\,\tau_1}$$

$$\tau_1 = (R_1 + R_2)C$$

$$\tau_2 = R_2\,C$$

Figure 3.3 An Active First Order Filter

$$I_n = \frac{1}{2\pi j} \int_{-j\infty}^{j\infty} H_n(s).H_n(-s)\, ds$$

$$H_n(s) = \frac{c_0 + c_1 s + c_2 s^2 + ... + c_{n-1} s^{n-1}}{d_0 + d_1 s + d_2 s^2 + ... + d_{n-1} s^{n-1}}$$

$$I_1 = \frac{c_0^2}{2.d_0.d_1} \qquad I_2 = \frac{c_0^2.d_2 + c_1^2.d_0}{2.d_0.d_1.d_2}$$

$$I_3 = \frac{c_2^2.d_0.d_1 + (c_1^2 - 2.c_0.c_2)d_0.d_2 + c_0^2.d_2.d_3}{2.d_0.d_3.(d_1.d_2 - d_0.d_3)}$$

Table 3.1 Table of Integral Solutions

noise ($\Delta f_R + \Delta f_{lo}$) and the shot noise differently. The equation suggests that if the pilot carrier to shot noise ratio is large then $\sigma_{\Delta\varphi}^2$ is inversely proportional to ω_n. In practical systems this would not be the case as the power penalty would be rather large. It also suggests that there is an optimum loop bandwidth at which point the effect of the noise is minimised. Figure 4 shows a plot of $\sigma_{\Delta\varphi}^2$ against ω_n with Δf = 1MHz. The optimum bandwidth is calculated by differentiating $\sigma_{\Delta\varphi}^2$ with respect to ω_n and setting the result equal to zero. This gives

$$\omega_{nopt} = \left[\frac{8P_C R\pi . \Delta f}{e(4\zeta^2 + 1)}\right]^{1/2} \qquad 3.2.21$$

which if substituted back into 3.2.20 gives an expression for the minimum phase error variance

$$\sigma_{\Delta\varphi min}^2 = \left[\frac{(4\zeta^2 + 1)e\pi . \Delta f}{8\zeta^2 RP_C}\right]^{1/2} \qquad 3.2.22$$

The natural frequency and the 3dB bandwidth are related by

$$\omega_{3dB} = \omega_n[\, 2\zeta^2 + 1 + ((2\zeta^2 + 1)^{1/2} + 1)^{1/2}]^{1/2} \qquad 3.2.23$$

This shows that increasing the damping factor increases the loop bandwidth. This however will also result in the loop having a poorer response to step changes[3].

Gardner has also empirically evaluated the pull out range for a loop with a sinusoidal phase detector. This can be written as

$$\Delta\omega_{po} = 1.8\omega_n(\zeta + 1) \qquad 3.2.24$$

For frequency steps greater than $\Delta\omega_{po}$ the loop will lose lock.

3.3 DESIGN CONSIDERATIONS

At this point in the chapter, it is useful to consider how a design engineer might go about building a coherent optical receiver given

Figure 3.4 Phase Error Variance vS. Loop Bandwidth
Beat Linewidth 1 MHz

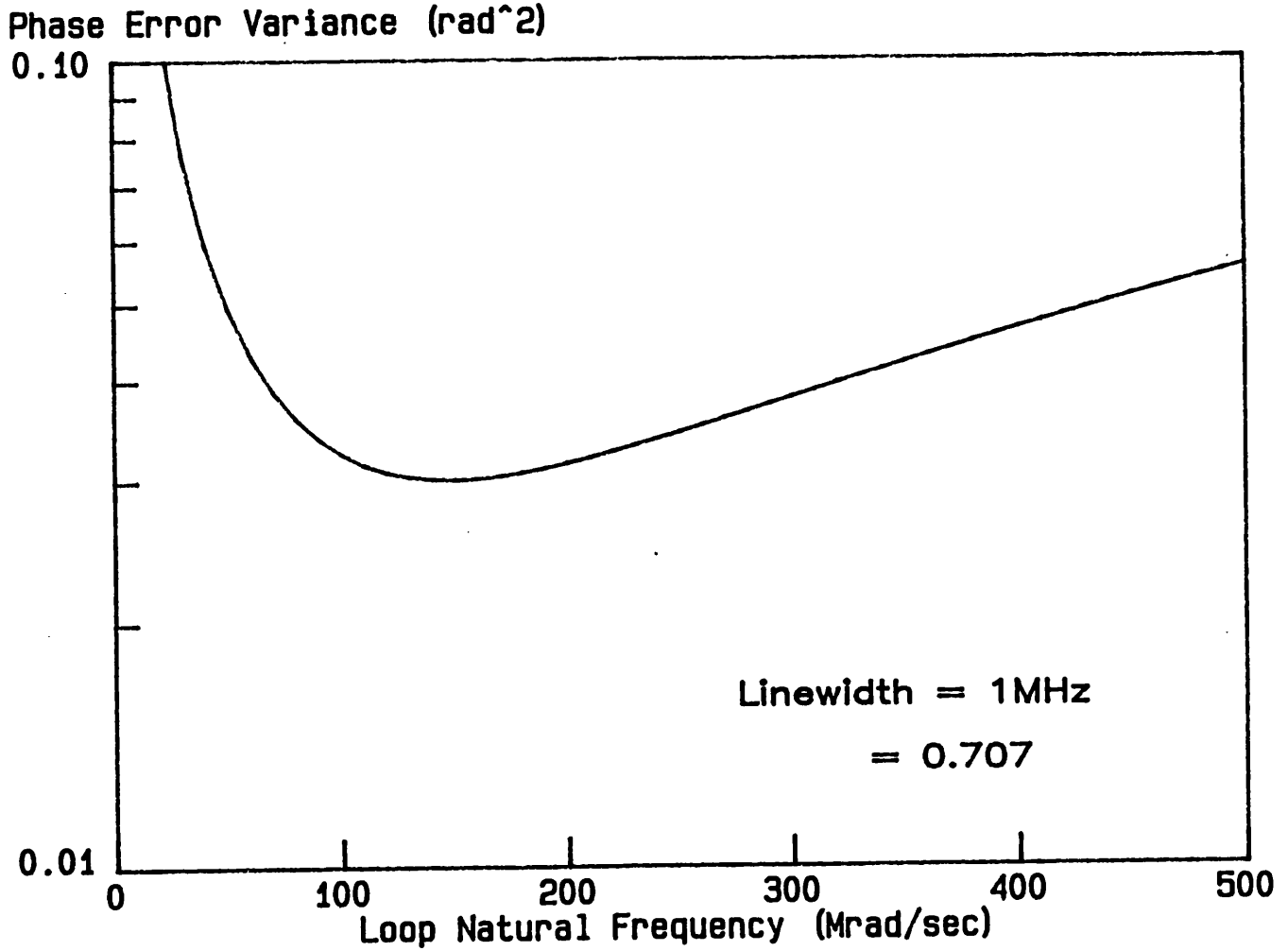

certain operating limits.

3.3.1 DESIGN EXAMPLE 1

If a system is designed to operate with a BER of 10^{-9} and with a total power penalty of only 1dB, 1/2dB as a result of carrier generation and 1/2dB due to the phase error variance, then it is possible to determine the minimum bit-rate to linewidth ratio permissible. To calculate this bit-rate an expression for $\sigma_{\Delta\varphi}^2$ in terms of f_B must be obtained.

In a pilot carrier system some of the optical power is transmitted at the carrier frequency, so that the OPLL has a signal to lock onto and track. Following the notation of Hodgkinson[7] the total received optical power can be written in terms of the theoretical receiver sensitivity as defined in chapter 2. For a PSK system P_{theory} is given by

$$P_{theory} = \frac{eQ^2 f_B}{4R} \qquad 3.3.1$$

and

$$P_T = K_S(K_C + 1)P_{theory} \qquad 3.3.2$$

$$K_S \geq 1 \quad \text{and} \quad K_C \geq 0$$

where P_T is the total power transmitted,S and C refer to signal and carrier powers respectively and so the carrier power may therefore be written as

$$P_C = K_C K_S \frac{eQ^2 f_B}{4R} \qquad 3.3.3$$

where Q is the normalised Gaussian variable. Substituting Eq 3.3.3 into Eq 3.2.22 gives

$$\sigma_{\Delta\varphi}^2 = \left[\frac{(4\zeta^2 + 1)\pi.\Delta f}{2\zeta^2 Q^2 f_B K_C K_S}\right]^{1/2} \qquad 3.3.4$$

It is clear from the last equation and from published curves[10] that for the system to suffer 0.5dB penalty, ie $\sigma_{\Delta\varphi}^2 = 0.03\text{rads}^2$, while

maintaining a 10^{-9} BER then:

$$\frac{f_B}{\Delta f} \geq 2000 \qquad 3.3.5$$

This expression is the justification for assuming that $\cos(\Delta\varphi(t))$ is quasi constant over the bit period when calculating the effect of phase noise upon the BER of a PSK detector in section 2.9.

3.3.2 DESIGN EXAMPLE 2

Alternatively one may be concerned with the total power penalty in a practical system if the bit rate is specified and the linewidth of the optical source is known. If the system operates with P_{data} 1dB away from the theoretical receiver sensitivity, 0.5dB as a result of the phase error variance and 0.5dB from polarisation mismatch at the receiver, then the total power penalty may be derived as follows. The total power transmitted is

$$P_T = P_{data} + P_{carrier} \qquad 3.3.6$$

For this example the same parameters will be used as in section 2.2. The laser linewidth is taken as 1MHz. The carrier power can be calculated from equation 3.2.22 since it is known that $\sigma_{\Delta\varphi}^2 = 0.03\text{rads}^2$ for 0.5dB power penalty at 10^{-9} BER. This results in $P_C = -63.0\text{dBm}$. The total power penalty is defined as:

$$\text{Power Penalty} = P_T - P_{theory} = 2.5\text{dB} \qquad 3.3.7$$

The optimum loop bandwidth may now be calculated by substituting the value for P_C into equation 3.2.21.

$$\omega_{nopt} = 148\text{Mrads/s} \qquad 3.3.8$$

It is useful at this point to calculate the power penalty and optimum bandwidth for loops where the linewidth of the beat signal is 15MHz, which corresponds to a system where two free running HLP1400 laser diodes are used and 100kHz is the beat linewidth which may be expected from two line-narrowed laser modules, see chapter 5. The results for both of these systems are displayed in table 3.2.

The results show the effect of laser phase noise upon a coherent

Linewidth	δf_{TOT}= 20kHz	δf_{TOT}= 1MHz	δf_{TOT}=15MHz
P_{DATA}	-59.2dBm	-59.2dBm	-59.2dBm
P_T	-59.16dBm	-57.7dBm	-50.7dBm
$\omega_{n\ opt}$	2.96Mrad/sec	148 Mrad/sec	2.22 Grad/sec
Total System Power Penalty	1.04 dB	2.5dB	9.5 dB

Table 3.2 Optimum Loop Parameters For Three Given Beat Linewidths

system. If the phase noise is small then the power penalty and loop bandwidths are also small. Similarly if the phase noise is large then the power penalty and loop bandwidth are also large. Although this is obvious, it is important to understand the relationship between bandwidth and phase noise of an OPLL.

In practice one cannot build a loop which is unconditionally stable if the bandwidth is large, ie $1/\omega_n$ is comparable to the propagation time around the loop. Under such circumstances, time delay has to be incorporated into the analysis used to determine loop performance.[9]

3.4 EFFECT OF FRONT END AMPLIFIER BANDWIDTH ON LOOP OPERATION

In the analysis so far the effect of the bandwidth of the front end amplifier has been ignored when determining the loop operation. It has been assumed that $B_{front\ end}$ has no effect, ie $B_{front\ end} = \infty$. This is clearly not true. In practice the bandwidth of the front end amplifier is dictated by the bit rate. $B_{front\ end} \geq f_B$. Therefore if the system has been designed so that the total power penalty is 1dB, as in design example 1, ($f_B/\Delta f \geq 2000$), then the front end bandwidth is much greater than ω_{nopt}. Under these circumstances the penalty introduced by incorporating $B_{front\ end}$ is negligble. It is only in systems where ω_n is comparable to $1/f_B$ that a significant change in loop performance will be observed. It has been shown[11] that provided $B_{front\ end} \geq 6\omega_n$ the power penalty introduced will be less than 1dB.

3.5 EFFECT OF PROPAGATION TIME DELAY UPON THE PERFORMANCE OF AN OPLL

This section will analyse a loop model which incorporates propagation delay within it. The section will start by deriving the loop transfer function. The stability criteria will then be evaluated in terms of the loop bandwidth and the time delay. The phase error variance will be expressed in terms of the new transfer function . Unfortunately there

is no simple analytical solution to the expression for $\sigma_{\Delta\varphi}^2$ and so the two integrals, the shot noise integral and the phase noise integral, are calculated numerically. All the assumptions that were made are given and the integration technique explained. The rest of the section is devoted to analysing the effect of the size of τ_d upon the loop operation.

3.5.1 OPLL MODEL INCORPORATING TIME DELAY

Time delay in the Laplace Domain is expressed as $e^{-s\tau}$. This term is included in the loop model, see Figure 3.5. The loop transfer function can then be expressed as

$$H(s) = \frac{K_{LO}K_D F(s)e^{-s\tau}}{s + K_{LO}K_D F(s)e^{-s\tau}} \qquad 3.5.1$$

If the same filter is used as in section 3.2.2 then Eq 3.5.1 may be rewritten as

$$H(j\omega) = \frac{K_{LO}K_D(1 + j\omega T_2)(\cos(\omega\tau_d) - j\sin(\omega\tau_d))}{(j\omega)^2T_1 + K_{LO}K_D(1 + j\omega T_2)(\cos(\omega\tau_d) - j\sin(\omega\tau_d))} \qquad 3.5.2$$

where $e^{-s\tau}$ has been written as [$\cos(\omega\tau_d)$ − $j\sin(\omega\tau_d)$] and $s = j\omega$.

The loop transfer function can now be expressed in terms of ω_n and ζ

$$H(j\omega) = \frac{(\omega_n^2 + 2\zeta\omega_n)(\cos(\omega\tau_d) - j\sin(\omega\tau_d))}{(\omega_n^2 + 2\zeta\omega_n)(\cos(\omega\tau_d) - j\sin(\omega\tau_d)) + j\omega 2} \qquad 3.5.3$$

Before substituting this expression into equation 3.2.15 to obtain an expression for $\sigma_{\Delta\varphi}^2$ which includes the effect of time delay, it is crucial that the limits of stability are evaluated. This was not done previously as the standard second order PLL is unconditionally stable, but it is evident from expression 3.5.3 that this is not necessarily so when a finite time delay is incorporated into the transfer function.

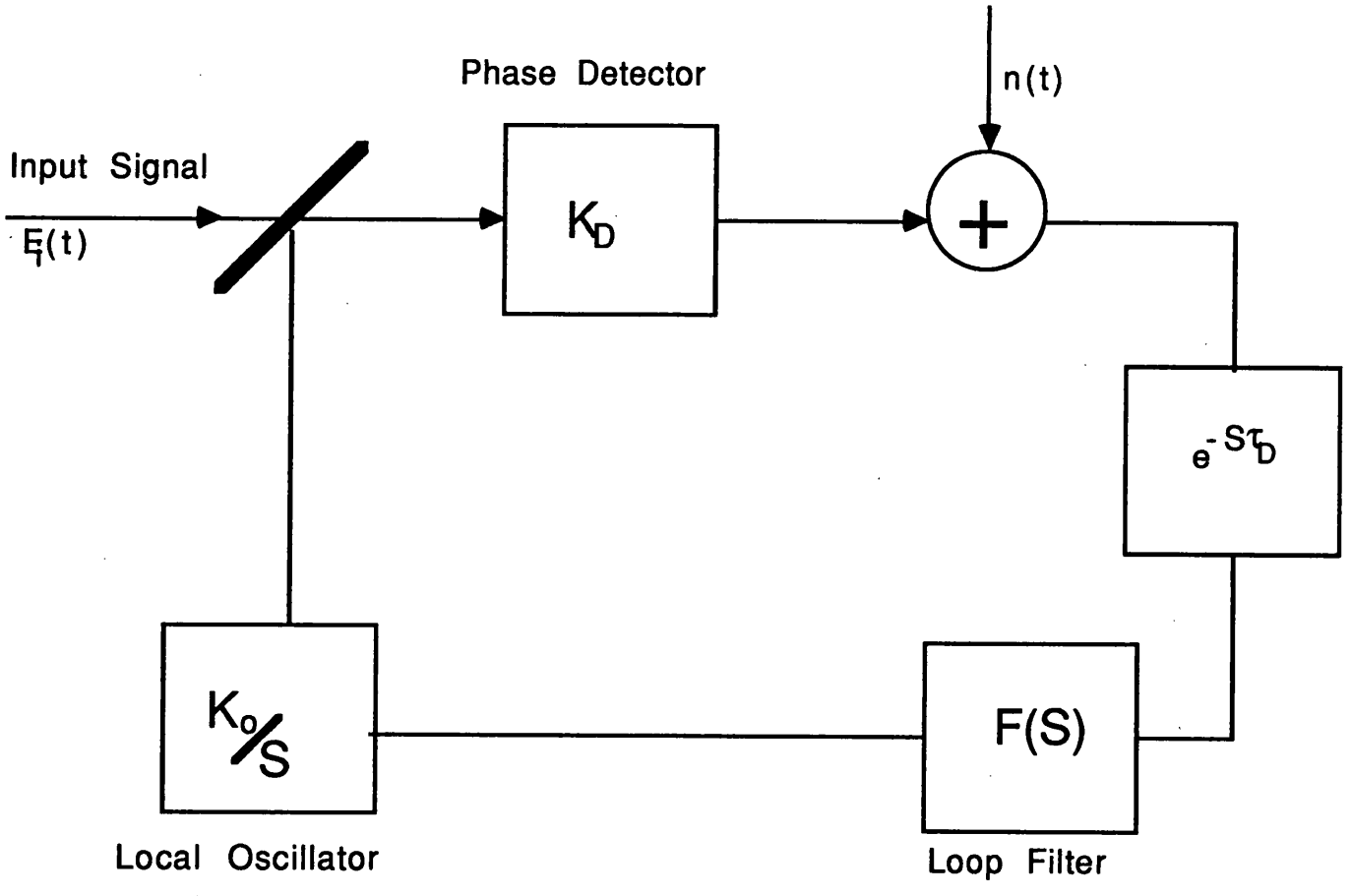

Figure 3.5. Schematic Diagram of an Optical Phase Lock Loop with Time Delay

3.5.2 LIMITS OF STABILITY

The stability criteria are easily determined using standard Nyquist Techniques. The open loop transfer function of the system is

$$G(j\omega) = \frac{\omega_n^2(1 + j\omega T_2)(\cos(\omega\tau_d) - j\sin(\omega\tau_d))}{-\omega_n^2} \qquad 3.5.4$$

The argument of this function is given by

$$\text{Arg}[G(j\omega)] = \arctan(\omega T_2) - \omega\tau_d - \pi \qquad 3.5.5$$

and the magnitude is

$$|G(j\omega)| = \omega_n^2(1 + (\omega T_2)^2)^{1/2} / \omega^2 \qquad 3.5.6$$

For the loop to remain stable it is required that when $\text{Arg}[G(j\omega)] = (2k - 1)\pi$, $k = (1,2,3 \ldots)$, the magnitude of the open loop function be less than one. The critical solution is the case where $k = 0$, giving

$$\omega\tau_d = \arctan(\omega T_2) \qquad 3.5.7$$

and

$$[\omega_n^2(1 + (\omega T_2)^2)^{1/2} / \omega^2] < 1 \qquad 3.5.8$$

These equations were solved numerically and an upper bound on the product $\omega_n\tau_d$ was found for $\zeta = 0.707$. The upper bound for absolute stability is

$$\omega_n\tau_d \leqslant 0.736 \qquad 3.5.9$$

3.5.3 NUMERICAL EVALUATION OF $\sigma_{\Delta\varphi}^2$

Substituting Eq 3.5.2 into Eq 3.2.15 gives

$$\sigma_{\Delta\varphi}^2 = \frac{e}{4RP_R}\int_{-\infty}^{\infty} \frac{\omega_n^4(1 + \omega^2T_2^2)}{\omega^4+\omega_n^4(1+\omega^2T_2^2)-2\omega^2\omega_n^2(\cos(\omega\tau_d)+\omega\tau\sin(\omega\tau_d))}d\omega$$

$$+\frac{\Delta f_{tot}}{2\pi}\int_{-\infty}^{\infty}\frac{\omega^2}{\omega^4+\omega_n^4(1+\omega^2T_2^2)-2\omega^2\omega_n^2(\cos(\omega\tau_d)+\omega\tau\sin(\tau_d))}d\omega \qquad 3.5.10$$

The author was unable to find an analytical solution to these integrals and so they were evaluated numerically.

Before any programs were written to calculate $\sigma_{\Delta\varphi}^2$, $|H(s)|^2$ was checked for continuity. It was found to be a monotonically decreasing function and so it was relatively simple to evaluate $\sigma_{\Delta\varphi}^2$. The integrations were calculated using a trapezoidal technique

$$\text{Integral} = \sum_{n=0}^{50\omega_n}\left[\frac{I_n + I_{n+1}}{2}\right]\Delta\omega \qquad 3.5.11$$

where $\Delta\omega = \omega_n/100$.

The limit of $100\omega_n$ on the sum was chosen as the value of the integrand at this point is 10^{-6} of its value at 1Mrad/s. The step size was found to be optimum for time and accuracy ,after experimenting with alternatives. The calculations were carried out on an IBM PC AT incorporating an 80287 maths co–processor.

3.5.4 ANALYSIS OF LOOP OPERATION

The effect of the propagation delay upon the loop operation will now be determined.

Figure 3.6 shows a plot of the normalised phase error variance integrals, with both the shot noise and phase noise contributions, plotted against the time delay bandwidth product. It is obvious from this graph that once $1/\tau_d$ is of the order of $0.2\omega_n$, the degradation, ie increase, of the phase error variance becomes quite severe.

The most informative way of analysing this effect is to examine what happens to ω_{nopt} as τ_d is varied. Figure 3.7, Δf = 1MHz, and Figure 3.8, Δf = 15MHz, show plots of $\sigma_{\Delta\phi}^2$ against ω_n for several different values of τ_d. It is immediately clear from these graphs that

Figure 3.6 Normalised Plot of Phase Error Variance Integrals

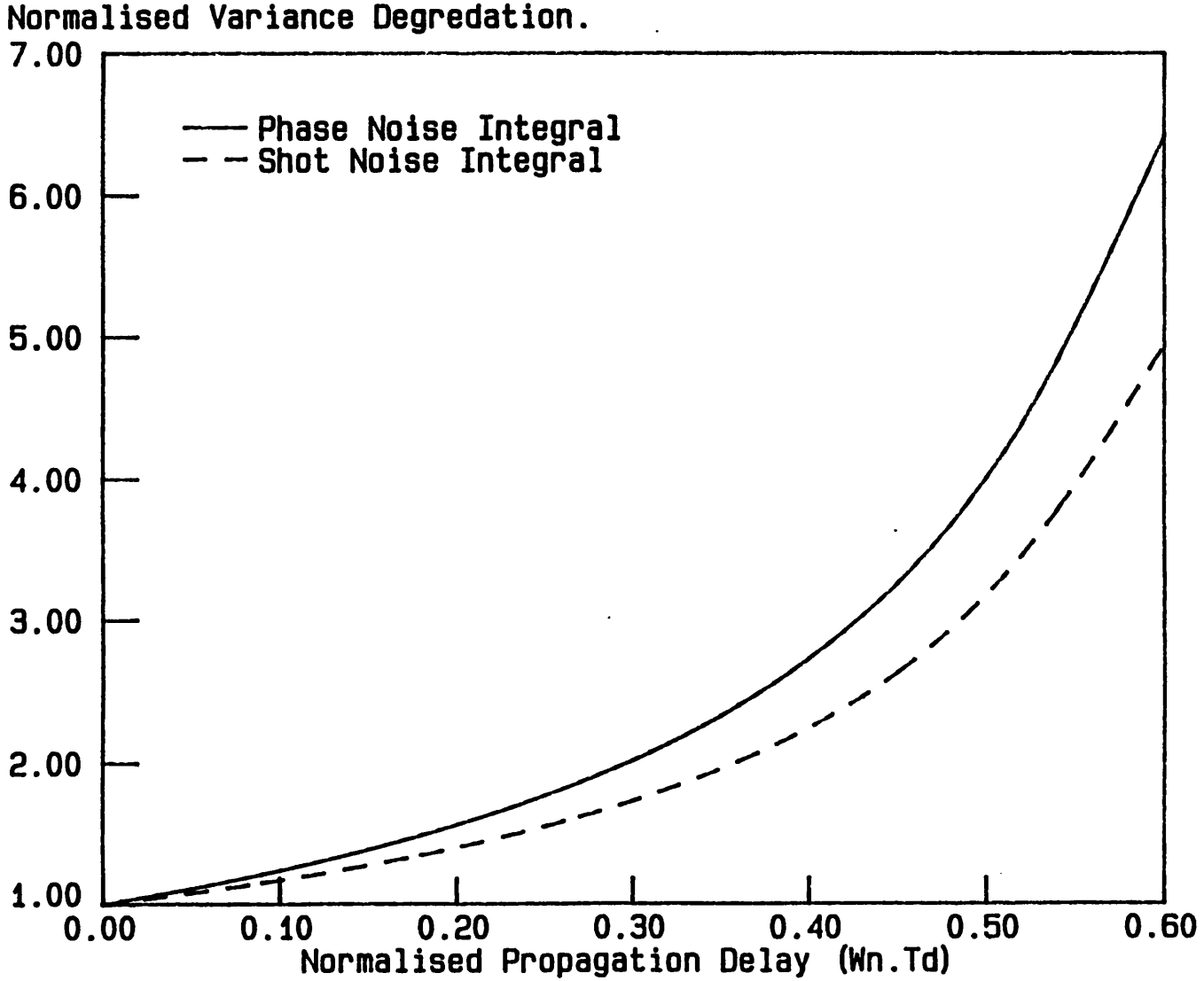

Figure 3.7 Loop Performance with a 1MHz Linewidth and Non Negligible Loop Delay

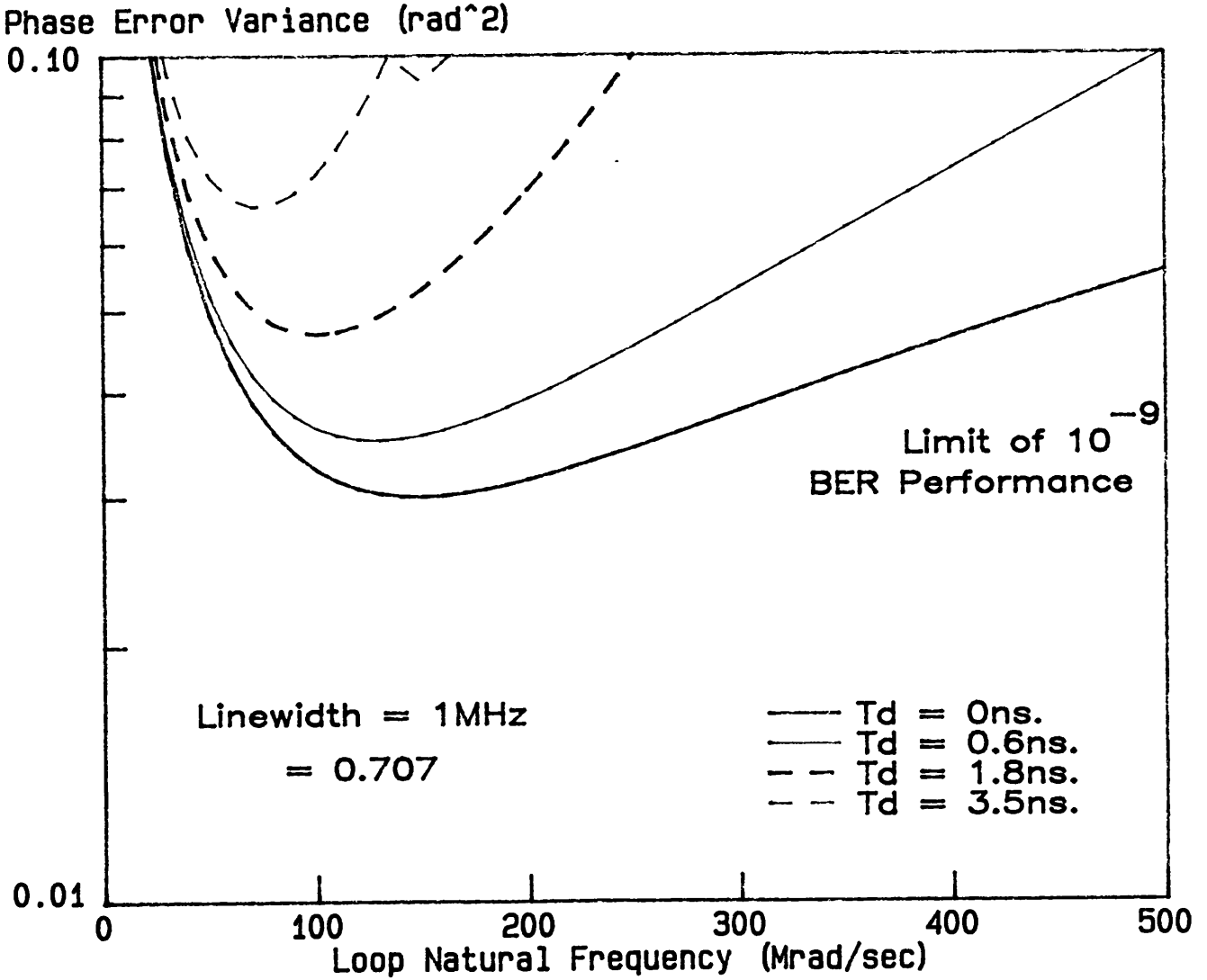

Figure 3.8 Loop Performance with a 15MHz Linewidth and Non Negligible Loop Delay

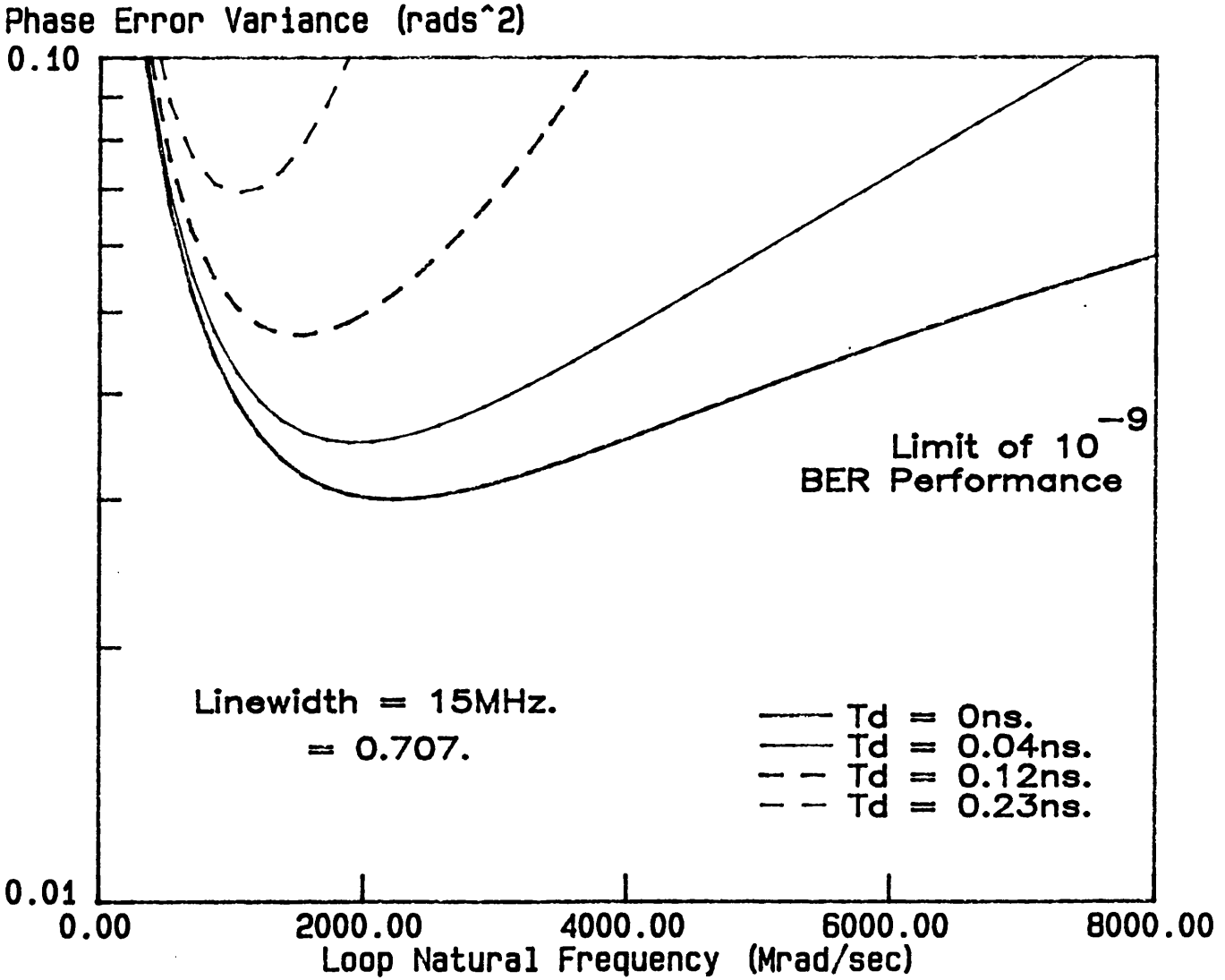

if a system is optimised for $\tau_d = 0$, ie no account is taken of τ_d, then the loop will operate with a much higher $\sigma_{\Delta\varphi}^2$ than is necessary as a result of the time delay. The optimum loop bandwidth is determined by all the loop parameters including τ_D.

3.5.5 EXAMPLE

If the system is designed as in design example 2 section 3.2.2 and τ_D is asumed to be zero, then ω_{nopt} = 148Mrads/s and $\sigma_{\Delta\varphi}^2 min$ = 0.03rads ^{2}. If it is then discovered that the loop has a propagation delay of 3.5ns $\sigma_{\Delta\varphi}^2$ will = 0.1rads^2. If the time delay had been incorporated at the design stage ω_{nopt} = 80Mrads/s and $\sigma_{\Delta\varphi}^2$ = 0.067rads^2.

Figures 9 and 10 show the locus of $\sigma_{\Delta\varphi min}^2$ against τ_d for laser linewidths of 1MHz and 15MHz respectively. Perhaps the most distressing thing from an engineering design point of view is that for a beat linewidth of 15MHz the propagation delay must be less than 0.5ns for the loop even to be capable of locking. In a system operating with two lasers of linewidth = 500kHz, the maximum allowable τ_d for stable lock is 10ns. It should be stressed that for 10^{-9}BER the allowed time delay for a 1MHz beat is around 1.5ns

This work has subsequently been developed by Norimatsu and Iwashita[13] who have evaluated the linewidth requirements of systems operating with non negligble time delays. They have shown both experimentally and theoretically that the linewidth requirement for a PSK system using homodyne detection is $\delta\nu * \tau = 2.04 * 10^{-3}$. The work by Norimatsu and Iwashita agrees well with the work presented in the earlier part of the chapter.

3.6 CONCLUSIONS

This chapter has presented an analysis of an OPLL incorporating both shot noise and laser phase noise. The operation of the loop was discussed in terms of the phase error variance. It was shown that the loop processes the two different types of noise in different ways and an expression for the optimum loop bandwidth was obtained. From

Figure 3.9 Phase Var. for Optimised OPLL.
Beat Linewidth = 1 MHz

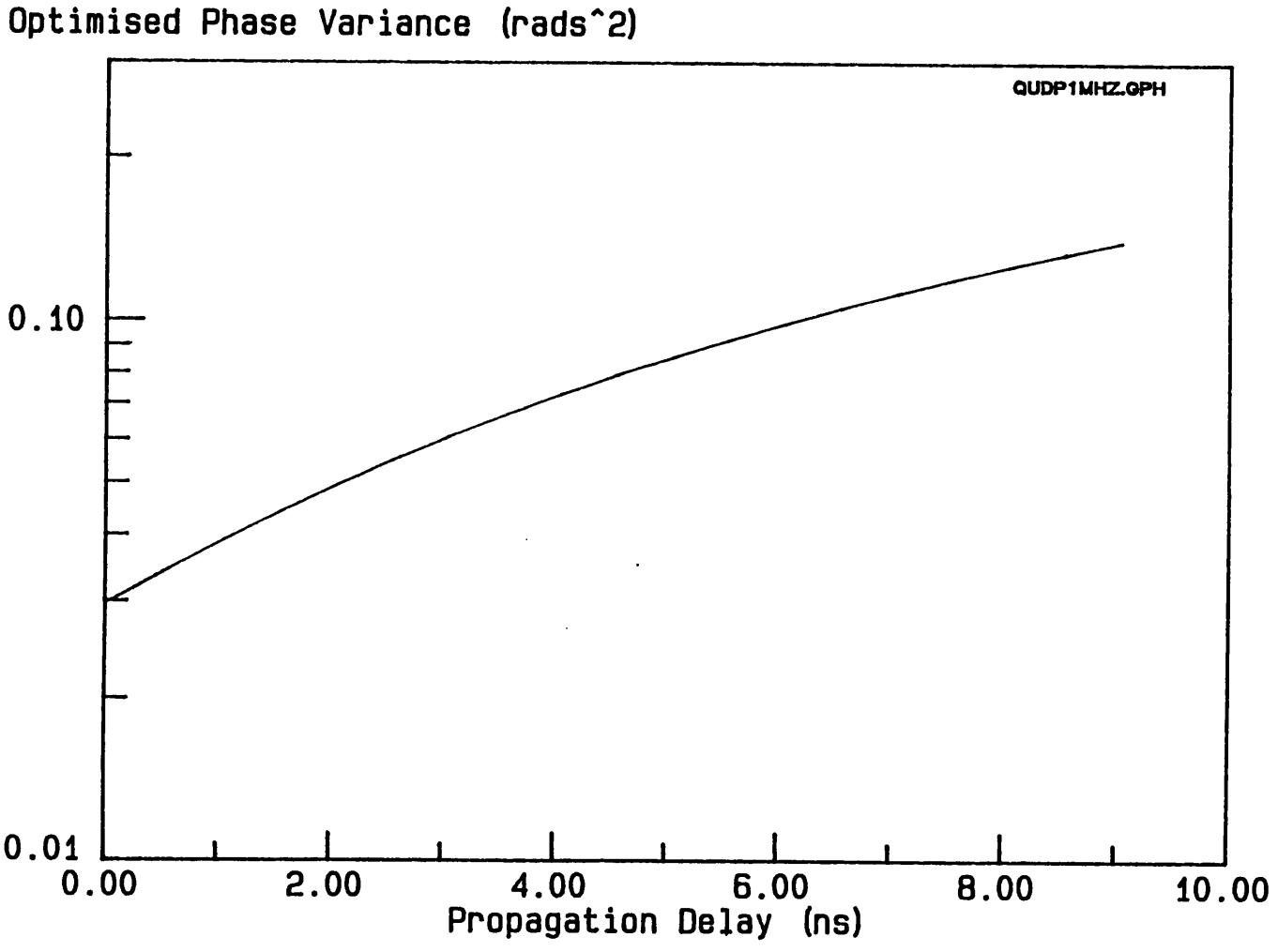

Figure 3.10 Phase Var Vs. Td for an OPLL
Beat Linewidth = 15 MHz

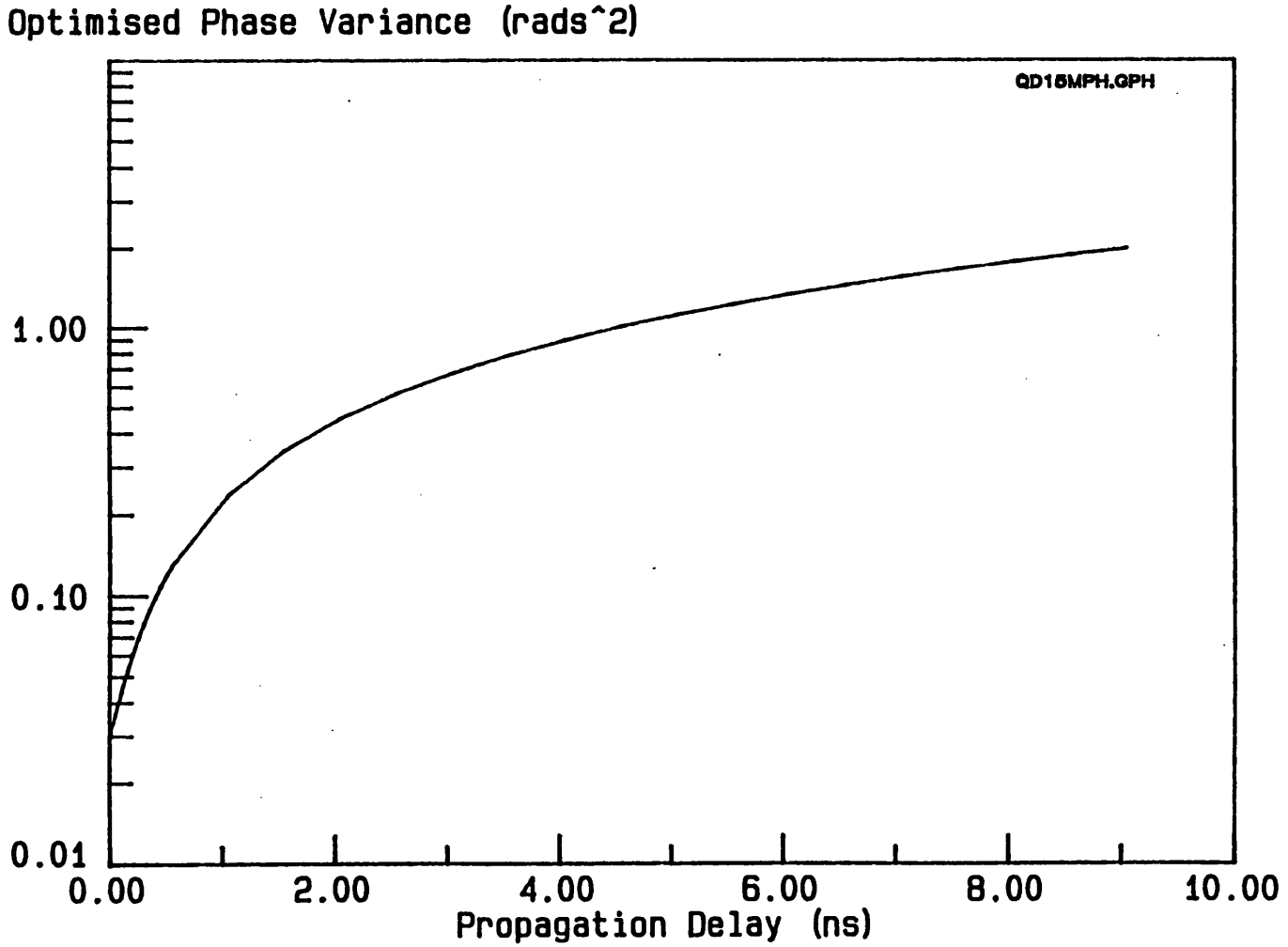

the expression for ω_{nopt} and $\sigma_{\Delta\varphi}{}^2{}_{min}$ it was shown that if the system power penalty is to be kept below 1dB then the bit rate to linewidth ratio must be of the order of 2000. It was also pointed out that in such a system it is permissible to neglect the effect of the bandwidth of the front end receiver. However if the bandwidth of the front end receiver is comparable to ω_n then the loop operation will be degraded since $\sigma_{\Delta\phi}{}^2$ is dependent upon the bandwidth of the front end receiver. It was also shown that in an optical system where the loop bandwidths are relatively large, when compared to the microwave case, that one must incorporate the loop propagation time in the analysis. If one does not incorporate τ_d the loop will not have been designed to operate at the true ω_{nopt}. The effect of the time delay upon loop operation was evaluated and it was shown that for the loop to operate stably $\omega_n\tau_d \leqslant 0.736$.

The end results of this analysis are that loop operation with Δf_{tot} = 15MHz is wholly impractical, with Δf_{tot} = 1MHz it is possible but a 10^{-9} BER will be very difficult to achieve but at Δf_{tot} = 100kHz a 10^{-9} BER should be easily achievable.

References

1. F.G. Stremmler "Introduction to Communication Systems" 2nd edition Addison– Wesely Inc. 1982

2. W.C.lindsey "Synchronous Systems in Communication and Control" Englewood Cliffs, N.J.: Prentice Hall 1972

3. F.M. Gardner "phaselock Techniques" New York: Wiley, 1979

4. A.Blanchard "Phase– Locked Loops. Application to Coherent Receiver Design." New York: Wiley 1971

5. J.J. Stiffler "Theory of Synchronous Communications" Prentice Hall Inc. 1971

6. J.B. Armor, Jr. "Phase Lock Control Considerations for Multiple, Coherently Combined Lasers" Master's Thesis, Air Force Institute of Technology, Wright Paterson Air Force Base, OH, Report GEO/EE/77D– 2 1977

7. L.G. Kazovsky "Balanced Phase– Locked Loops for Optical Homodyne Receivers: Performance Analysis, Design Considerations and Laser Linewidth Requirements" J. Lightwave Technology vol.LT– 4(2) 1986 pp 182– 194

8. T.G. Hodgkinson "Phase– Locked Loop Analysis for Pilot Carrier Coherent Optical Receivers" Electronic Letters vol. 21 1985. pp1202– 1203

9. B. Glance "Performance of Homodyne Detection of Binary PSK Optical Signals" J. Lightwave Technology 4(2) 1986 pp2228– 235

10. V.K. Prabhu "PSK Performance with Imperfect Carrier Phase Recovery" IEEE Transactions on Aero. and Elect. Syst. vol AES 12(2) 1976 pp275 – 286

11. W.C. Michie "Carrier Phase Recovery for Coherent Optical Transmission Systems" Phd. Thesis, Glasgow University 1989

12. M.A. Grant, W.C.Michie. M.J. Fletcher "The Performance of Optical Phase– Locked Loops in the Presence of Non– Negligble Loop Propagation Delay" J. Lightwave Technology vol. LT– 5(4) 1987 pp592– 597

13. S. Norimatsu and K. Iwashita "PLL Propagation Delay Time Influence on Linewidth Requirements of Optical PSK Homodyne Detection" J. Lightwave Technology 1991, LT– 9, pp 1367 – 1375

CHAPTER 4

4.1 INTRODUCTION

Although coherent optical communications systems offer many advantages over intensity modulation/direct detection systems they do place very stringent requirements upon the spectral properties of the lasers used. The lasers have to be monomode and must also have a very narrow linewidth, ideally less than 100kHz. It was shown in the previous chapter that for the system to suffer a power penalty of no more than 0.5dB due to carrier regeneration the required bit−rate−to−linewidth ratio is of the order of a few thousand for a PSK homodyne system. This ratio decreases for less sensitive modulation / demodulation formats. The linewidth required for a 565Mbit/s PSK system is therefore around 100kHz. The lasers used must also be relatively stable. To obtain a beat signal from two independent devices the frequencies have to be controlled to 10^{-7} of their absolute frequency.

Semiconductor lasers have been chosen as the most promising optical source for coherent optical communications for several reasons.

1. Low cost
2. Tunability
3. Small size
4. Reliability
5. Potential for wholly integrated receiver
6. Wavelengths which can be matched to the low loss windows in optical fibre
7. Low power consumption
8. High efficiency
9. Mature manufacturing technology

Unfortunately many of these lasers are multimode with linewidths of the order on tens of megahertz. The lasers used in this project were Hitatchi HLP 1400 laser diodes. These lasers are monomode and side mode suppression is greater than 30dB, with linewidth−power products of the order of 100MHzmW. The object of this chapter is to provide a summary of how the devices operate and how their properties arise.

The chapter then goes on to describe a full characterisation of the Hitachi HLP1400 laser diode and in doing so to point out its inadequacies as a source for coherent communication systems. Chapter 5 goes into detail on how the properties of semiconductor lasers can be improved presenting both theory and results.

4.2 SEMICONDUCTOR LASER

Unlike the situation for other lasers, the light generation process in semiconductor diodes characteristically takes place between two relatively wide distributions of energy, rather than between discrete energy levels. This results in semiconductor lasers having relatively broad gain profiles. Light is generated when electrons in the conduction band recombine with holes in the valence band and emit photons. This process is known as injection luminescence[1,2,3,4].

There are several different types of electron transition which occur between the conduction and valence bands in a semiconductor laser. Some of these transitions are not optically radiative. An electron may drop down into the valence band in several stages, emitting phonons with different wavelengths as it does so. The phonons only serve to heat up the material. Transitions of this kind hinder laser operation. The number of non– optically– radiative transitions can be reduced by using high quality material with fewer lattice defects and by putting a premium on the control of the epitaxial growth process.

There are three different electron transitions which are of interest when studying the properties of diode lasers: these are absorption, spontaneous emission and stimulated emission.

Absorption, in the most important case, takes place when a photon of energy greater than the band gap energy excites an electron from the valence band up into the conduction band, see Fig 4.1a. There is also free carrier absorption but this is not dealt with here. Spontaneous emission is a random process and is simply the emission of a photon when an electron transition takes place, see Fig 4.1b. Photons emitted in this fashion are of random phase and intensity. It will be shown later in this chapter that spontaneous emission is the major source of

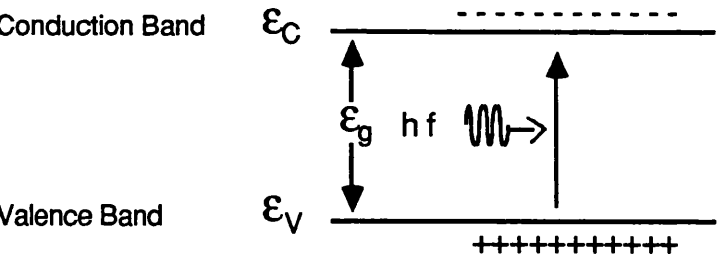

a) Absorption

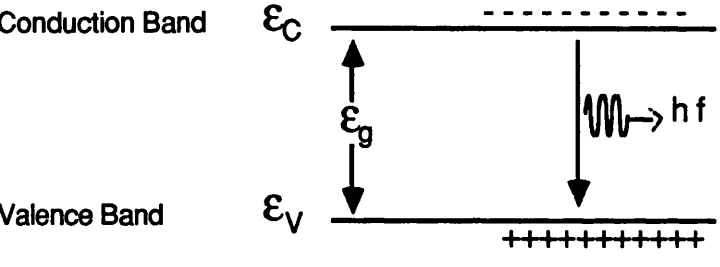

b) Spontaneous Emission

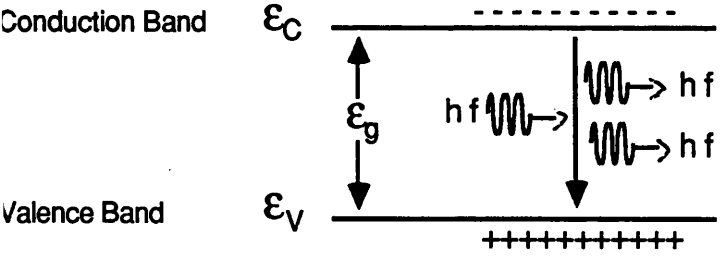

c) Stimulated Emission

Figure 4.1 Electron - Hole transistions in semiconductor material

noise in laser oscillators. The third type of transition is stimulated emission. This occurs when a photon interacts with the material in such a way as to cause an identical photon to be emitted, see Fig 4.1c. Einstein in 1917 developed relationships between the rate of stimulated emission and spontaneous emission. There will now be two photons travelling in the same direction with identical phase and intensity. It is this process which gives the laser its high degree of spectral purity. The light which is emitted has a free space wavelength given by

$$\lambda = \frac{hc}{E_c - E_v} \qquad 4.1.1$$

where h is Planks constant, c is the speed of light, E_c is the energy level of the electron in the conduction band and E_v is the energy level of the hole in the valence band measured in Joules. The theory behind the shape and the population of the energy bands within a semiconductor laser will not be described in this thesis. It is sufficient to know that electron/hole recombination takes place between two bands of energy and that the levels are dictated by Fermi–Dirac statistics and density of states theory[1,2,3].

At thermal equilibrium there will always be more electrons in the valence band than in the conduction band and so absorption dominates the emission processes. To achieve laser oscillation, a population inversion must exist, where many electrons are available in the conduction band to recombine with holes in the valence band. This condition is satisfied at the boundaries of the depletion region in a forward biased PN junction, where majority carriers are injected across the depletion region and are available to recombine within it, see Fig 4.2. When this condition is satisfied laser oscillation is possible.

The second condition which must be satisfied before lasing can take place is that there must exist some form of optical feedback mechanism to set up oscillation. In a semiconductor laser this is achieved by cleaving the material along two parallel crystal planes. The boundaries between the semiconductor material and the outside world then act as mirrors. Lasing may now take place when the

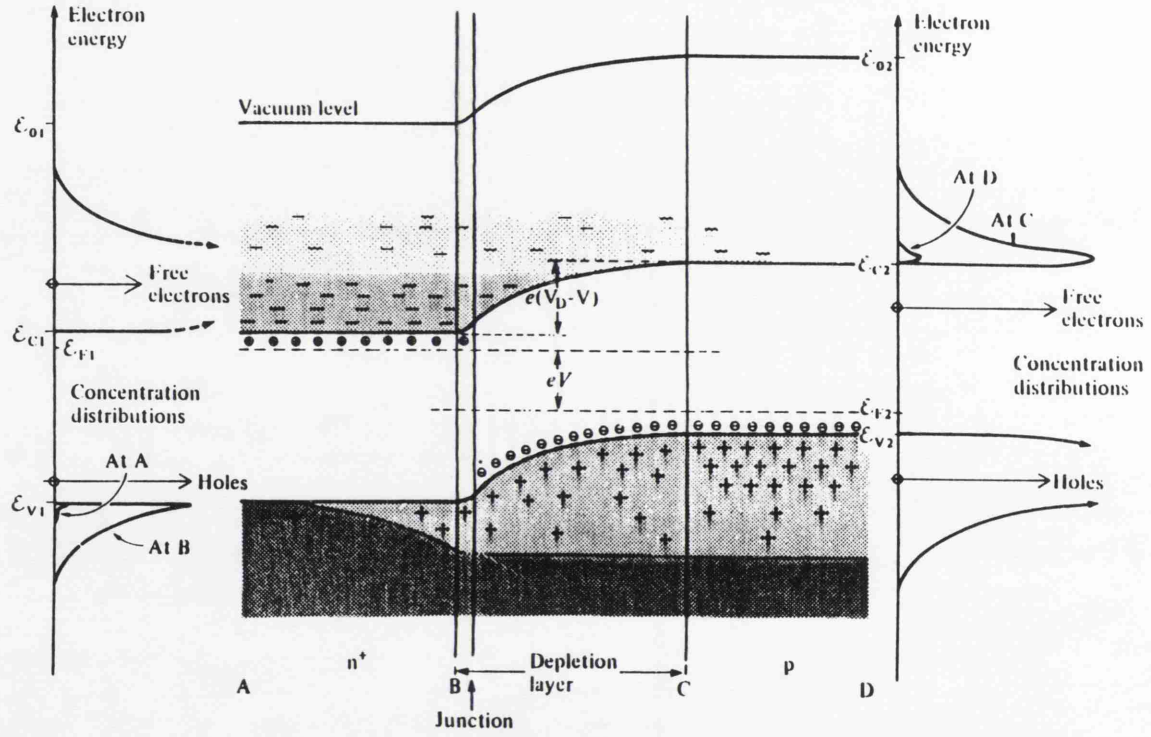

Figure 4.2 Electron energy levels across a forward-biassed n^+p junction.

Here the concentrations of free-electrons and holes in any given range of energies will vary with position because of the carrier diffusion that takes place outside the depletion layer. For electrons in the conduction band the distribution remains in quasi-equilibrium from A to C. Diffusion between C and D causes the electron concentration to fall until the equilibrium concentration distribution characteristic of the bulk material is reached. Holes remain in quasi-equilibrium from D to B. Diffusion between B and A causes the hole concentration to fall until the equilibrium concentration, p_{n0} is reached.

injection current is increased until the total gain equals the total losses. Above threshold, the power increases uniformly with current, as shown in Fig 4.3.

There are many more aspects to the theory of laser action in semiconductors: concerning the materials which can be used, the doping concentrations and theory regarding the setting up of quasi Fermi levels. These topics will not be covered here as they are not necessary for an understanding of the properties of semiconductor lasers which are of interest in the present context. For more information on semiconductor laser theory and their operation see references[1,2,3,4,5].

The above section was included in order to emphasise that the coherent light generation process takes place via transitions between two distributions of energy and not between discrete levels, that the optical resonator is firstly within the lasing material and is not formed by two external mirrors and finally that it is the injection of free carriers into the active region which allows laser oscillation to take place. These three criteria dictate to a large extent the spectral characteristics of semiconductor lasers.

4.3 PHYSICAL STRUCTURE

Most diodes in use today are double heterostructure (DH) devices as their operation is far superior to lasers which have been manufactured in only one material, single homojunction lasers. It is of benefit to state briefly the reasons for the superior operation of double heterojunction devices.

Figure 4.4 shows a schematic diagram of the physical structure of a typical channeled substrate planar (CSP) DH AlGaAs/GaAs laser diode because the Hitachi lasers used in this work were of this type.

As can be seen from the diagram, the laser is a multilayer device consisting of three layers of AlGaAs, of different compositions, and one layer of GaAs on top of a GaAs substrate. The active region is the central GaAs layer, this may even be a suitably composed AlGaAs

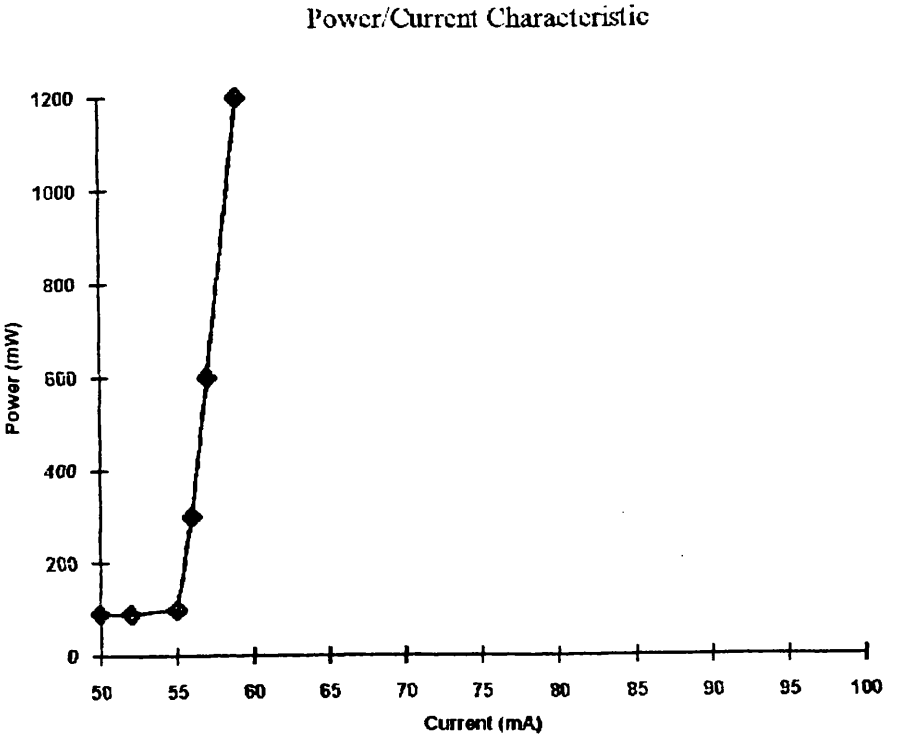

Figure 4.3 Optical Power vs Current Characteristic of a typical laser diode, Hitachi HLP1400

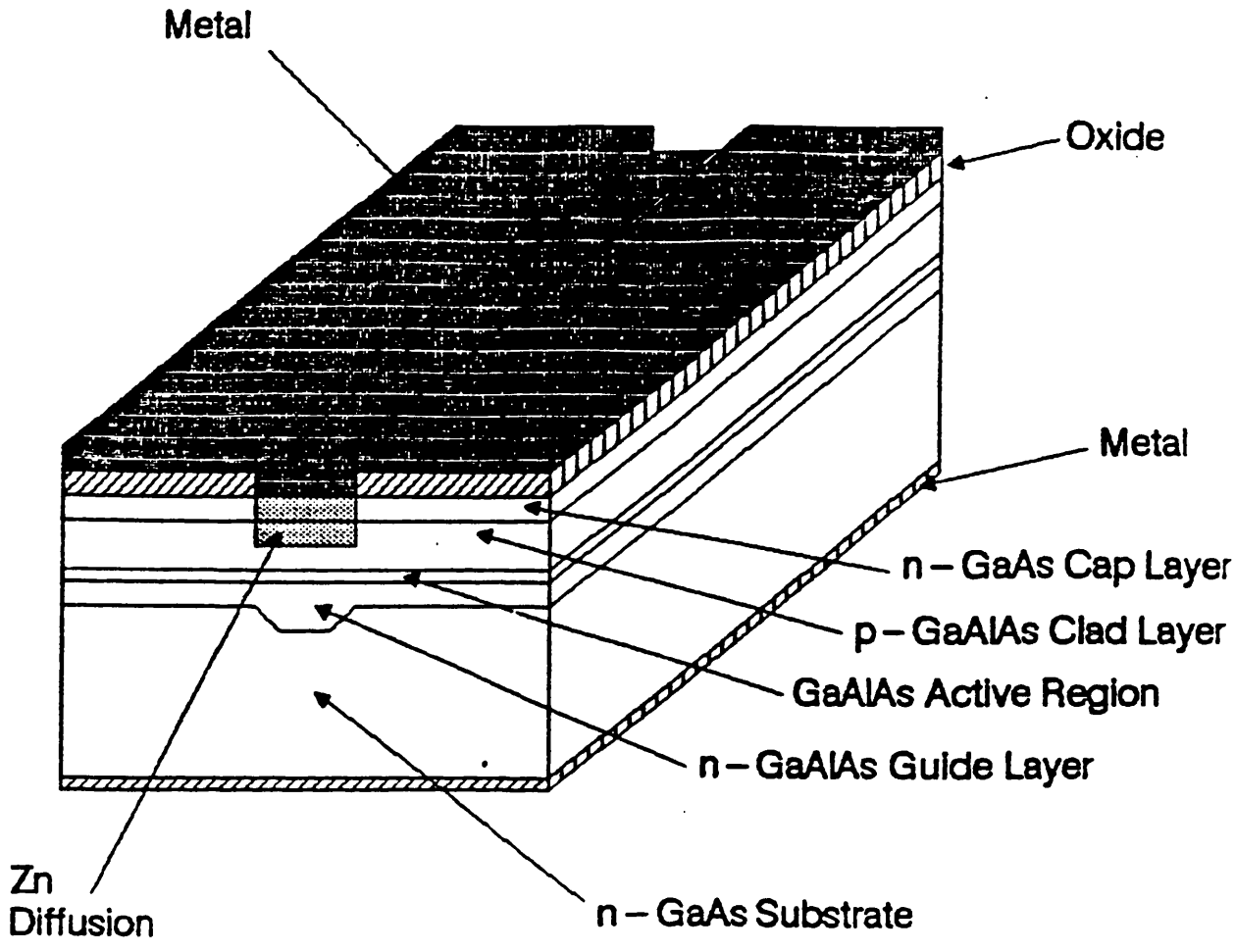

Figure 4.4 Schematic Structure of an HLP 1400 AlGaAs Semiconductor Laser Diode

layer, which is of higher refractive index and lower band gap than the two cladding layers. The higher refractive index of the active region aids laser operation by confining the light in the horizontal plane. The lower energy band gap of the active region helps to confine carriers within it as there are potential barriers set up at either side by virtue of the composition change. The current is confined laterally by the stripe metal contact on the GaAs layer. The GaAs layer is used as an ohmic contact in preference to AlGaAs because of its lower energy band gap. This information is summarised in Fig 4.5. The laser itself is a tiny device, typically 300μm long and 100–300μm broad with the substrate around 100μm thick and the cladding layers of the order of 1μm. The active region thickness is only about 0.1μm. These dimensions dictate, to a great extent, the modal properties of the device. The laser is usually mounted p–side down for thermal reasons, ie so that the junction is closer to the heatsink. A photograph of one of the diodes used in this project is shown in Fig 4.6.

4.4 FREQUENCY STABILITY, MODULATION CHARACTERISTICS AND MODAL PROPERTIES.

Semiconductor lasers have relatively large spectral gain profiles, up to 60nm, resulting from the light being generated between two distributions of energy. It is possible for the laser to oscillate over the whole range of these frequencies, given suitable circumstances. The particular mode in which the laser oscillates is determined by the cavity geometry and, in the absence of external reflections, is usually situated around the peak in the gain profile. There are many possible modes and these are separated in frequency by

$$\Delta\nu = \frac{c}{2nl} \qquad 4.4.1$$

where n is the refractive index of the active region and l is the length of the cavity. $\Delta\nu$ for an AlGaAs/GaAs diode of 300μm length is around 120GHz, and the corresponding $\Delta\lambda$ around 0.3nm. This would imply that a semiconductor laser of this size would lase with many modes present. In reality the lasers used in this project were all

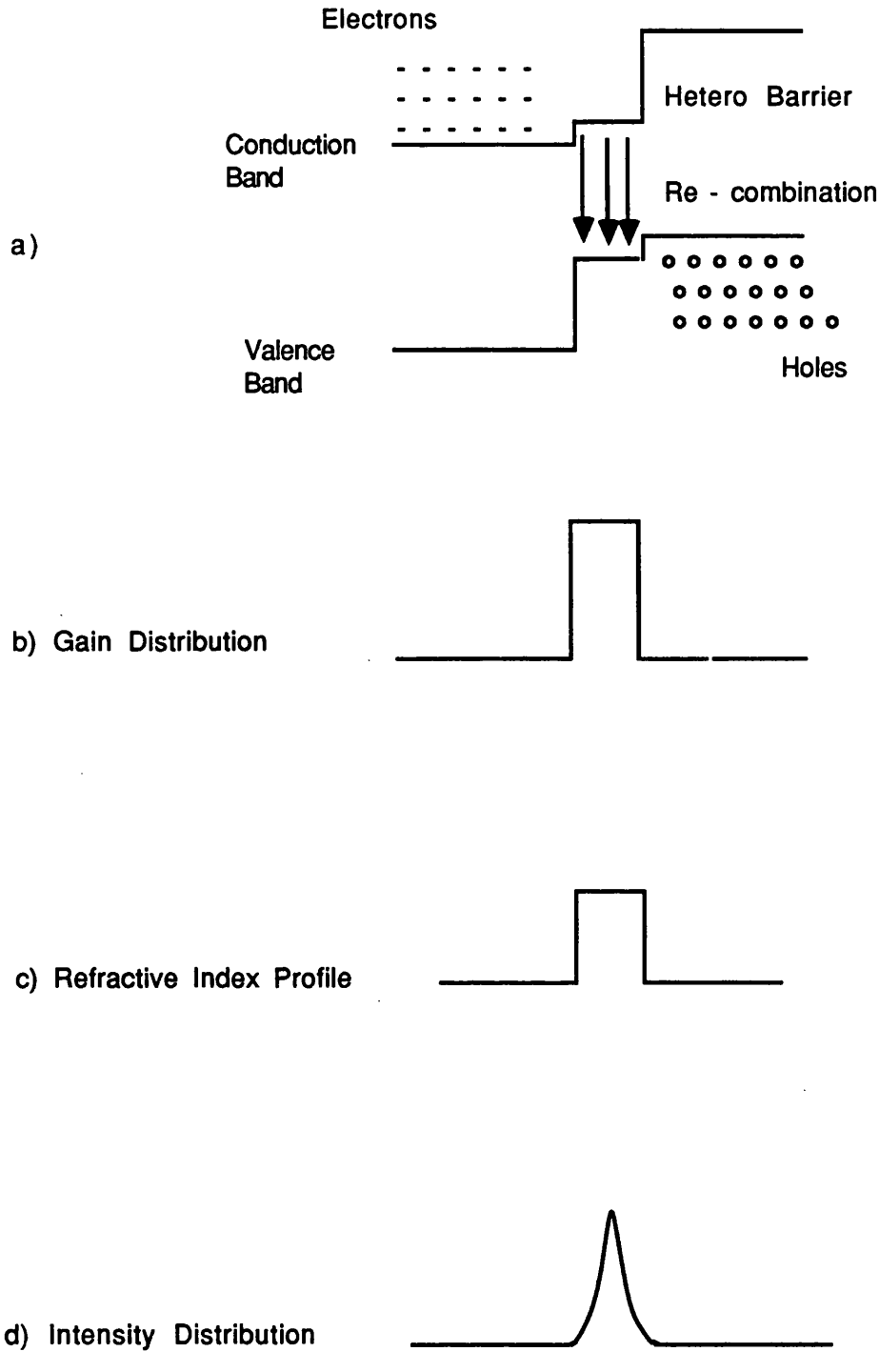

gure 4.5 The effect of a Double Hetero-Junction various properties of a Semiconductor Laser Diode

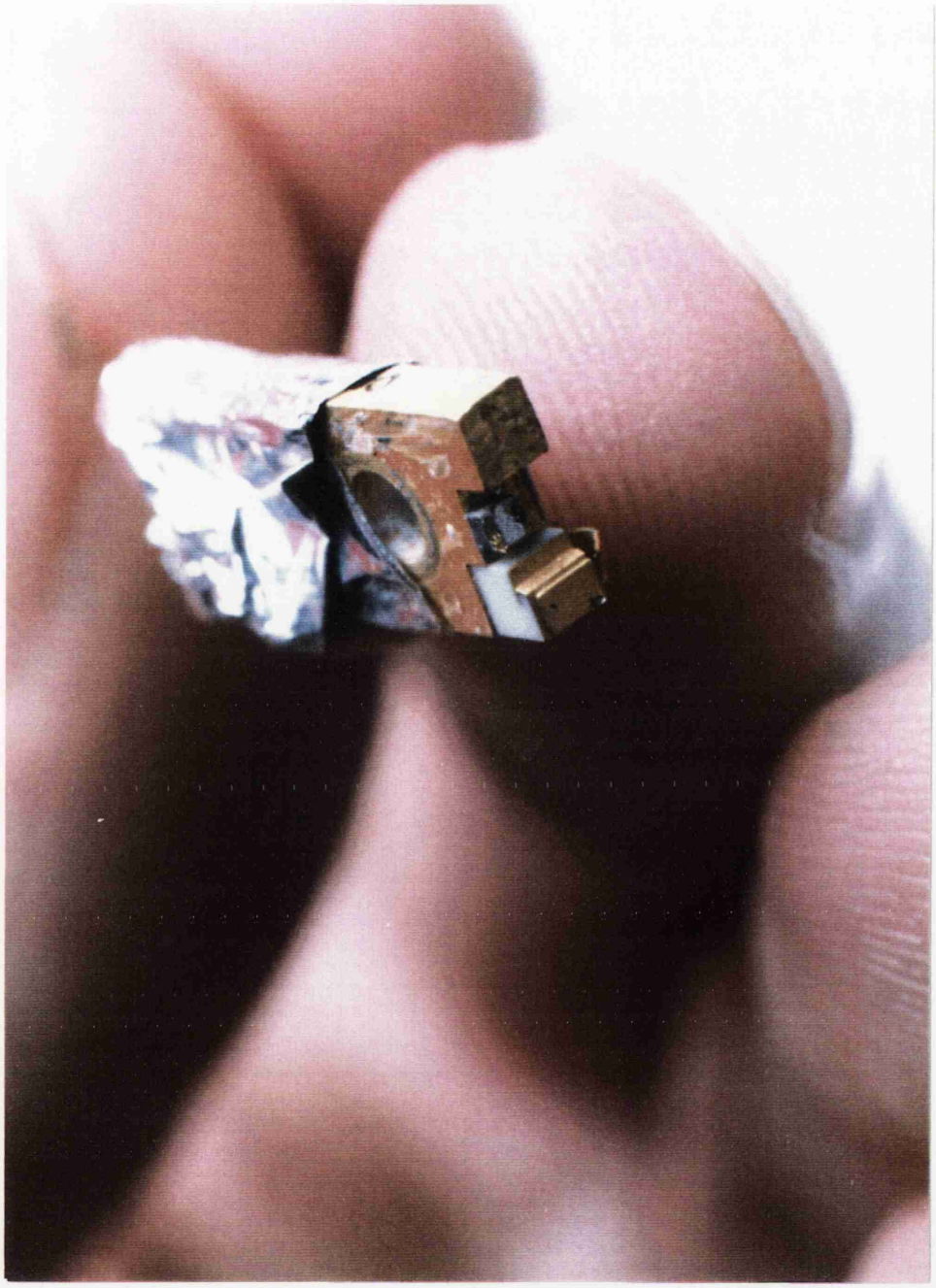

Figure 4.6 Hitachi HLP1400 Laser Diode as Received From Manufacturers

monomode, better than 20dB side mode supression, under free runing conditions. This indicates that Hitachi HLP1400 laser diodes are homogeneously broadened.

This however does not explain why all semiconductor lasers do not operate monomode. Some manufacturers guarantee monomode operation in some of their product lines, Hitachi and Sharp, where as most others do not. Multimode operation is in contradiction to the assumption of a homogeneous active layer and to the idea of homogeneous broadening.

One possible explanation is that Hitachi and Sharp are better at making laser diodes and that the reason most lasers are multimode is that they have impurities and or defects in the material. It is possible that material defects could cause a nonuniform distribution of charge within the active region. This could cause multimode operation.

It is of crucial importance that laser designers fully understand what causes some Fabry Perot semiconductor lasers to operate monomode and others to operate multimode[1,2,6].

The mode on which a Fabry–Perot semiconductor laser operates is determined by the optical length of the cavity. This dictates that for the laser frequency to remain stable it must operate in a controlled temperature and current environment. A change in any of the laser operating parameters could cause the laser to mode–hop. The most informitive way to picture this effect is to examine some plots of wavelength against current. Before doing so it has to be mentioned that if there are any external reflections back into the cavity, then the modal properties may change drastically. This effect will be dealt with in great detail in the next chapter. To minimise external reflections, an optical isolator is placed immediately after the laser collimating lens. In a bulk system the isolator can be angled slightly to avoid reflections back into the laser.

The optical isolator used in this work consisted of a piece of polaroid followed by a 1/4 wavelength plate orientated at 45^0 to the optical axis. The polaroid is aligned for maximum transmission. The light

leaving the polaroid is linearly polarised and after going through the $\lambda/4$ plate is either right or left circularly polarised. After the light is reflected the polarisation changes from right to left or left to right. On passing back through the $\lambda/4$ plate the light is again linearly polarised but perpendicular to the orientation of the polaroid sheet and so it is blocked. Additional isolation is achieved by slightly misaligning the optics. Since no isolation can be placed before the collimating lens, it is most important that the lens is anti–reflection coated and that it is stably mounted. There are other magnetooptic isolators available on the market but there were none available for this work.

The modal properties of the HLP 1400 semiconductor laser were observed by directing the emitted light through the optical isolator and then through a 50/50 beam splitter. One of the output beams was then directed into a 1m Rank Hilger monochromator which uses a 1200 line/mm grating, giving the device a potetial resolution of better than 1 Angstrom. The second beam was fired into a Tecoptics Scanning Fabry Perot Interferometer(SFPI), providing the function of an optical spectrum analyser. The experimental arrangement is shown in figure 4.7.

The Fabry–Perot interferometer used in this experiment had a free spectral range of 2GHz and a maximum finesse of 170. The typical finesse however was around 140. This gave the device a resolution of around 14MHz. In the presence of external reflections the laser spectrum may change quite drastically. Figure 4.8 show typical laser spectra traces with and without feedback. Once it was clearly shown that no feedback effects were present, the laser current was increased and the wavelength monitored. Experiments have shown that more than 55dB of optical isolation is required for the lasers to be unaffected by reflections.

Some plots of the modal characteristics of HLP1400 lasers are shown in figure 4.9. It can be seen from these that as the current increased the wavelength also increased. The wavelength of the laser was observed using the 2GHz SFPI. It was found that the laser tuned continuously at a rate of 22GHz/^{o}C until the mode hopping occured.

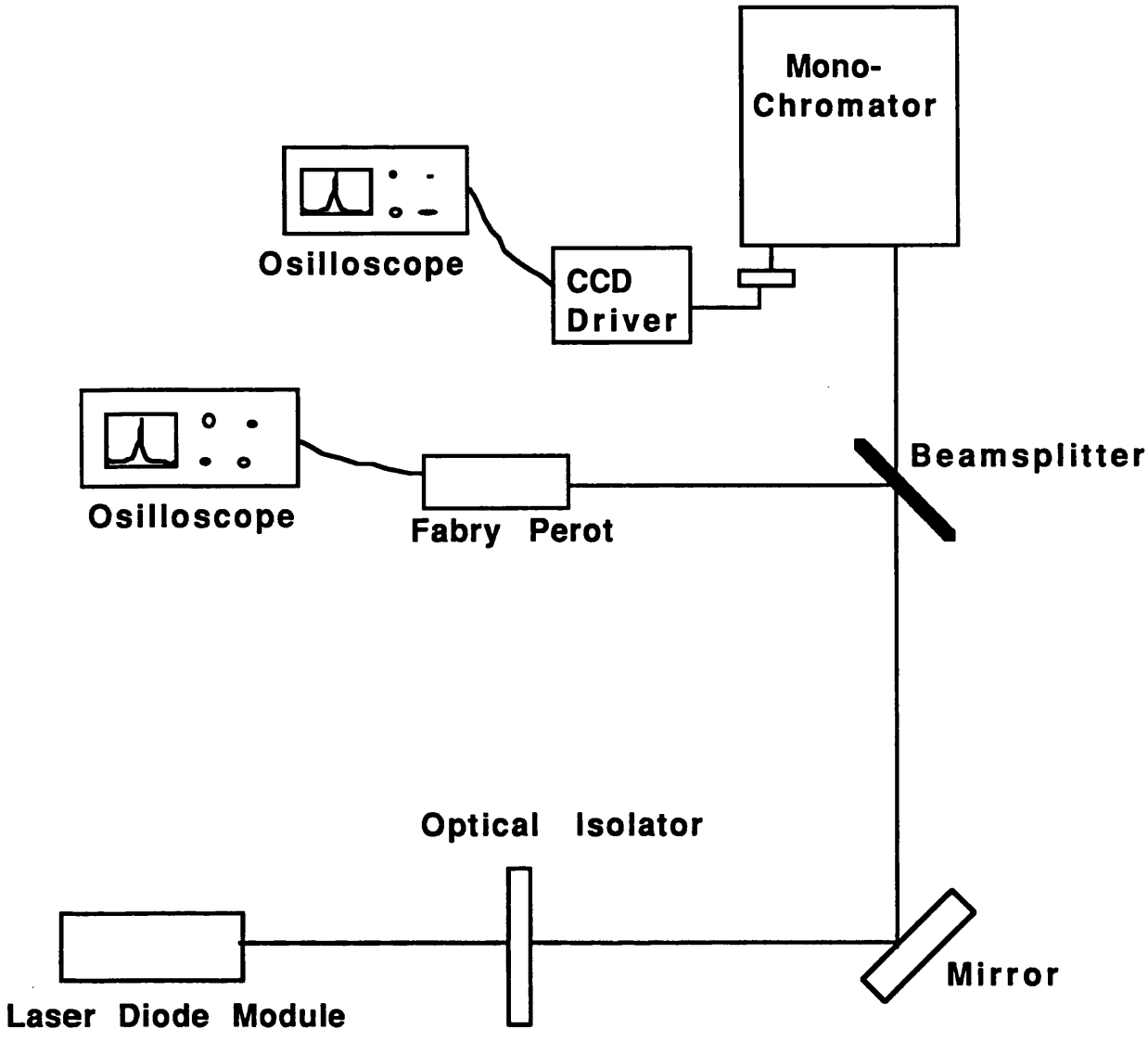

Figure 4.7 Experiment to Measure Absolute Wavelength and Modal Stability of Laser Diode

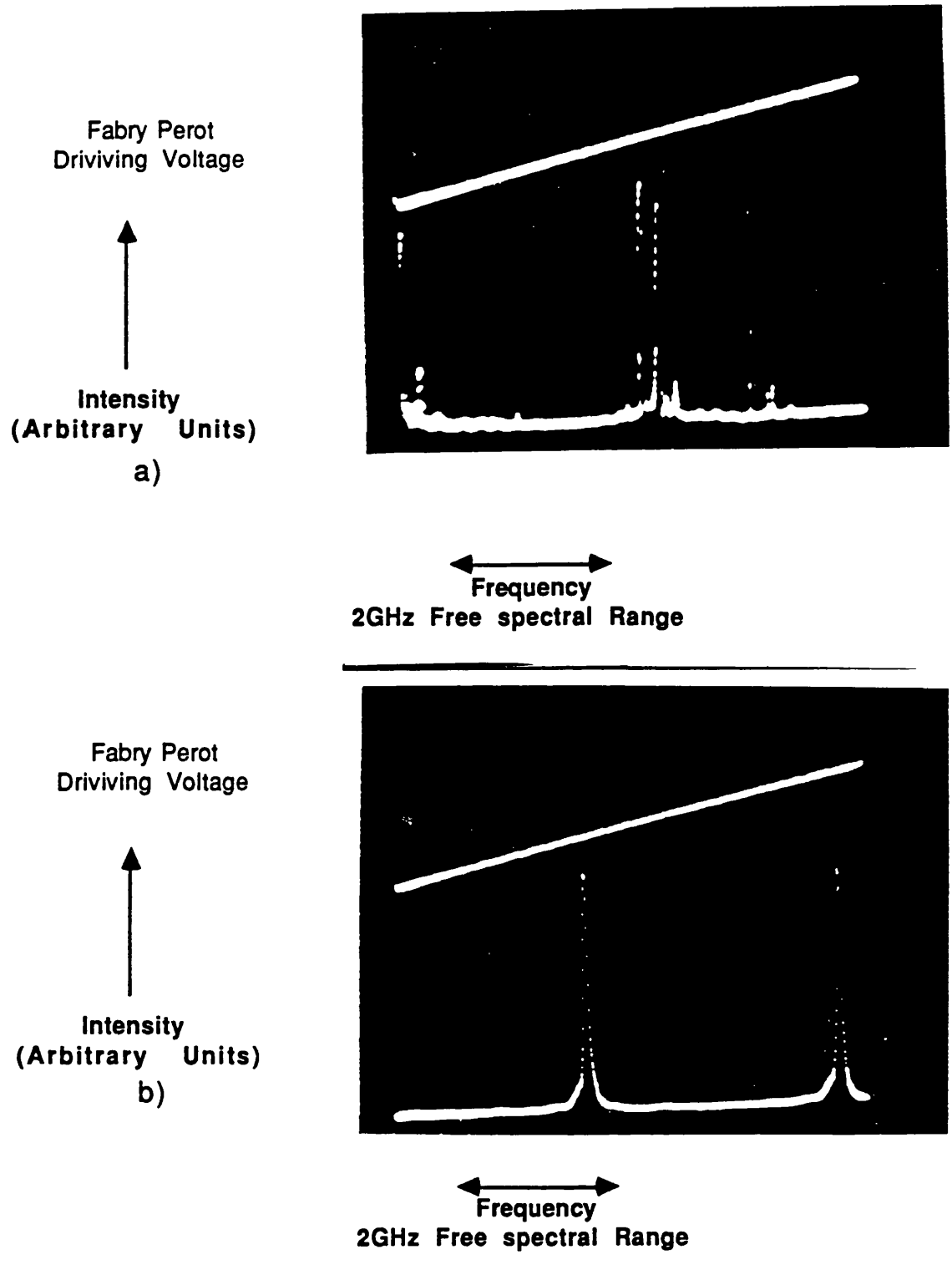

Figure 4.8 Laser Spectra observed on a 2GHz Free Spectral Range Scanning Fabry Perot a) suffering from feedback and b) without feedback

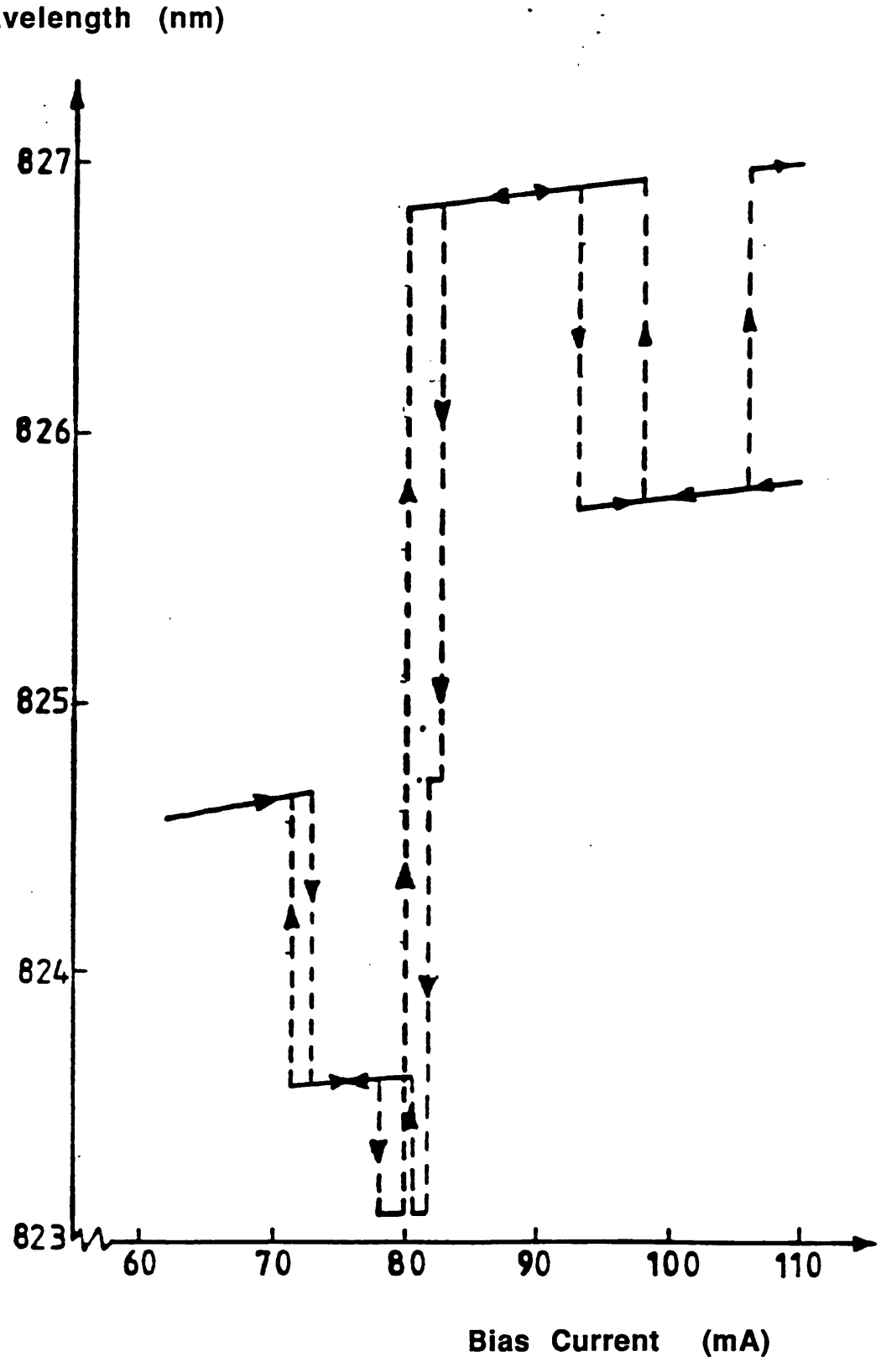

Figure 4.9a

Graph of Laser Wavelength against Bias Current
HLP 1400 No 5E3070
Operating Temperature 290.8 K

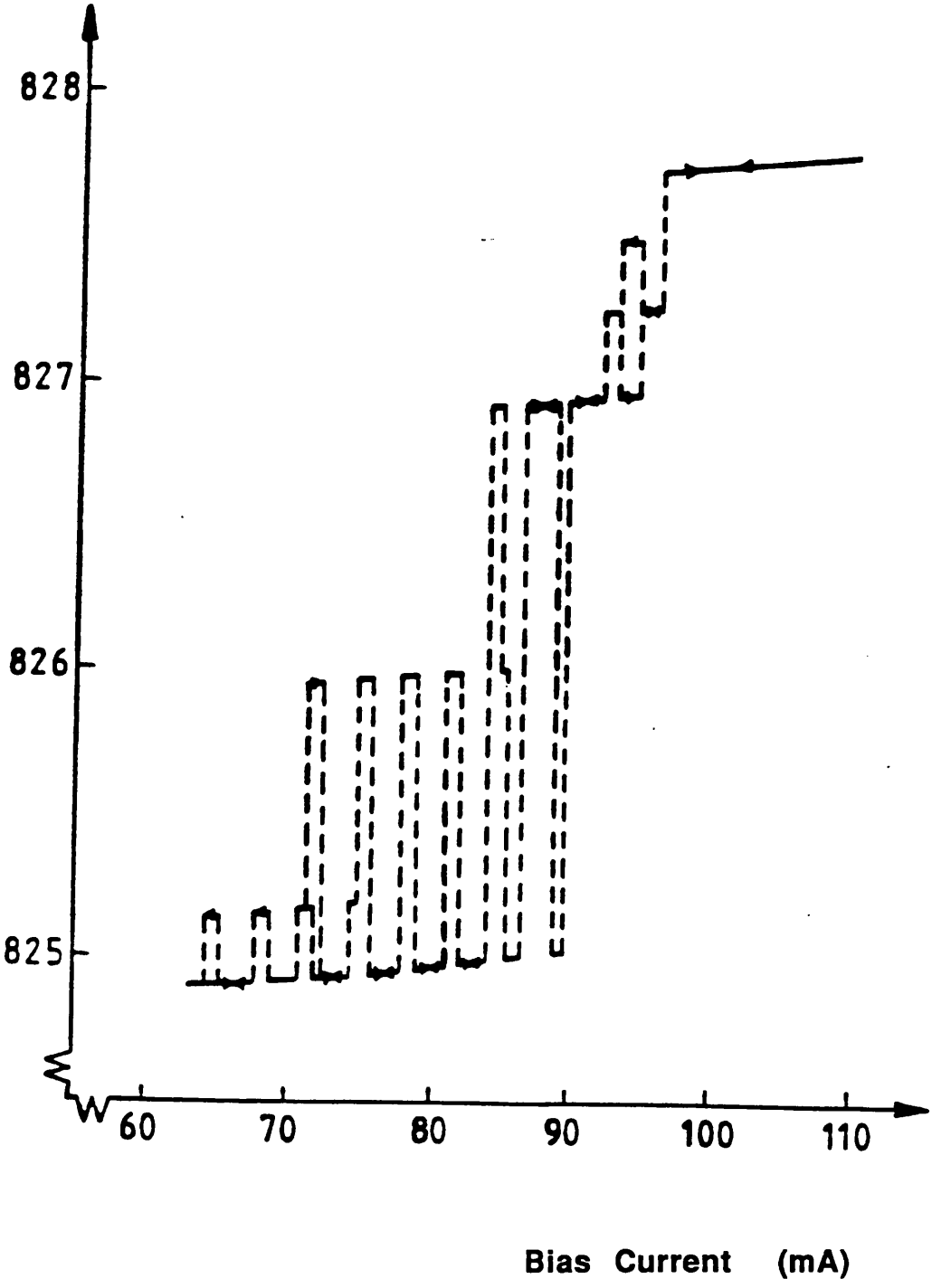

Figure 4.9b

Graph of Laser Wavelength against Bias Current
HLP 1400 No 2M0861
Operating Temperature 290.8 K

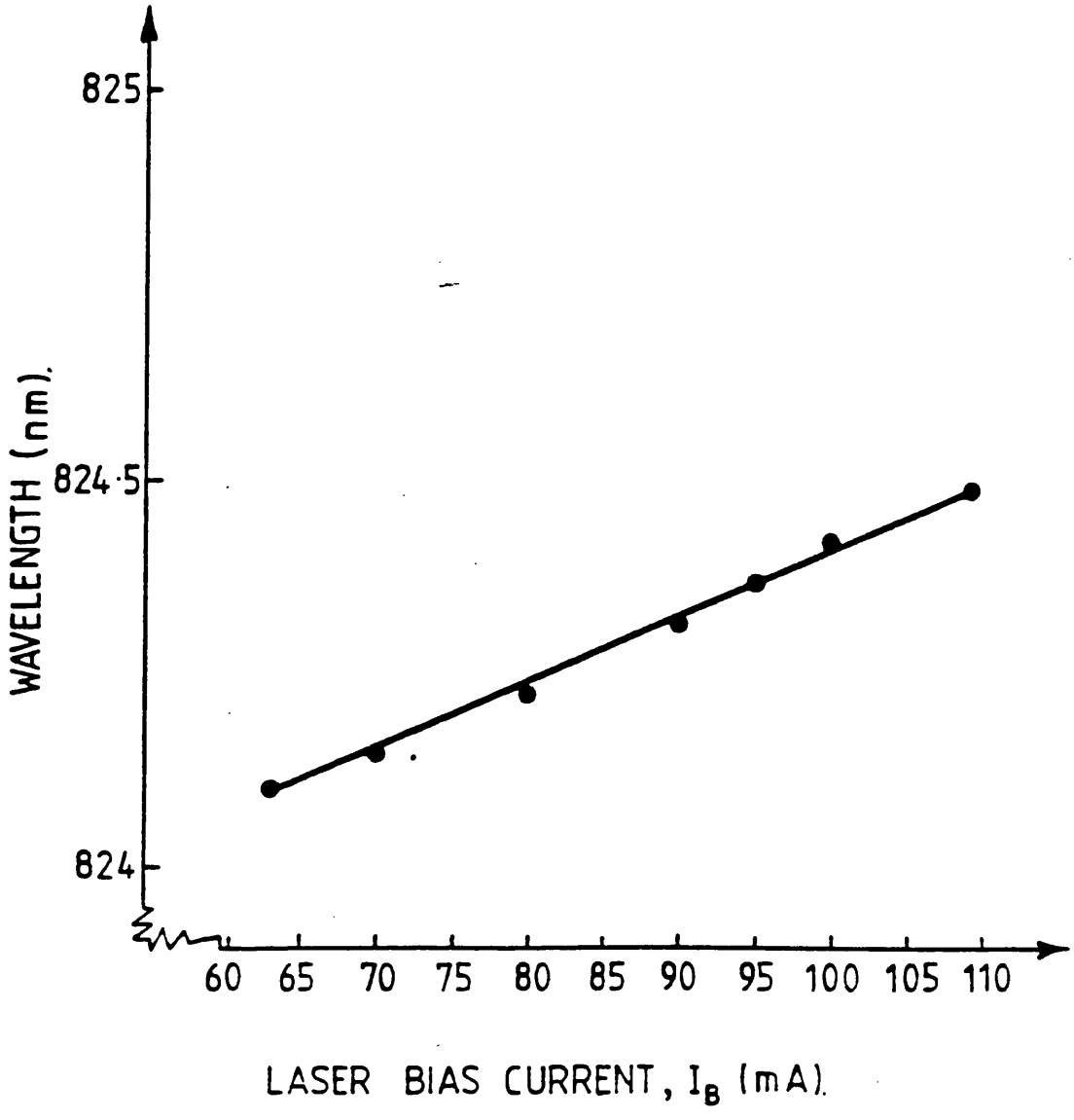

Figure 4.9c

Graph of Laser Wavelength against Bias Current
HLP 1400 No 5E3072
Operating Temperature 293.0 K

When the laser mode hops the trend should always be in the same direction unless there is some external feedback present. The number of modes by which the emmision wavelength changes appeared to be fairly random, but in integral multiples of $\Delta\nu = c/2nl$. There was also a hysteresis effect in that the laser did not necesarily reproduce the same mode hoping profile when decreasing current as it had displayed while increasing the current. Figure 4.9c displays a laser operating on a continuously tuning mode. This was most unusual. Indeed when this laser was operated under slightly different conditions the laser mode hopped in a similar fashion to those displayed in figures 4.9a and b.

4.5 STABILITY AND MODULATION CHARACTERISTICS

In a heterodyne or homodyne system two or more optical fields must be mixed. In practise this is done by multiplying the two signals together. This is achieved by spatial alignment and good polarisation control of the optical beams. They are then focussed onto a photodiode. The intrinsically square law in the response of the diode effectively multiplies the signals together. The low frequency component of the output is a signal which is the difference frequency of the two lasers. Practically, the bandwidth of the receiver will be no more than a few Gigahertz, and possibly much less, so the frequency of each laser has to be controlled to one part in 10^7 of its absolute frequency, $5 \cdot 10^{14}$ Hz, if a beat is to be detected.

Unfortunately the frequency of a typical semiconductor laser is extremely sensitive and drifts with both changes in temperature and changes in current. The frequency depends upon the optical length, nl, of the cavity and when the temperature changes both the length and the refractive index change, where as when the current changes only the refractive index changes, providing the current change is faster than the thermal response of the diode. Otherwise a change in current alters the temperature of the diode.

$$\nu = \frac{mc}{2nl} \qquad 4.5.1$$

$$\Delta\nu = \left[\frac{-mc}{2nl}\right]\frac{\Delta(nl)}{(nl)^2} \qquad 4.5.2$$

To measure the frequency deviation with respect to temperature is quite simple. The laser beam was directed through an optical isolator before being split into two beams by a 50/50 beamsplitter. One beam was then directed into a Rank Hilger Monochromator to monitor the absolute frequency of the laser and more especially to check that the laser did not mode-hop during the course of the experiment. The second beam was then directed into the Scanning Fabry-Perot Interferometer (SFPI) as in the set-up described in section 4.4. The output of the SFPI was observed on an oscilloscope and as the temperature changed so the trace moved across the screen. The frequency drift was then determined by counting the number of passes that the peaks in the laser spectra made across the screen.

The temperature of the laser was controlled using a feedback circuit and was monitored using a 100Ω ceramic resistance thermometer in a bridge circuit. This signal was processed using an "in-house" three-term controller, before being fed back to a Peltier thermoelectric element which changed the laser temperature. Using this controller, the temperature was controlled to better than 0.01K. This accuracy was determined by monitoring the laser spectra on the SFPI. If the Fabry Perot is assumed to be relatively stable then a change in frequency of the laser causes the laser spectrum to move across the display on the oscilloscope. Since the separation between peaks is known to be 2GHz it is possible to determine the stability of the laser temperature providing its frequency sensitivity is known.

The frequency drift of the laser can be calculated using

$$\frac{\Delta\nu}{\Delta T} = \frac{1}{l}\frac{dl}{dT}\nu_0 - \frac{1}{n}\frac{dn}{dT}\nu_0 = 22\text{GHz/°C} \qquad 4.5.3$$

where $\Delta\nu$ is frequency drift, ΔT is temperature drift, l is the length of the laser cavity and n is the refractive index of the laser cavity. It

should be noted that the rate of change of length with respect to temperature has a different polarity than the rate of change of refractive index with respect to temperature.

The output of the SFPI, as the temperature of the laser diode was changed, is shown in Fig 4.10. The separation between the peaks in Fig 4.10 was 2GHz, the free spectral range of the interferometer. This effect was not bias current dependent. The variation of frequency against current was not quite so simple to measure. Whenever the bias current was changed the device heated up or cooled down slightly and so the temperature modulation effect was always present for dc changes in current. To observe the current modulation effect the current has to be modulated at a rate faster than the thermal response time of the laser diode. The thermal time constant is typically in the range of $10^{-6} - 10^{-7}$s.

An amplitude modulation signal was superimposed on the DC bias and the laser spectrum was observed using the SFPI. The frequency drift with current was easily determined if the modulation current was increased until the sidebands had the same power as the carrier. At this point

$$\frac{\Delta f}{f_m} = 1.5 \qquad 4.5.4$$

where Δf is the frequency excursion and f_m is the modulation rate. This is a standard result from frequency modulation experiments and theory[6]. Figure 4.11 shows a typical spectrum for an FM-modulated laser. As can be seen from the photograph the sidebands are slightly asymmetric. This is a result of AM modulation which is always present when the current is changed.

At low frequencies it is known that $\Delta f/\Delta I$ is large. When this is the case, $\Delta f/f_m > 20$, it is then possible to measure Δf directly by measuring the seperation between the two sideband peaks on the scanning Fabry Perot[7]. The modulation was supplied diectly to the laser diode which was in series with a 47Ω resistor. It was assumed that the laser resistance was a few ohms.

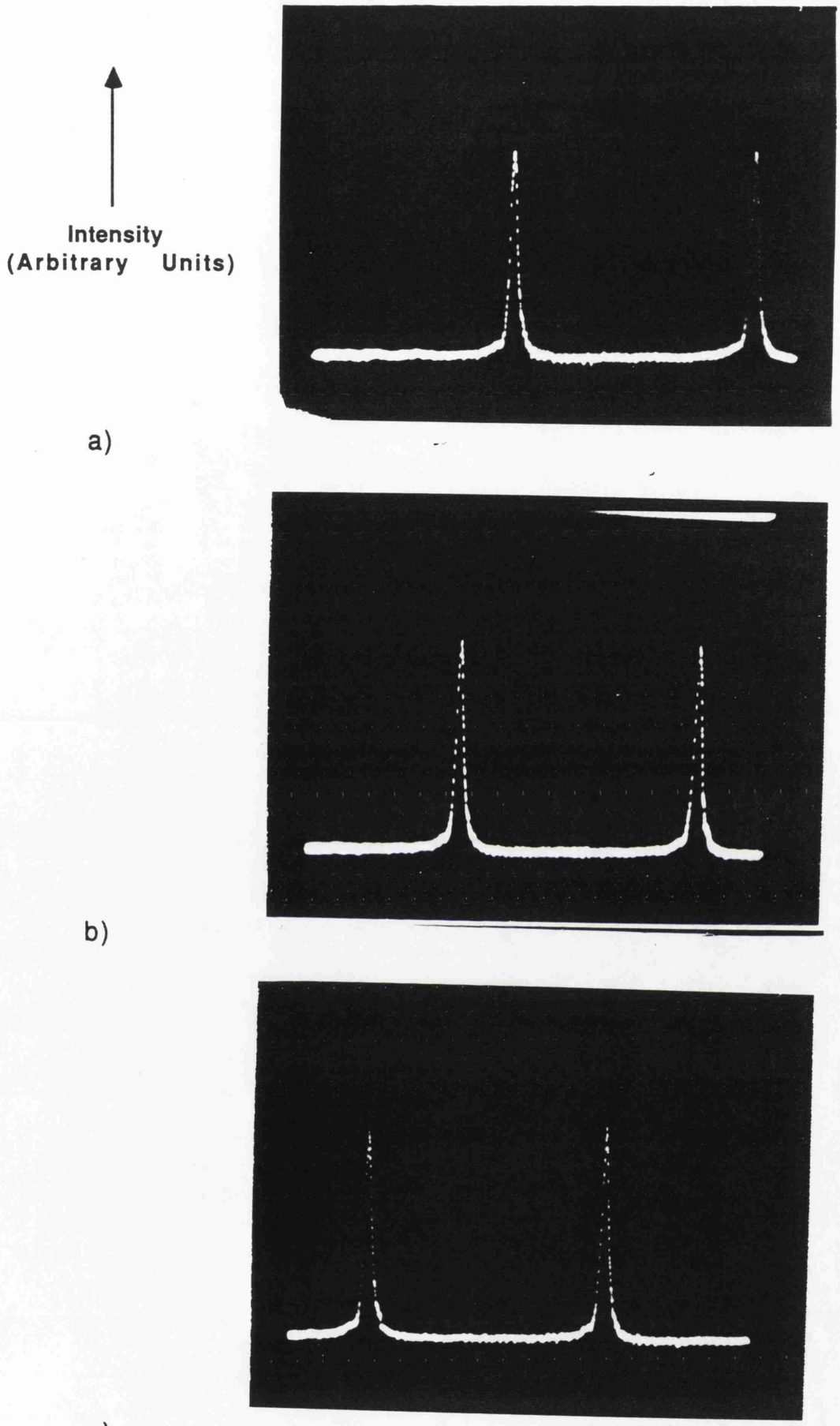

Figure 4.10 Figures a, b and c display the drift of the laser mode with temperature as observed on Scanning Fabry Perot.. 2GHz between the peaks.

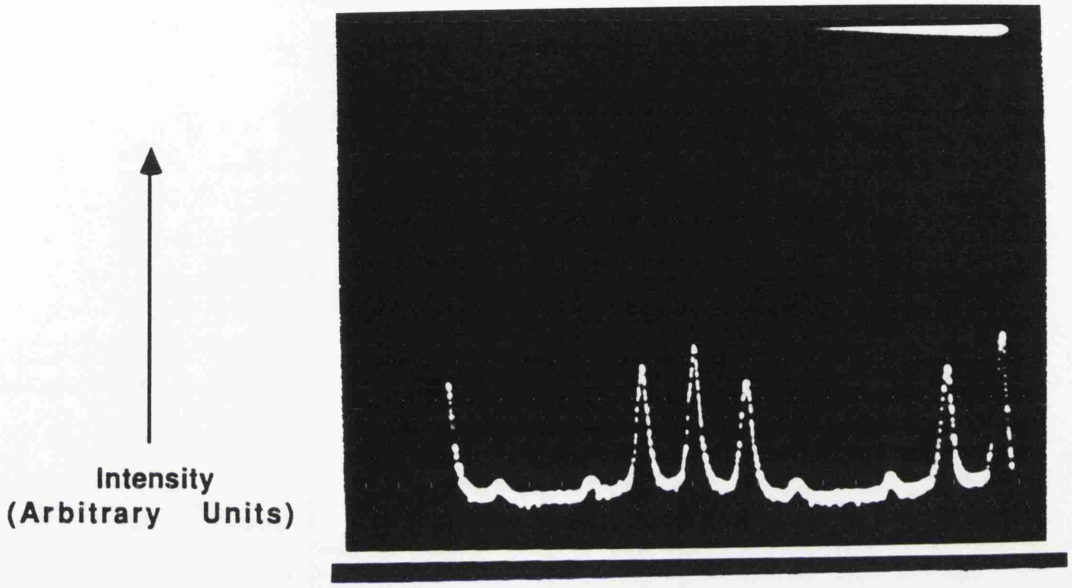

Figure 4.11

Fabry Perot Spectrum of a FM modulated HLP1400 Laser Diode.. Modulation Frequency = 330MHz
Free Spectral Range of Fabry Perot = 2GHz

The above experiment was carried out at many modulation frequencies in the range from dc to 990MHz and the results are shown in Fig 4.12a. It can be seen from this graph that the temperature modulation effect dominates at low frequencies, i.e. up to 1 − 2MHz which corresponds to the thermal time constant, and then the current modulation effect has a fairly flat response thereafter. The relaxation oscillation resonance present in all semiconductor lasers was never observed for any of the HLP1400 Laser Diodes. This is hardly surprising as the experiment was only carried out at modulation rates upto 990MHz.

What appeared to be a relaxation oscillation was observed during other experiments when using a Hitachi HLP1600 laser diode. It was always observed ar 2.8 GHz and it did not move around. The spectrum from a self heterodyne experiment is shown in figure 4.12b. The HLP1600 is sold as being identical to the HLP1400 except for the packaging.

4.6 PHASE NOISE AND LASER LINESHAPE

Ideally a laser would emit a perfectly monochromatic signal of zero spectral width. This however is not the case since no oscillator can ever emit a completely pure signal. There is a fundamental limit set by the Heisenberg Uncertainty Principle

$$\Delta\nu \geq \frac{1}{\Delta t} \qquad 4.6.1$$

where $\Delta\nu$ is the fwhm of the spectral lineshape and Δt is the finite time taken to generate the signal.

In the case of a semiconductor laser there are other broadening mechanisms present. The laser linewidth can be thought of as being due to fluctuations in the phase or frequency of the laser field. These fluctuations arise primarily as a result of spontaneous emission. Every time that there is a spontaneous emission event both the phase and intensity of the laser are instantaneously altered in a discontinuous fashion, see Fig 4.13. There is also a delayed phase change as a result of the coupling which exists between intensity and phase in a

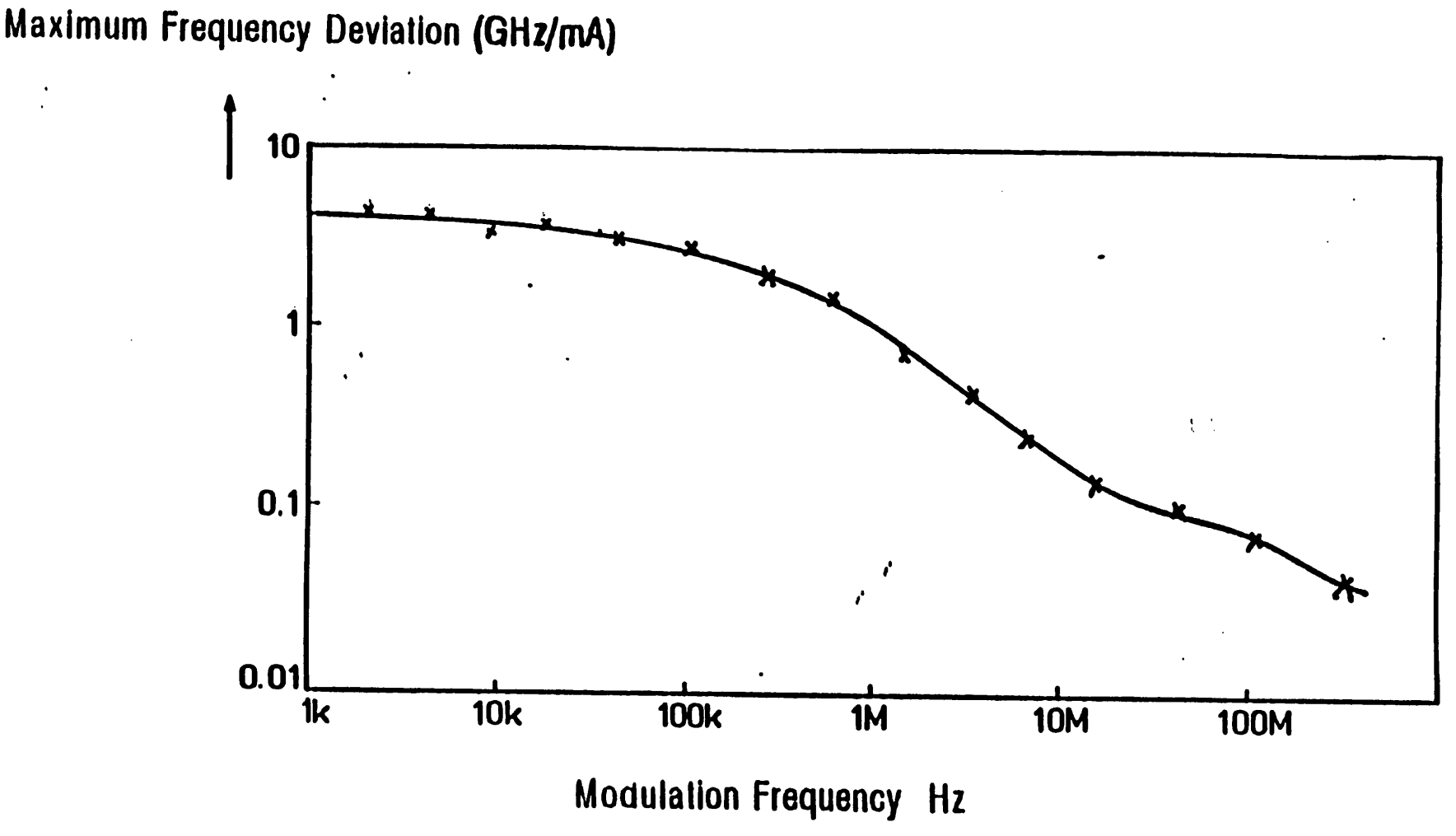

Figure 4.12 Modulation Characteristics of HLP1400 Laser Diode

Reference Level

Marker Frequency

Horiz. Scale MHz/div

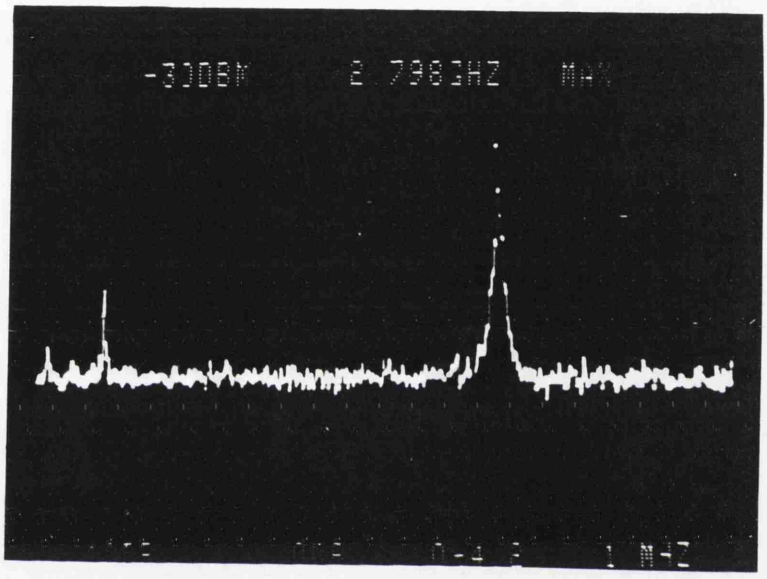

Vertical Scale dB / Div

Input Attenuation

Freq. Span GHz

Resolution Bandwidth

Figure 4.12b

HLP1600 Laser Diode Relaxation Oscillation

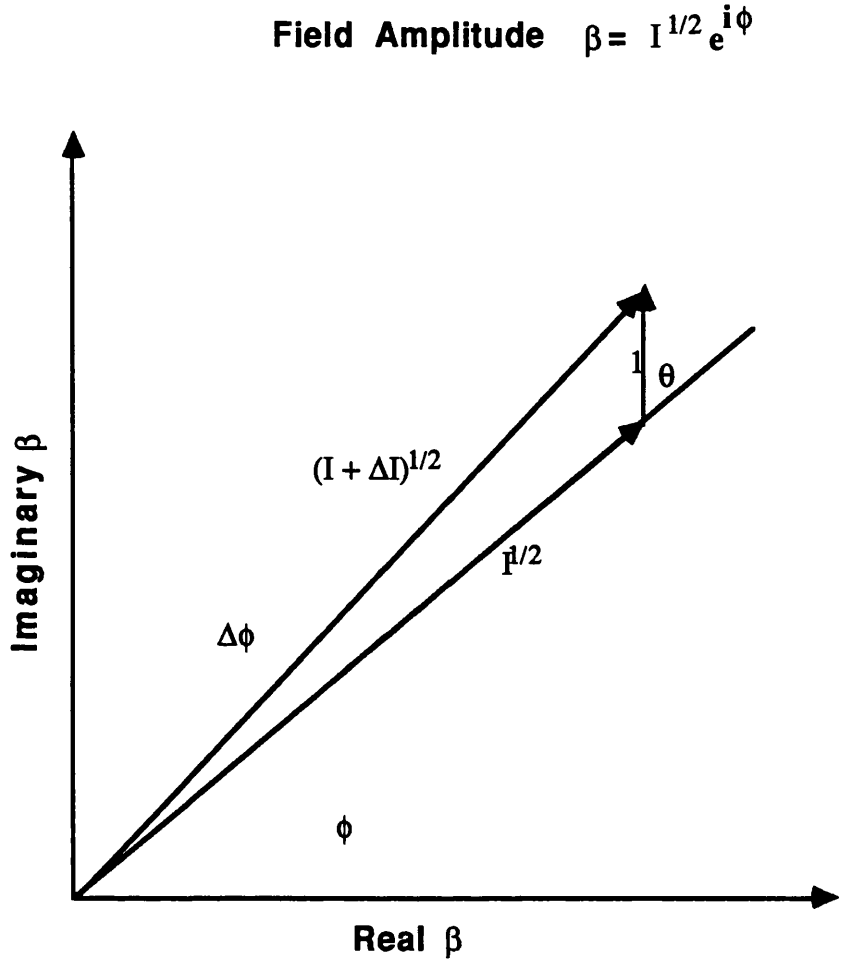

Figure 4.13 The instantaneous changes of the phase ϕ and intensity I of the optical field brought on by the i th spontaneous emission event [8]

semiconductor laser. The following theory is largely based upon the work of C.H. Henry[8,9,10].

Whenever the carrier density is altered by a spontaneous emission event, the intensity of the laser is increased. In order to maintain steady state operation, and as a result of gain saturation, the laser will undergo relaxation oscillations. During this time there will be a net gain change which can be written as:

$$\Delta g = \frac{-2\omega\Delta n''}{c} \qquad 4.6.4$$

where $\Delta n''$ is the change in the imaginary part of the refractive index caused by a change in carrier density of the active layer, Δg is the change in gain, ω is angular frequency and c is the free space velocity of light.

There will also be a change in the real part of the refractive index which will result in an additional phase shift. This causes the lasing mode to shift in such a way as to keep the real part of the propagation constant,

$$k' = \frac{\omega n'}{c} \qquad 4.6.2$$

constant, resulting in the angular frequency being changed by

$$\Delta\omega = \frac{-\omega v_g \Delta n'}{c} \qquad 4.6.3$$

where $\Delta n'$ is the change in the real part of the refractive index, v_g is the group velocity and k' was the propagation constant.

The simplest way to get a physical understanding of phase and frequency fluctuations in a laser is to consider what happens after each spontaneous emission event. Whenever the carrier density in the active region changes, so do the intensity and phase of the laser. The laser must now alter its gain in order to return to the steady

state output intensity. In altering the gain the laser changes its carrier density, which in turn alters the phase. This secondary phase change is a result of gain saturation[8] and only takes place when the laser is operated above threshold.

It was mentioned earlier that there was a peak at around 2GHz in the laser modulation spectrum. This peak is as a result of the effect described above. Whenever the laser tries to readjust to the steady state it undergoes relaxation oscillations with a period, for a Hitachi HLP1400, of around 0.5ns.

4.7 MATHEMATICAL ANALYSIS OF LASER SPECTRUM

This section on the mathematical analysis of the laser spectrum has been included for the sake of completeness as many papers analyse lasers using the following techniques.

The fundamental laser wave equation can be written as[13,14]

$$\frac{d}{dt} E(t) = \left[i\omega(N) + \frac{1}{2} (G(N) - 1/T_p) \right] E(t) \qquad 4.7.1$$

where $E(t) = \sqrt{I(t)} \exp [i(\omega t + \varphi(t))]$ is the laser field, G(N) is the carrier density dependent modal gain per second, N is the carrier number and T_p is the photon lifetime.

$\omega(N)$ can be expanded to first order with respect to carrier number using $\Delta N = N - N_{th}$ where N_{th} is determined by $G(N_{th}) = 1/T_p$. $\omega(N)$ can be written as[14]

$$\omega(N) = \omega_o - \frac{\omega_o}{n^*} \frac{dn}{dN} \Delta N = \omega_o + \frac{\alpha G_N}{2} \Delta N \qquad 4.7.2$$

where

$$n^* = n + \omega_0(\partial n/\partial \omega) \qquad 4.7.3$$

is the effective refractive index and

$$\alpha = -\frac{2\omega}{n^*G}\frac{\partial n}{\partial N} \qquad 4.7.4$$

is called the linewidth enhancement factor. Also G(N) can be written as

$$G(N) = G_{th} + \Delta G \qquad 4.7.5$$

Using $\Delta G = G_N \Delta N$, equation 4.7.1 can be rewritten as

$$\frac{d}{dt} E(t) = \left[i\omega_o + \frac{\Delta G}{2}(1 + i\alpha) \right] E(t) \qquad 4.7.6$$

It is now possible to obtain rate equations for φ and I, that is for the phase and intensity of the laser field, respectively

$$I(t) = \Delta G I + R \qquad 4.7.7$$

$$\dot{\varphi}(t) = \frac{\alpha \Delta G}{2} \qquad 4.7.8$$

where R is the average spontaneous emission rate. Before taking this analysis further it is necessary to introduce Langevin Forces.

4.8 LANGEVIN FORCES

Consider a multivariable time dependent system, in this instance a semiconductor laser. In the simplest useful case the variables are the phase, the carrier number and the intensity. The Langevin rate equations of such a system are[8,9,10]

$$\begin{aligned} \dot{\varphi} &= f(\varphi, I, N, t) + F_{\varphi}(t) \\ \dot{I} &= g(\varphi, I, N, t) + F_I(t) \\ \dot{N} &= h(\varphi, I, N, t) + F_N(t) \end{aligned} \qquad 4.8.1$$

where $F_i(t)$ are the Langevin Forces.

The Langevin Forces are included in the analysis to describe how the statistical distribution of the variables change in time. Langevin Forces

obey the following rules. Since the fluctuations are computed with reference to an equilibrium state f,g and h are chosen so that $\langle F_i(t)\rangle = 0$. The forces are also assumed to be Markoffian, ie they have no memory and so the correlation of their products function is a delta function.

$$\langle F_i(t)F_j(u)\rangle = 2D_{ij}\delta(t-u) \qquad 4.8.2$$

where D_{ij} is called the diffusion coefficient. A variable with a δ– function autocorrelation is often described as completely random.

The Langevin Forces for I,N and φ are given by

$$\begin{aligned} F_\varphi(t) &= \sum_i I^{-1/2}\sin(\theta_i)\delta(t-t_i) \\ F_I(t) &= \sum_i 2I^{1/2}(\cos(\theta_i))\delta(t-t_i) \qquad 4.8.3 \\ F_N(t) &= -\sum_i \delta(t-t_i) \end{aligned}$$

The δ functions are necessary in order to model the discontinuous changes in N,I and φ during spontaneous emission events. The Langevin Force have been obtained by considering the instantaneous changes after each spontaneous emission event, see figure 4.13.

The lineshape is the Fourier transform of the autocorrelation of the electric field, E(t):

$$S_E(\omega) = \int_{-\infty}^{\infty} R_E(\tau)\exp(-i\omega t)dt \qquad 4.8.4$$

where

$$R_E(\tau) = \overline{E(t+\tau)E^*(t)} \qquad 4.8.5$$

$$= I\exp(i\omega_o t)\exp\left[i\int_t^{t+\tau}\varphi(t')dt'\right] \qquad 4.8.6$$

In general this is difficult to evaluate but since $\varphi(t)$ is a normally

distributed ergodic process, R_E can be written as[15]

$$R_E = I \exp(i\omega_o t)\exp[-1/2\langle\Delta\varphi(t)^2\rangle] \qquad 4.8.7$$

The problem has now reduced itself to calculating the variance of $\Delta\varphi(t)$. $\Delta\varphi$ can be written as:

$$\Delta\varphi = \int_0^t F_\varphi(t)dt - \frac{\alpha}{2I}\int_0^t F_I(t)dt \qquad 4.8.8$$

$$\langle\Delta\varphi(t)^2\rangle = \frac{R}{2I}(1+\alpha^2)t \qquad 4.8.9$$

substituting this back into 4.8.4 and 4.8.6,the lineshape is given by

$$S_E(\omega) = E_o^2 \frac{\Delta f}{2\pi[(f-f_0)^2 + (\Delta f/2)^2]} \qquad 4.8.10$$

where

$$\Delta f = \frac{R}{4\pi I}(1+\alpha^2) \qquad 4.8.11$$

Equation 4.8.11 can be rewritten as

$$\Delta f = \frac{v_g^2 n_{sp} h f (1+\alpha^2) \ln(1/R_m)^2}{8\pi P_o \eta L^2} \qquad 4.8.12$$

where Δf is the FWHM of the laser spectrum, v_g is the group velocity and n_{sp} is the spontaneous emission factor which accounts for the fact that there is an incomplete population inversion.

Equations 4.8.10 and 4.8.12 predict that the laser will have a Lorentzian lineshape of linewidth Δf, where Δf is $(1 + \alpha^2)$ greater than that predicted by Schalow and Townes[14]. It can be seen from the above equation that the reason that semiconductor lasers have very large linewidthis is that they have a very low cold cavity Q which is

defined as

$$Q = \frac{\nu}{\Delta\nu_c} \qquad 4.8.13$$

where

$$\Delta\nu_c = \frac{c}{2\pi n}\left[\alpha_1 - \frac{1}{L}\ln(\sqrt{R_1R_2})\right] \qquad 4.8.14$$

where n is the refractive index, R_1 and R_2 are the facet reflectivities and L is the length of the cavity. Equations 4.8.11 and 4.8.12 show that the laser linewidth depends upon the length of the cavity and on the reflectivity of the facets as well as upon many other material properties. This suggests that one possible technique for improving the spectral characteristics is to alter R and L. This topic is covered in chapter 5.

4.9 LASER LINEWIDTH MEASUREMENT

Δf for a free running semiconductor laser is typically in the range from 5MHz to 100MHz. Measurements of the linewidth of such lasers can be performed using a high finesse SFPI of low free spectral range, around 300MHz. Such instruments have a resolution of around 1MHz.

If the laser linewidth is reduced in any way or if high resolution measurements are required, a slightly different approach is needed. With the advent of optical fibre it has become possible to build very compact interferometers with rather large path differences in the two arms.

Using optical fibre for the optical path in one arm of a Mach–Zender interferometer Okoshi[16] devised the self heterodyne/homodyne experiment, see Fig 4.14. The beam from the laser is collimated out and directed through an optical isolator before being split into two paths using a 50/50 beamsplitter. The beam in one arm is coupled into the fibre delay line while the other beam may be frequency shifted using a Bragg cell. The beams are then spatially aligned, using a beamsplitter. The combined signal is then focussed onto a photodiode.

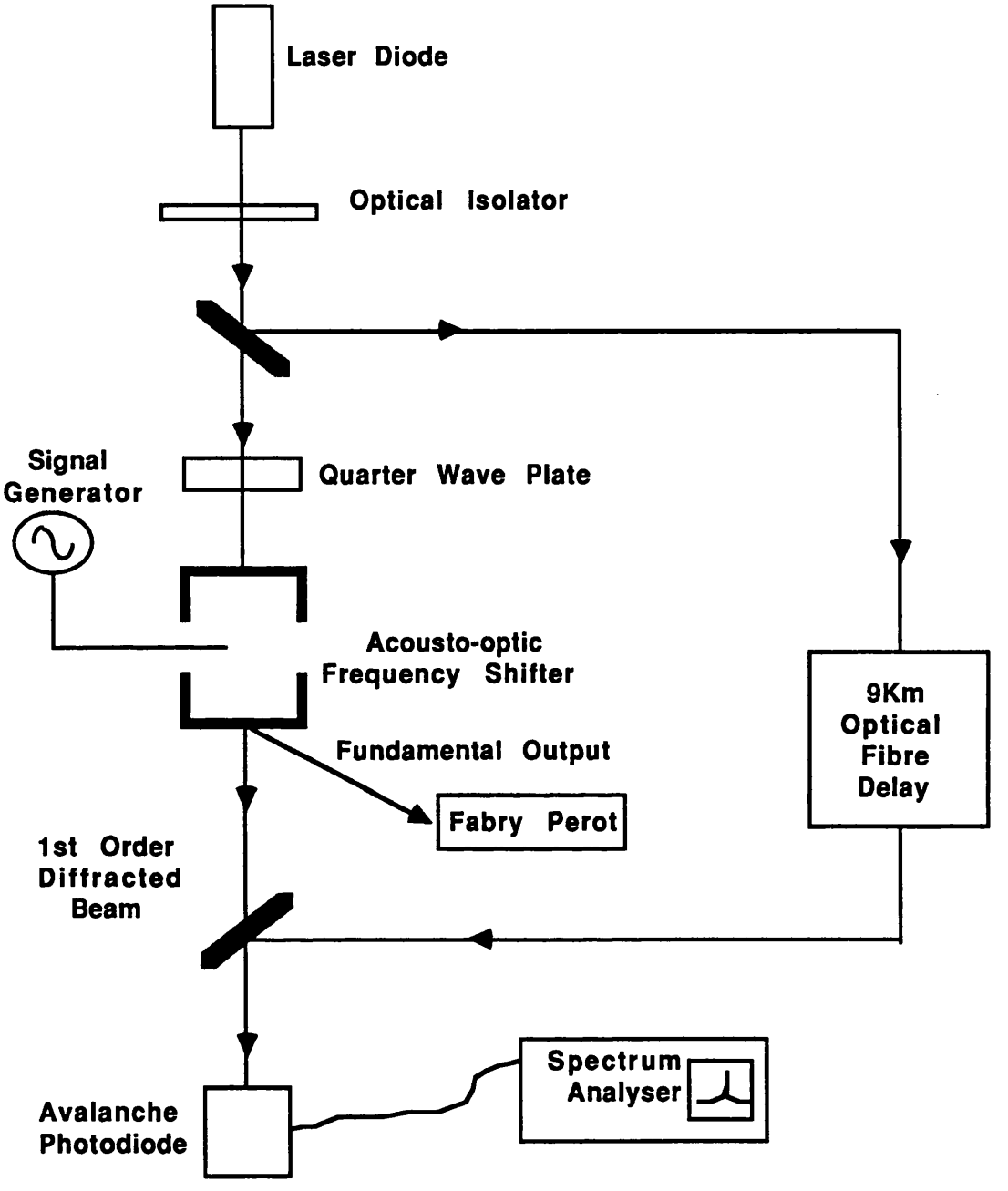

Figure 4.14 Schematic of Self-Heterodyne Experiment

While the above experiment is being performed it is important to monitor the laser spectrum on a SFPI to ensure that the laser is operating monomode and to ensure that there are no uncontrolled reflections entering the laser cavity.

If the time spent by the light in the fibre is longer than the coherence time of the laser, then the recombined beams will behave like two independent lasers of the same frequency beating together. If this signal is then sent to a r.f.spectrum analyser, a spectrum which is twice the width of the laser spectrum will be observed.

Gallion[17] has shown that the delay time should actually be twice the laser coherence time for an accurate measurement to be made. The photocurrent power spectrum is given by

$$S_i(\omega) = \langle i\rangle^2 \delta(\omega) + e\langle i\rangle/2\pi + \alpha^2\langle i\rangle^2 \exp(-\Delta f\tau)\,\delta(\omega-\Omega)$$

$$+ \alpha^2\langle i\rangle^2 \frac{\Delta f/\pi}{(\Delta f)^2 + (\omega - \Omega)^2}$$

$$\left[1 - \left[\Delta f\tau \frac{\sin(\omega - \Omega)\tau}{(\omega - \Omega)\tau} + \cos(\omega - \Omega)\tau \right]\exp(-\Delta f\tau)\right] \qquad 4.9.1$$

where α is a parameter which accounts for the relative wieght between the amplitudes of the signal and the local oscillator waves, Δf is the full width at half maximum of the laser field spectrum, τ is the delay and Ω is the shift frequency.

The first two terms of the equation can be ignored from a spectral analysis point of view. They represent the dc current due to incident optical powerr and the corresponding random shot noise. The third term represent any existing correlation between the two beams and the fourth term is the Lorentzian part of the spectrum.

Figure 4.15 displays a plot of measured linewidth against actual linewidth. It is obvious from the plot that when $\tau \geq 2\tau_c$ the measurement is reasonably accurate.

Figure 4.15

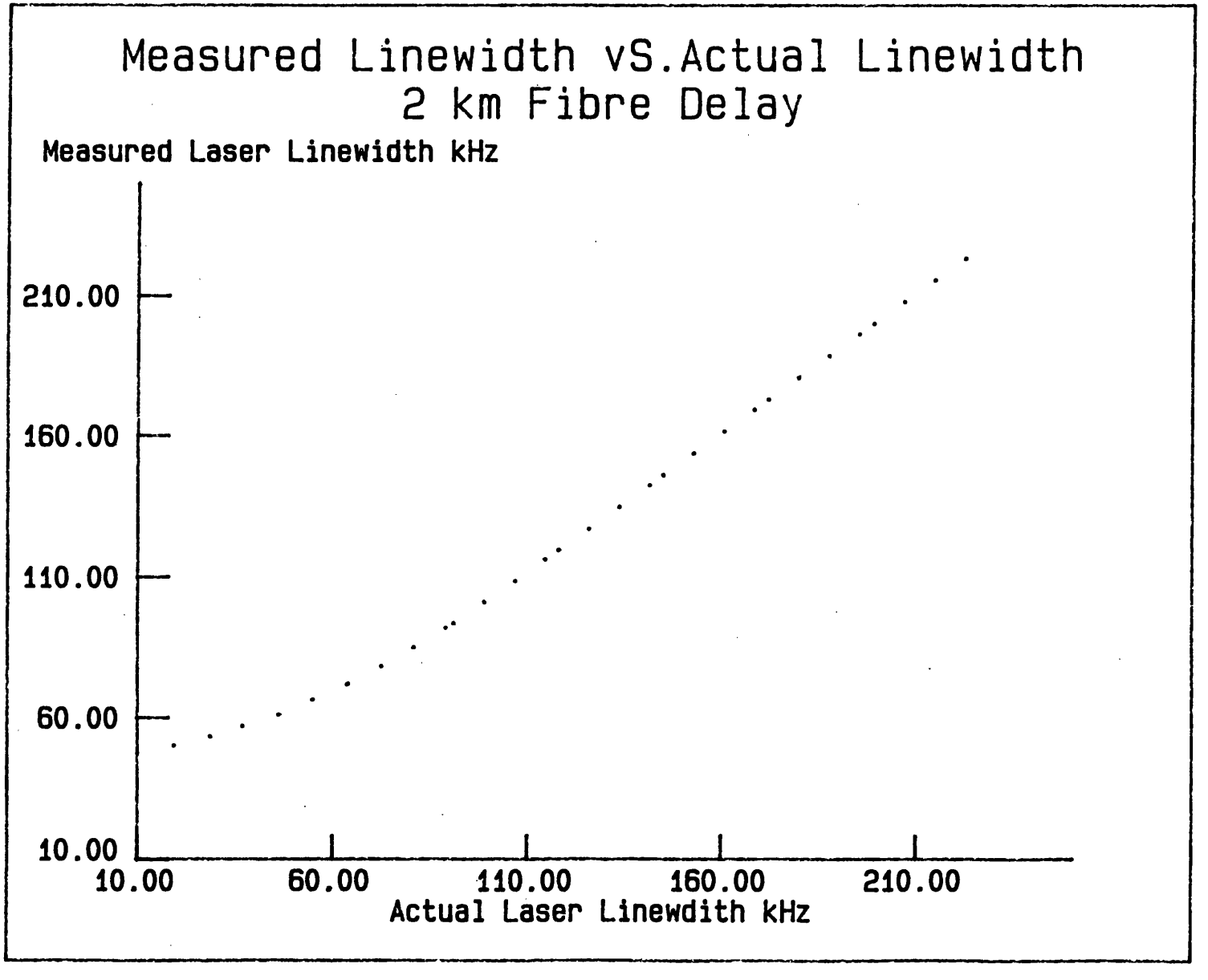
Measured Linewidth vS.Actual Linewidth
2 km Fibre Delay
Measured Laser Linewidth kHz
210.00
160.00
110.00
60.00
10.00
10.00
60.00
110.00
160.00
210.00
Actual Laser Linewdith kHz

Figure 4.16a shows spectra obtained when using a self heterodyne experiment with a delay of 9km. These HLP1400 lasers had linewidths of the order of 10MHz.

Figure 4.16b shows a more recent measurement on a newer set of HLP1400 laser diodes, which have much narrower linewidths. This improvement is most probably due to improved manufacturing procedures resulting in higher quality material and better thermal properties.

4.10 CONCLUSION

In this chapter the properties of semiconductor lasers which are important to coherent optical communications, namely linewidth, tunability and modal stability have been discussed, analysed and measured. The operation of the device has been explained and the importance of good optical, thermal and acoustic noise isolation has been stressed. An analysis of how phase noise causes a broadening of the laser line has been given using Langevin Forces and the self heterodyne experiment for measuring linewidth has been discussed.

In characterising the Hitachi HLP1400 laser diode it has been shown that the laser has a typical linewidth—power product of around 100MHzmW indicating a linewidth of around 10MHz at an output power of 10mw. This linewidth is too large to be of use in a coherent system. The laser was also shown to be extremely sensitive to reflections of its emitted light returning to the diode cavity. The laser was shown to be tunable with typical sensitivities $\Delta f/\Delta T$ = 22GHz/^{0}C and $\Delta f/\Delta I$ varied from greater than 1GHz/mA at low frequencies, < 1kHz, to 200MHz/mA at higher frequencies, > 100MHz. The temperature effect dominated at low frequencies, below 1Mhz while the current effect dominated higher up. Unfortunately the laser also tended to mode hop in an unpredictable fashion, typically the laser would jump in frequency several times its modal spacing of 0.3nm.

In conclusion the Hitachi HLP1400 laser diode has been shown to be an inadequate source for use in a phase lock loop. However, as the

spectralproperties of a laser diode largely depend upon the physical dimensions of the cavity and the reflectivity of its facets there is scope for physically improving their operating characteristics to the point where phase locking may be achieved. This subject will be addressed in the next chapter.

Reference Level

Marker Frequency

Horiz. Scale MHz/div

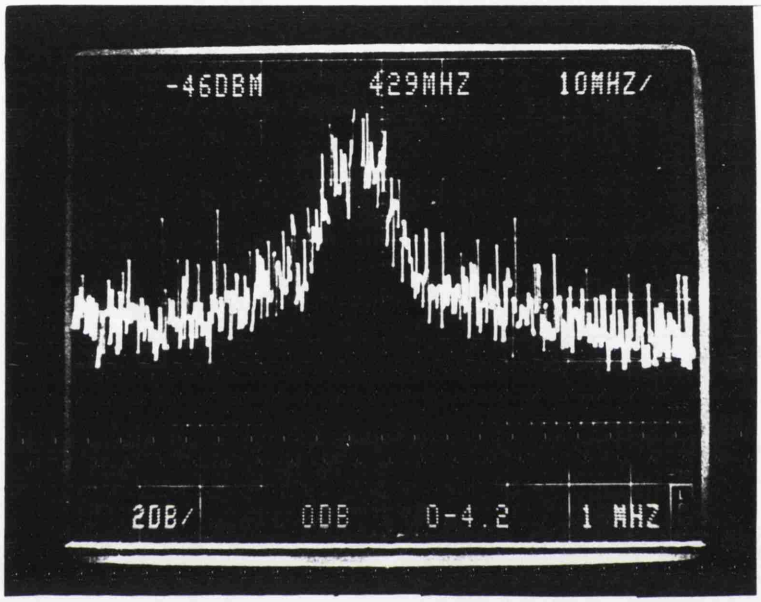

Vertical Scale dB / Div

Input Attenuation

Freq. Span GHz

Resolution Bandwidth

Figure 4.16a

Self Heterodyne Beat Indicating Linewidth to be around 10MHz

Reference Level

Marker Frequency

Horiz. Scale MHz/div

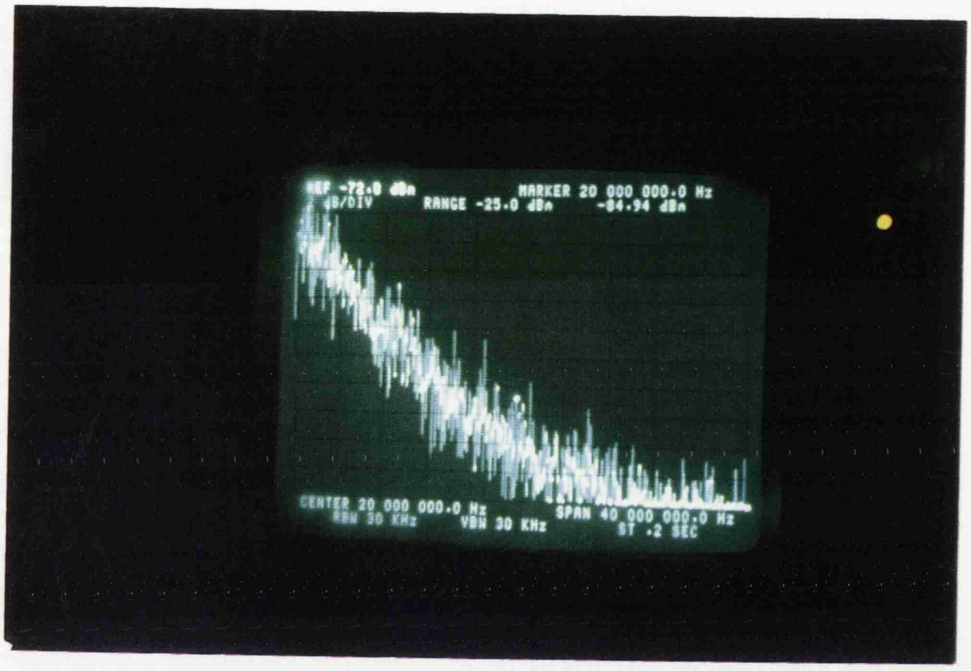

Vertical Scale dB / Div

Input Attenuation

Freq. Span GHz

Resolution Bandwidth

Figure 4.16b

Self Homodyne Beat Indicating Linewidth to be around 2 -3MHz

REFERENCES

1. H. Kressel and J.K. Butler Semiconductor Lasers and Heterojunction LEDsNew York: Academic 1977

2. H.C. Casey and M.B. Parish Heterostructure Lasers, Part A: Fundamental Principles. New York: Academic, 1978

3. A. Yariv, Quantum Electronics, 2nd ed. Ney York: Wiley, 1975

4. J. Gowar, Optical Communication Systems, Prentice Hall International Series, 1984

5. J. Dale Barry,"Design and System Requirements Imposed by the selection of GaAs/GaAlAs Single Mode Laser Diodes for Free Space Communications" IEEE J. Quantum Electronics Vol. QE−20. No 5 May 1984

5. R.P. Salathe, Diode Lasers Coupled to External Resonators, Applied Physics,vol 20, 1979 pp. 1−18

6. F.G. Stremmler "Introduction to Communication Systems" 2nd ed. Addison − Wesely Inc. 1982

7. S. Kobayashi et al, Direct Frequency Modulatioon in AlGaAS Semiconductor Lasers, IEEE J. Quantum Electronics, vol QE−18(4) 1982 pp582−597

8. C.H. Henry, Theory of Linewidth of Semiconductor Lasers, IEEE J. Quantum Electronics, vol QE−18(2) 1982 pp259−264

9. C.H. Henry, Theory of Phase Noise and Power Spectrum of a Single Mode Injection Laser, IEEE J. Quantum Electronics, vol QE−19(9) pp1391−1397, 1982

10. C.H.Henry, Phase Noise, IEEE J. of Lightwave Technology 4, 1986 pp288−297

11. B. Daino et al, Phase Noise and Spectral Lineshape in Semiconductor Lasers, IEEE J. Quantum Electronics, vol−19(3) 1983. pp266−270

12. P. Spano et al, Phase Noise in Semiconductor Lasers: A Theoretical Approach, IEEE J. Quantum Electronics, vol QE−19(7) 1983. pp 1195−1199

13. R. Lang and K. Kobayashi, External Feedback Effects on Semiconductor Injection Laser Properties, IEEE J. Quantum Electronics vol QE−16(3) 1980 pp347−355

14. B. Tromborg et al, Stability Analysis for a Semiconductor Laser in an External Cavity,, IEEE J. Quantum Electronics, vol. QE−20(9) 1984 pp1023−1032

15. A. Papoulis, "Probability, Random Variables and Stochastic Processes" New York: Mgraw−Hill 1965

16. T.Okoshi et al, Novel Method for High Resolution Measurement of Laser Output Spectrum, Elect. Lett. 16(16) 1980. pp630−631

17. P. Gallion et al, Single−Frequency Laser Phase Noise Limitation in Single Mode Optical Fibre Coherent Detection Systems With Correlated Fields, J. Opt. Soc. America vol. 72, No 9/September 1982.

CHAPTER 5

5.1 INTRODUCTION

In the previous chapters it has been shown that the linewidth– power product of free running semiconductor lasers is too large for the diodes to be of use in a coherent optical communications system. The Hitachi HLP1400 laser diodes which were used in this project have linewidth– power products of around 100MHz.mW. It was also shown that these lasers are very sensitive to changes in temperature and current and that they have a tendency to mode hop. These are the three main areas of laser operation which require improvement before semiconductor lasers can be used in coherent communications.

It is the aim of this chapter to explain how the properties of laser diodes can be improved to the point where they are of use in coherent systems. To this end the theory behind compound cavity, weak optical feedback, and external cavity, strong optical feedback, laser modules is given, as well as experimental results characterising their operation. Alternative laser structures such as distributed feedback, cleaved coupled cavity and integrated passive cavity semiconductor lasers will be discussed. There is also a section on the reduction of the laser linewidth by means of electrical feedback.

The chapter concludes with the authors opinion regarding the future use of the semiconductor laser in coherent optical communications.

5.2 COMPOUND CAVITY

It was mentioned in the previous chapter that one has to be very careful to eliminate all reflections of laser light back into the semiconductor cavity, when measurements are being made, because uncontrolled reflections drastically alter the spectral and modal characteristics of the diode. Feedback effects previously observed are linewidth broadening, line narrowing, improved frequency stability , observations of multi mode lasers being made to lase monomode and vice versa[1–10].

This section will discuss the theory of weak optical feedback before giving the experimental results of compound cavity operation. The model used for the analysis is shown in figure 5.1. R_1 and R_2 are the reflectivities of the semiconductor laser diodes facets. For an AlGaAs/GaAs diode, $R_1 = R_2 = 31\%$. The reflectivity of the external reflector is denoted by r, where L is its distance from the diode and nl is the optical length of the diode.

5.2.1 THEORY

It is useful to think of external feedback as a form of self injection locking. The laser field is locked onto a part of the field which was emitted one or more roundtrip times of the cavity earlier. For the purpose of this analysis it is assumed that the feedback is weak enough to count only one roundtrip of the light as having any effect. It is possible to analyse this effect by adding a feedback term to the standard laser wave equation 4.7.6.:

$$\frac{dE}{dt} = \left[-i\omega_0 + \frac{\Delta G}{2}(1 - i\alpha)\right]E(t) + KE(t - \tau) + F_E(t) \qquad 5.2.1$$

where τ is the roundtrip cavity time in the external part of the cavity, $F_E(t)$ is the langevin force and K is a feedback parameter. All other terms are as they were defined previously. K may be expressed as:

$$K = \frac{(1 - R)}{\tau_d}\left[\frac{r}{R}\right]^{1/2} \qquad 5.2.2$$

and can be derived by considering the combination of the semiconductor facet and external reflector as one entity having an effective facet reflectivity. τ_d is the time spent by the light in the diode.

The linewidth of the compound cavity module can now be evaluated in a similar manner to that used in the previous chapter for evaluating the linewidth, Δf, of a free running laser. Agrawal[8] has carried out the required calculation and the result is

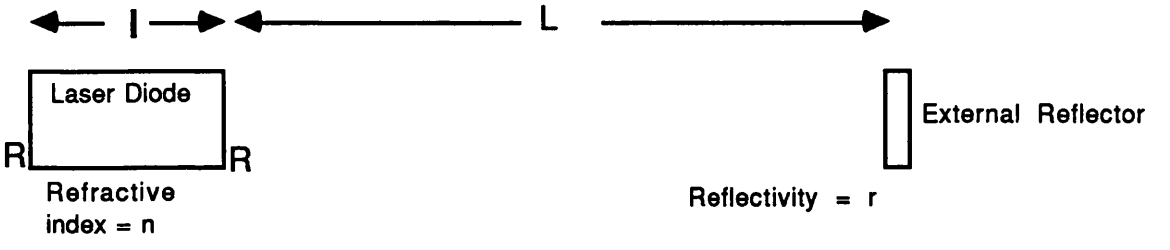

Figure 5.1 Schematic of a three facet model of a Compound Cavity Laser Module

$$\Delta f = \frac{\Delta f_0}{[1 + X\cos(\varphi_0 + \varphi_r)]^2} \qquad 5.2.3$$

where $X = K\tau(1 + \alpha^2)^{1/2}$, $\varphi_r = \tan^{-1}\alpha$, τ is the roundtrip time in the external part of the compound cavity and Δf_0 is the full width half maximum of the free running laser diode spectrum.

It is clear from this equation that depending on the value of the external cavity phase shift, $\varphi_0 = \omega_0\tau + \varphi_m$, both line narrowing and line broadening are possible. Φ_m represents a constant phase shift at the external mirror.

There are, however, other effects which are evident at the onset of feedback. When feedback is present the change in steady state gain and laser oscillation frequency, $\omega - \omega_0$, are given by:

$$\Delta G = -2K\cos(\omega\tau) \qquad 5.2.4$$

$$\omega - \omega_0 = -K(\sin(\omega\tau) + \alpha\cos(\omega\tau)) \qquad 5.2.5$$

In general 5.2.5 has multiple solutions corresponding to many compound cavity modes. However, it is possible, in principle at least, to obtain monomode oscillation if $K\tau$ is less than one.

Using a simple 3 mirror compound cavity model, Goldberg[6] showed that there are three distinct regimes where the modal characteristics of the compound cavity module are quite different. He identified a regime where, if the power P coupled back into the diode is below a certain value r_aP, then the laser module operates with only one longitudinal mode. Goldberg also identified a regime where at least three modes were present if the power returned to the diode was greater than r_bP. The third area is the intermediate one where, depending upon the phase of the signal which is fed back the laser can operate on one or three modes, $r_a < r < r_b$. The expressions for r_a and r_b are

$$r_a = \frac{(nl)^2 R}{L^2(1-R)} \qquad 5.2.6$$

$$r_b = (1.047)\left[\frac{3\pi}{2}\right]^2 \frac{(nl)^2 R}{L^2(1-R)} \qquad 5.2.7$$

For a 12cm long cavity and R = 0.31 r_a = 0.0039% and r_b = 0.009%.

Compound cavity operation also effects the stability of laser operation. Differentiating equation 5.2.5 with respect to the distance to the external mirror and also w.r.t. changes in the diode frequency gives:

$$d\omega = -\frac{K\omega}{c}(\cos(\omega\tau) - \alpha\sin(\omega\tau))dL \qquad 5.2.7$$

$$d\omega = \frac{d\omega_o}{1 + X\cos(\omega\tau + \varphi_0)} \qquad 5.2.8$$

where φ_0 = arctan(α).

Equation 5.2.7 states that the frequency of the compound cavity module is dependent upon the stabiltity of the external reflector. Equation 5.2.8 states that changes in free running frequency are altered by $1/[1 + X\cos(\omega\tau + \varphi_0)]$ and that the size of frequency deviation is phase sensitive. These two equations suggest that compound cavity operation will be extremely sensitive to changes in any of the parameters of the module.

5.2.2 EXPERIMENTS

Figure 5.2 shows a photograph of the compound cavity module used in this project.The laser used in the module was a Hitachi HLP1400 laser diode. The diode package was shown in figure 4.5. The diode package was mounted on an aluminium heatsink. Light was collimated out of the front facet using a single element 97% transmission diode lens with a relatively long working distance of 5mm and a numerical aperture of .45. The lens was AR coated to reduce unwanted

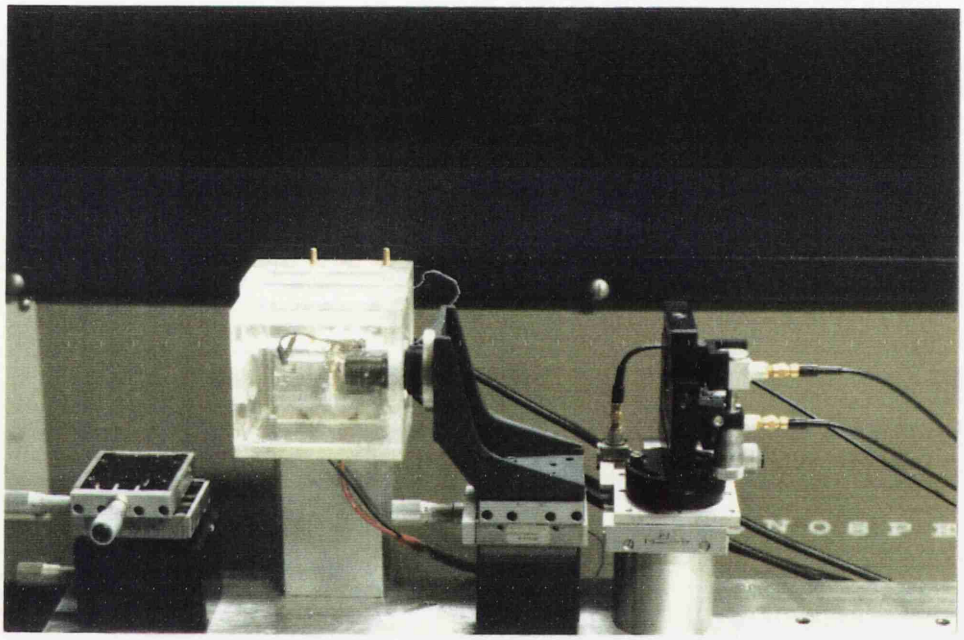

Figure 5.2

Photograph of the Compound Cavity Laser Module

reflections (lens serial number FLA40 and was supplied by Newport). The lens was mounted on an x,y,z micrometer driven translation stage. A partially reflecting mirror which was held in a piezoelectrically controlled gimbal mount was placed in the beam path. The gimbal mount sat on a piezo controlled longitudinal stage. (All the piezo equipment was supplied by Physik Instrumente) Each of the components was then mounted on an aluminium baseplate. The mirrors used in this experiment were 1 inch, around 2.5cm, in diameter and were specified as being flat to better than $\lambda/10$ at λ = 780nm over their whole surface area. A variable attenuator was placed in the external cavity to control the power fedback to the diode. The temperature of the diode was controlled using the unit described in section 4.5. It was impractical to attempt to control accurately the temperature of the whole laser mount.

The experiments carried out on the compound cavity module consisted of measurements of the laser linewidth under various levels of feedback, measurements of the modulation characteristic, observations of the modal structure and of the laser frequency stability. The experiments have all been described in chapter 4.

5.2.3.RESULTS AND OBSERVATIONS

5.2.3a LINEWIDTH

The linewidth of the compound cavity module was measured using the self homodyne technique described in section 4.9 with a 2km optical fibre delay. This gives the experiment a resolution of around 100kHz. Figure 5.3 shows the results of some of these measurements. The linewidth has been reduced from around 10MHz down to around 200kHz. These experiments were carried out using a mirror with 4% reflectivity. The power being coupled back into the diode cavity being substantially less than that

5.2.3b MODAL CHARACTERISTIC

It is possible even with a 4% reflector to collapse the laser mode completely into many modes. Figure 5.4c shows a photgraph of a

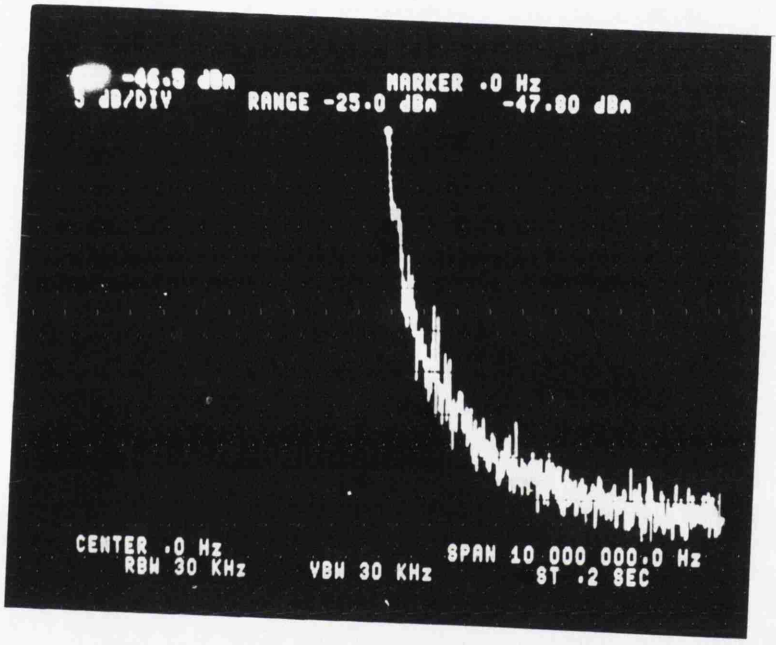

Figure 5.3a

Linewidth measurement of compound cavity laser diode module. Diode No 2206
Linewidth = 235kHz

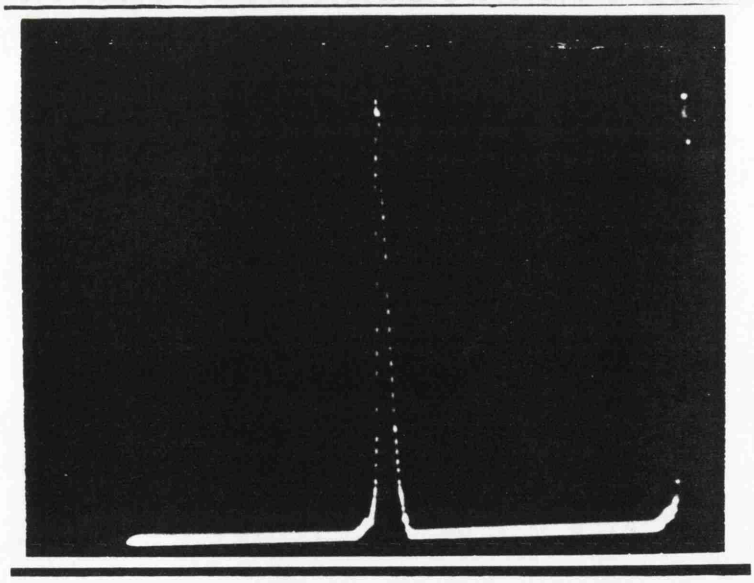

Intensity
(Arbitrary Units)

a)

$r < r_a$ guaranteed monomode operation

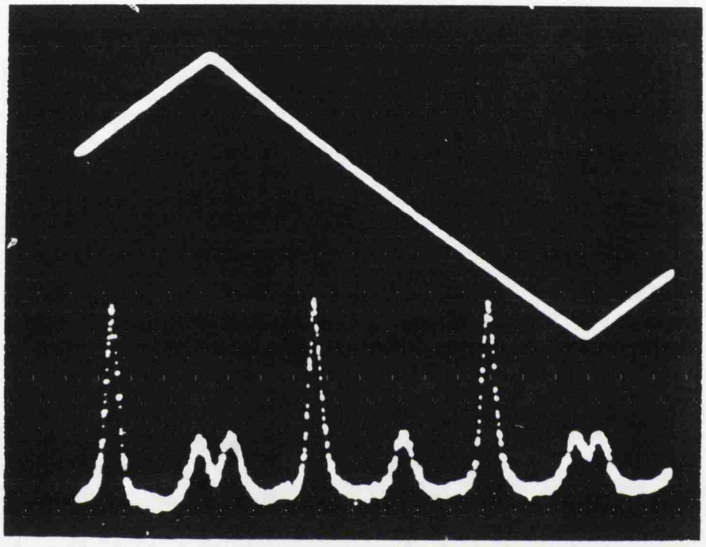

b)

$r_a < r < r_b$ one or three modes present
phase sensitive

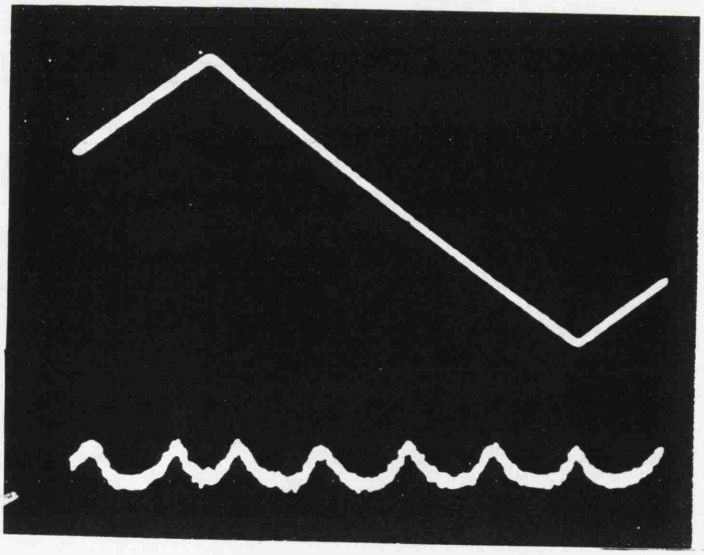

c)

$r > r_b$ multimode operation

frequency

Figure 5.4 Modal Structure of compound cavity laser module for different levels of feedback displayed on a Scanning Fabry Perot with 2GHz Free Spectral

trace obtained from a 2GHz free spectral range SFPI when the laser has too much feedback. Figure 5.4b shows a photograph with the feedback slightly reduced and only three modes present. Finally, Figure 5.4a shows only one line– narrowed mode.

With the feedback aligned for only one mode to be present several plots of wavelength against current were made. An example of these is shown in figure 5.5. An expanded scale is used around each diode mode to indicate that the laser module mode hopped in between the air cavity modes around each diode cavity mode.It can be seen clearly that these traces are extremely erratic. The compound cavity module was extremely sensitive to changes in any of its parameters. It is extremely difficult and, in practice, impossible, to predict λ to better than a few times the mode separation of the air cavity even if the feedback is well controlled and the laser is on a stable diode mode. Otherwise the laser mode may hop by two or three positions. On many occasions the laser was oscillating between two modes.

5.2.3c STABILITY

The frequency instability was measured using a FPI in a nonscanning mode of operation. The FP mirror separation was adjusted until the FP transmission was held at about 50% of the resonance peak maximum. In this set up, frequency fluctuations of the laser source are observed as relatively large deviations in the FP transmission intensity.

The FPI was aligned so that the finesse was around 20, while the free spectral range was 2GHz. With this set up, a frequency fluctuation of 10MHz corresponded to a 20mV change in the photodetector output voltage. It can be seen from figure 5.6, that the module was extremely unstable.The frequencies of oscillation involved were between 10Hz and 500Hz. The deviations shown in figure 5.6 are of the order of 50 to 100MHz. A servo loop was built to stabilise the external mirror. This is described in section 5.3.6e.

In normal operation the laser module behaved as shown in 5.4 until it drifted into complete instability, where it tended to mode hop

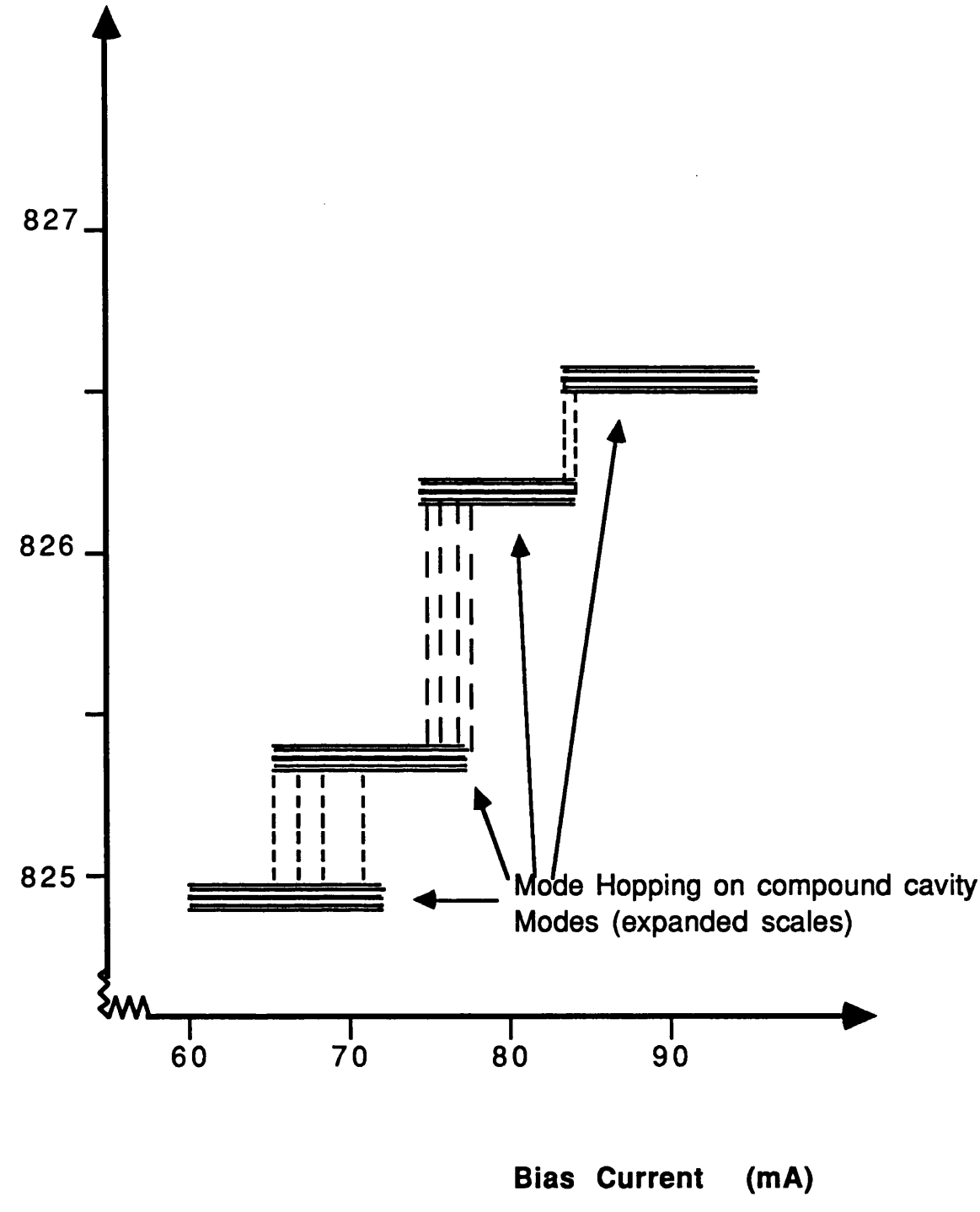

Figure 5.5

Graph of Laser Wavelength against Bias Current for a Compound Cavity Laser Diode Module

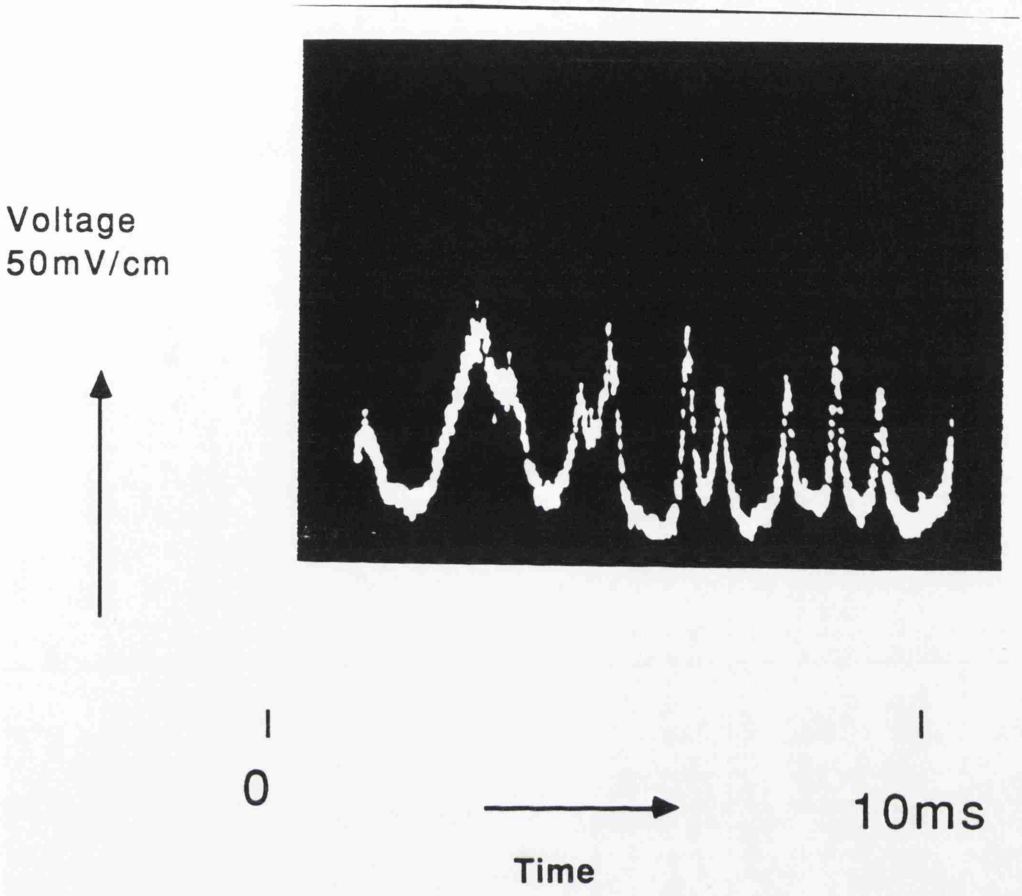

Figure 5.6

Frequency Fluctuations observed from Fabry Perot in Non Scanning Mode of Operation

uncontrollably. The module then tended to drift in and out of these different regions.

5.2.3d MODULATION CHARACTERISTICS

Equation 5.2.8 states that the modulation sensitivity of the laser will be reduced by a factor $1/(1 + X\cos(\omega T + \varphi_0))$ when operating in a compound cavity. This effect can be confirmed by observing the laser spectrum while being modulated.

Figure 5.7 displays the spectra observed when the laser was modulated with a signal of frequncy of 500MHz with amplitude 158mV. Figure 5.7a was obtained when the laser was operated without feedback and Figure 5.7b was obtained when the laser was operated under feedback. By measuring the relative intensity of the peaks it is possible to calculate the modulation sensitivity in both instances. The feedback parameter X can also be calculated if it is assumed that $\cos(\omega T + \varphi_0)$ equals 1.

Under free running conditions	$\Delta f/\Delta I = 160$ MHz/mA
Under feedback conditions	$\Delta f/\Delta I = 40$ MHz/mA
Feedback parameter	$X = 3$

These experiments were extremely difficult to carry out as the laser module tended to mode hop whenever modulation was applied, unless the optics were extremely well aligned. The module tended to drift in and out of this condition as a result of vibration and thermal expansion of the laser mount.

Limits could also be placed on the extent to which the laser would tune before mode hopping. In practice the laser module tended to mode hop once the frequency had changed by approximately F/2, where F is the free spectral range of the compound cavity.

5.2.3e CONCLUSIONS ON COMPOUND CAVITY MODULE LASER OPERATION

Using weak optical feedback it is possible to reduce the linewidth of a

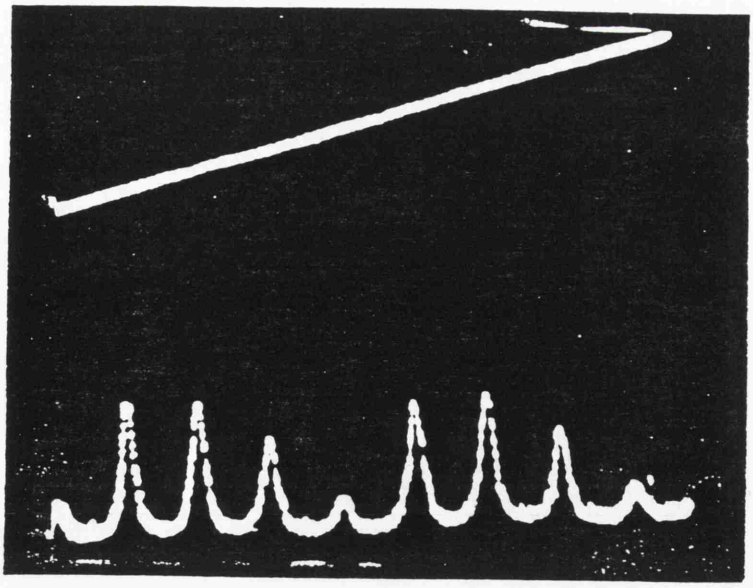

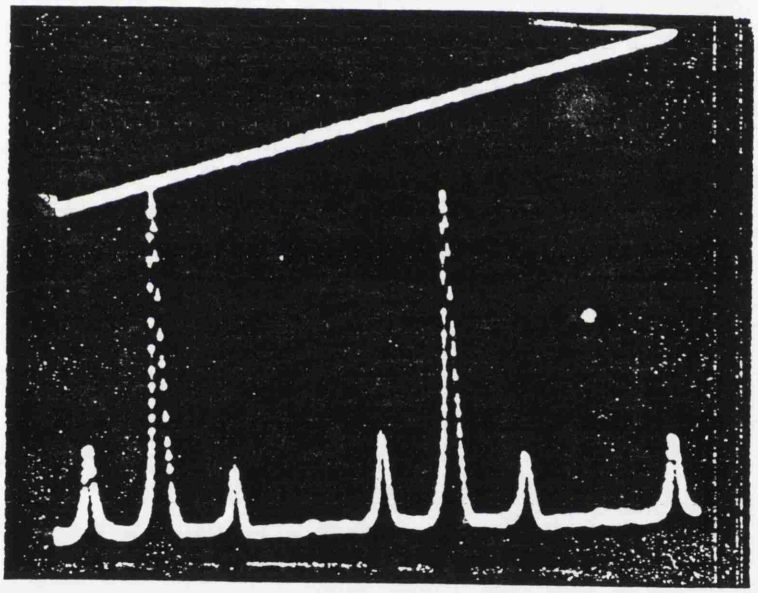

Figure 5.7

Laser Spectra observed on a 2GHz Free SpectralRange Scanning Fabry Perot
a) Free running diode under direct FM Modulation
b) Compound Cavity Module under direct FM Modulation
In both cases the modulation frequency was 500MHz and the modulation voltage was 158mV.

semiconductor laser to the point where it can be of use in a coherent system. The absolute stability of the semiconductor laser can also be improved.

However the modal instability and the inability to predict the wavelength at which the laser will operate render the compound cavity unsuitable for phase–sensitive systems.

5.3 EXTERNAL CAVITY MODULE

The most effective way to reduce the laser linewidth is to add a long passive section to the semiconductor laser in a "true external cavity."

To operate in a true external resonator the semiconductor laser cavity modes must be suppressed. The diode cavity modes can be suppressed by placing an anti–reflection (AR) coating on one of the diode facets. Once this has been done a mirror or diffraction grating can be used to feed light back into the diode and initiate lasing. It is the object of this section to detail the theory, design and operating characteristics of an external cavity module.

5.3.1 ANTI REFLECTION COATING

Standard wave theory states that at a boundary between two materials of different refractive index, partial reflection will take place at normal incidence. This is true unless a third layer of material is placed between the original two and that this material is also exactly 1/4 λ thick and of refractive index:

$$n_m = (n_1 n_2)^{1/2} \qquad 5.3.1$$

where n_m is the refractive index of the matching layer and n_1 and n_2 are the refractive indices of the original two materials. When these conditions have been met 100% transmission of the wave is possible.

The refractive index of the active region of the the HLP1400 laser diodes used in this project is approximately 3.5. The wavelength of the light emitted by the diode was 830nm. Using these figures, and asuming that the refractive index of air is one, the refractive index of

the matching material should be $(3.5)^{1/2}$ and of thickness 207.66nm.

As the department did not have facilities readily available for placing such a coating on a laser diode this work had to be contracted outwith the department. The coating had to be placed on the diodes at temperatures below 80^0C, otherwise the properties of the lasers would be substantially degraded.

Lasers were sent to two different companies for AR coatings. Initially one diode was sent to "Kendal and Hyde Optical Coatings." This company placed a cold V multi layer dieletric coating on the diode, which reduced the reflectivity of the facet from 31% to 2.3%. Another diode was sent to Optical and Eletrical Coatings who placed a TiO_2 coating on the laser. This coating reduced the reflectivity of the diode facet to around 0.3%.

Unfortunately, when a group of diodes which were matched in wavelength to better than 0.1nm was sent to OEC, the quality of the coating was drastically different. The three diodes which had been sent off together, were returned with the following reflectivities

Diode 2203 R = 0.6%
Diode 2207 R = 1.1%
Diode 2209 R = 31%

No satisfactory reason could be established for this spread in R. The three diodes all came from the same batch, with consecutive serial numbers. All the diodes were coated at the same time under the same conditions. The only obvious reason, other than extreme lack of care at the coating stage, is that the diodes had been coated previously with a passivating layer to protect the facet. However for this to have been the cause of the spread in R the passivating layers must all have been of different thicknesses. Although laser 2209 was sent for coating on more than one occassion the reflectivity of the laser mirror never altered. It is unclear why this was the case, but it did however point up the fact that the coatings were of variable quality.

Folowing further dialogue with the company, more diodes were sent

for coating. On this occasion the reflectivity of the diodes did not change at all. No further contact was made with this company.

After the above events had taken place the last diode was sent to Kendal and Hyde with the following result:

Diode 2206 R = 5%

5.3.2 MEASUREMENT OF THE REFLECTIVITY OF THE AR COATING

It is possible to measure the reflectivity of an AR coated facet of a semiconductor laser by comparing its new spectrum with its original spectrum[9]. This comparison has to be carried out at the original threshold current of the diode. The reflectivity is calculated by measuring the Fabry Perot modulation index which is superimposed upon the spontaneous emission profile of the diode, see Figure 5.8.

For a laser diode at threshold, the power modulation index, m, is unity, where m is defined as:

$$m = \frac{P_{max} - P_{min}}{P_{max} + P_{min}} \qquad 5.3.2$$

After coating, m is less than one, at the same driver current.

The roundtrip amplification factor for a laser can be written as

$$a = (R_1 R_2)^{1/2} \exp(2j\beta L) \exp 1/2(G_+ + G_-) \qquad 5.3.3$$

where G_+ and G_- are the power gain terms, β is the propagation term and R_1 and R_2 are defined as before. For a symmetrical AlGaAs diode with cleaved facets, $R_1 = R_2 = 31\%$ and $G_+ = G_- = G_1$.

The amplification factor a is related to m by

$$m = \frac{2|a|}{1 + |a|^2} \qquad 5.3.4$$

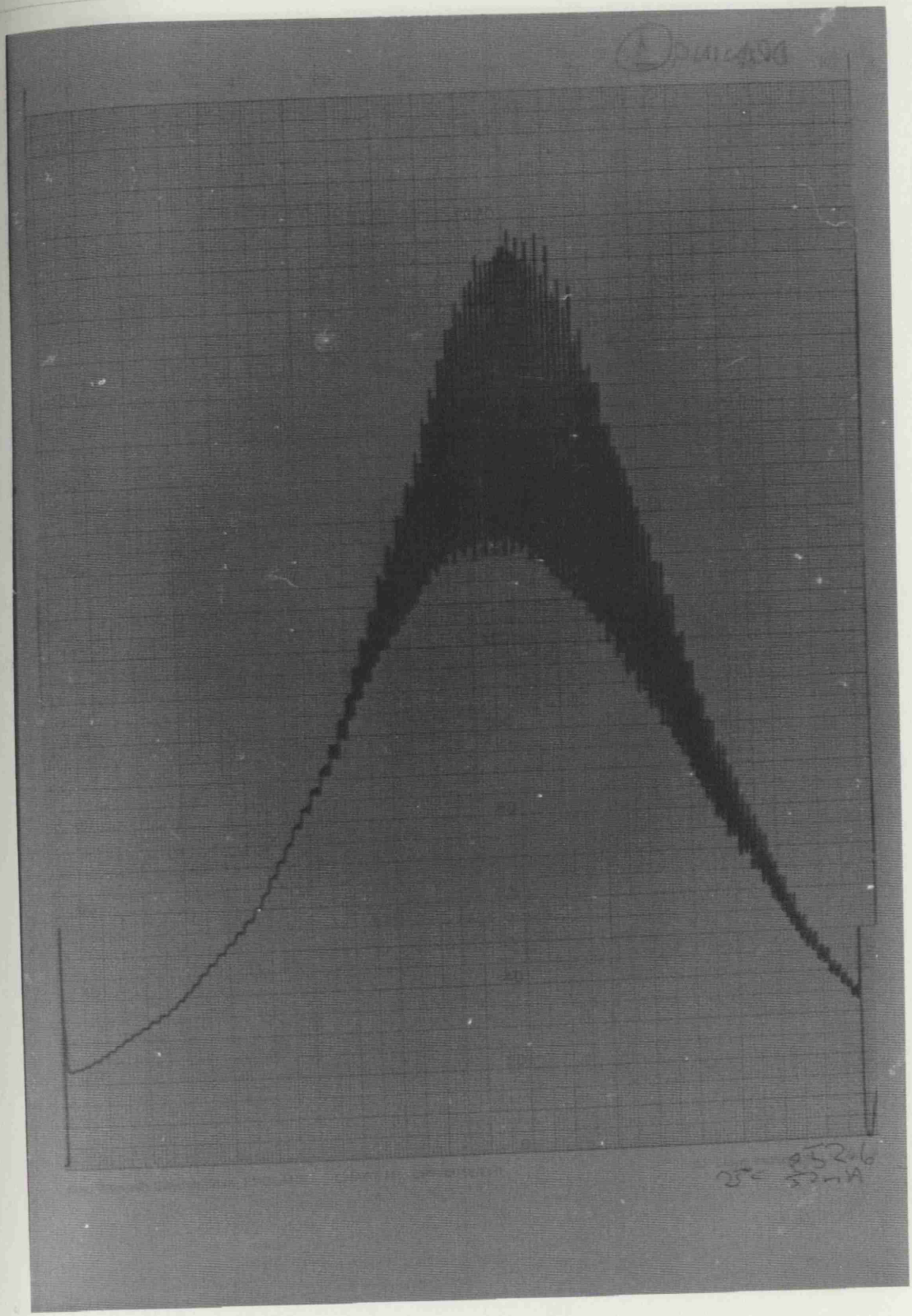

Figure 5.8a)

Spontaneous Emission Profile of HLP1400 Laser Diode
After Deposition of Titanium Dioxide AR Coating.
Facet Reflectivity = 0.3%
Measurement Range 807 - 852nm

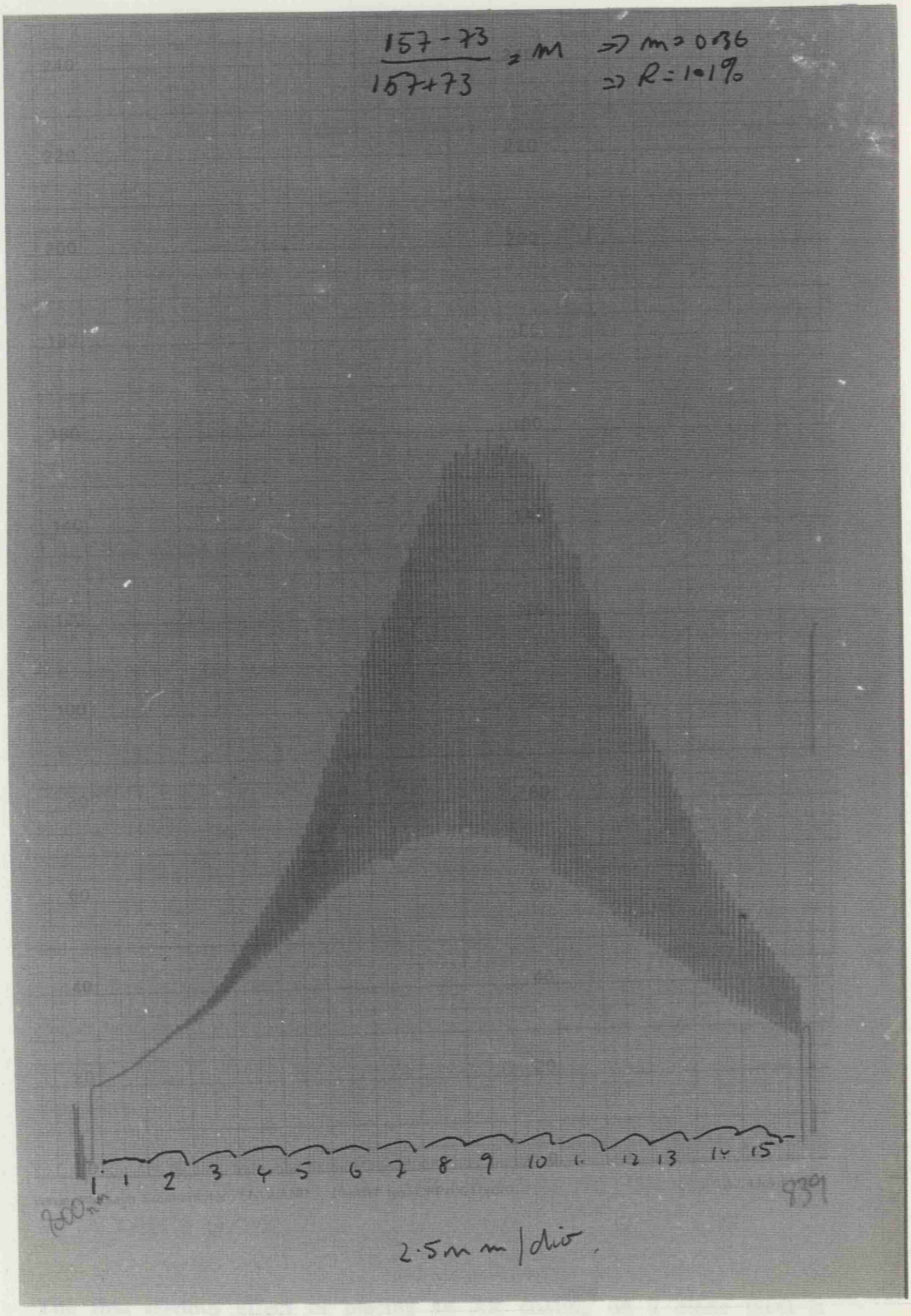

Figure 5.8b)

Spontaneous Emission Profile of HLP1400 Laser Diode No 2203 after Deposition of Titanium Dioxide AR Coating.
Facet Reflectivity = 1.1%
Measurement Range 800 - 839nm

Assuming a = 1 at threshold,

$$R_{AR} = |a|^2 R_1 = .32|a|^2 \qquad 5.3.5$$

The residual Fabry Perot modulation index has to be measured at the original threshold of the laser for the previous equation to be valid, as only then can gain saturation be neglected. M can be measured by driving the laser at I_T and directing the beam into a scanning monochromator. The resolution of the monochromator should be better than c/2nl so that peaks and troughs in the spectra may be resolved. The output from the monochromator must be monitored on a power meter. Figure 5.8 shows spectra from the coated lasers.

5.3.3 EXPERIMENTAL MODULE

Figure 5.9 shows a photograph of the external cavity module used in this project. The laser diode was mounted on an aluminium heatsink which was temperature controlled using the controller described in 4.5. Light was coupled out of both facets using FLA40 collimating lenses. The beam from the AR coated front facet was fired onto a diffraction grating which was mounted with its grating lines perpendicular to the active layer. The grating,which was blazed for 750nm, was aligned to feed light back into the cavity. Light from the rear facet was used in the measurement set up. The lenses were mounted on Micro–Controle translation stages and the grating was held in a Physik Instrumente piezo–electrically controlled gimbal mount that also had longitudinal motion. All of these components were mounted onto an aluminium baseplate.

5.3.4 EFFECTS OF PLACING AN AR COATING ON ONE FACET OF A LASER DIODE

The first obvious effect of placing an AR coating on a diode facet is that the threshold current of the diode increases. Figure 5.10 shows plots of the power–current characteristics of a coated diode, both before and after coating. The diode used for this experiment was the first to be coated with Titanium Dioxide. The threshold current increased by about 55%, from 56mA to 80mA. This was in line with

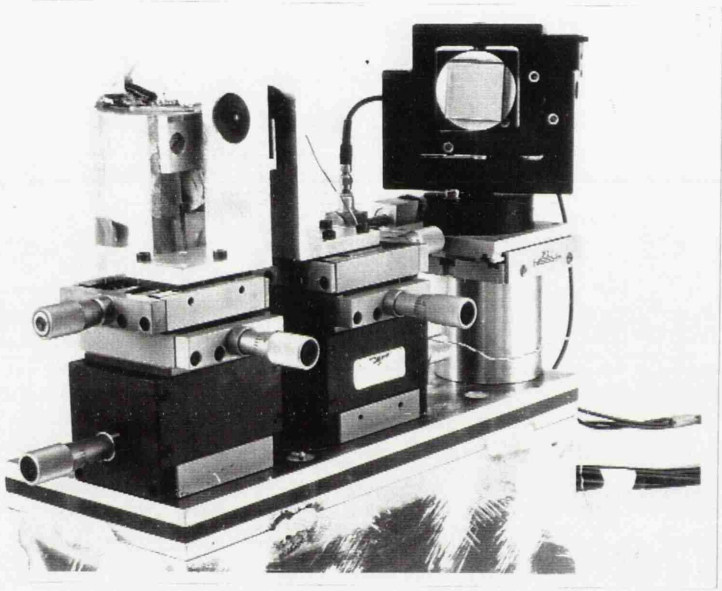

Figure 5.9

Photograph of the External Cavity Laser Module

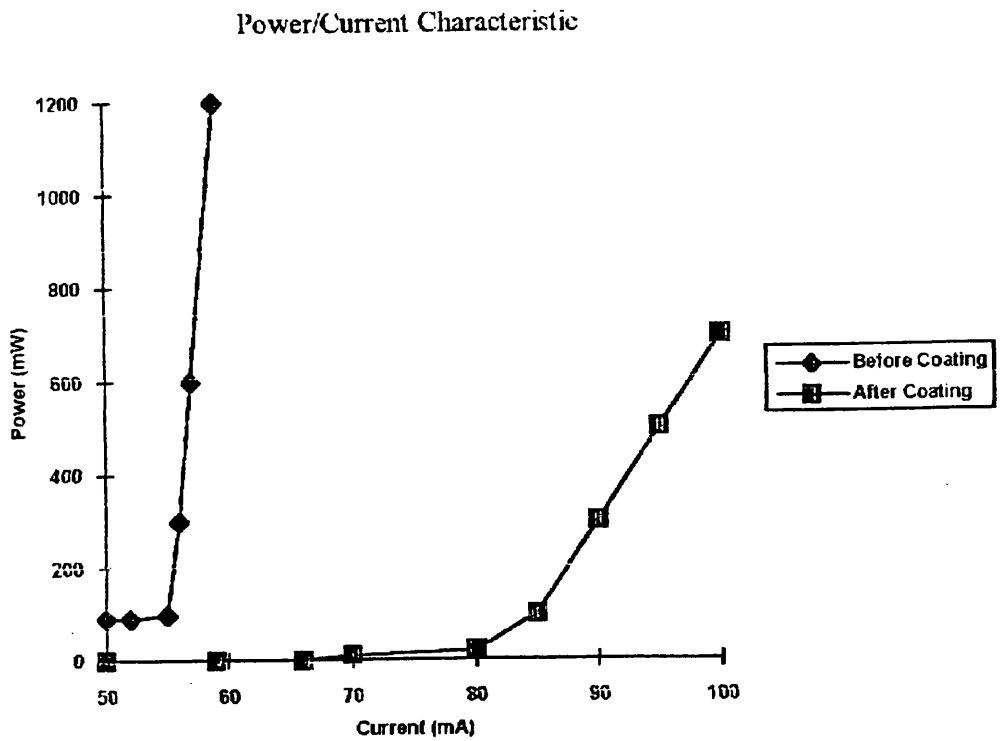

Figure 5.10 HLP 1400 Power/Current Characteristics both before and after deposition of a TiO_2 Anti-Reflection Coating

expectations.

The spectral spread of frequencies available to feed light back into the diode is also much increased as the bandwwidth of the cold cavity has been increased. Figure 5.11 shows a plot of output power against wavelength when light was fed back from a blazed diffraction grating. The diode used in this experiment had an original threshold current of 56mA and a new one of 77mA. During the experiment it was biased at 66mA. At all points on the graph the side mode suppression was greater than 13dB and at the peak the suppression was greater than 26dB. Unfortunately the tuning was not continuous but rather the wavelength changed in discrete steps of 0.3nm. This was as a result of a residual reflectivity of the AR coated lasers facet. It was possible however to access any wavelength within the tuning range by adjusting the current or temperature. Some periodic tuning was also possible by adjusting the length of the cavity.

EVIDENCE OF HOMOGENEOUS BROADENING

The external cavity module operated in a single longitudinal mode when the grating was replaced by a plane mirror. The wavelength of the module was then adjusted by adjusting the length of the cavity.

When no frequency selective elements were used in the external cavity the laser still exhibited monomode operation. This suggests that the laser was homogeneously broadened.

5.3.5 THEORY OF LINEWIDTH REDUCTION AND MODAL STABILITY OF AN EXTERNAL CAVITY SEMICONDUCTOR LASER MODULE

It was shown in section 4.3 that the FWHM of a semiconductor laser spectrum varies inversely with the square of the cavity length. If a passive section is added to the cavity the linewidth will therefore decrease as $1/L^2$. The physical reasons for this reduction are that the relative average spontaneous emission rate into the lasing mode has been reduced and that the number of lasing photons in the mode has increased. Both of these effects depend upon the size of the cavity

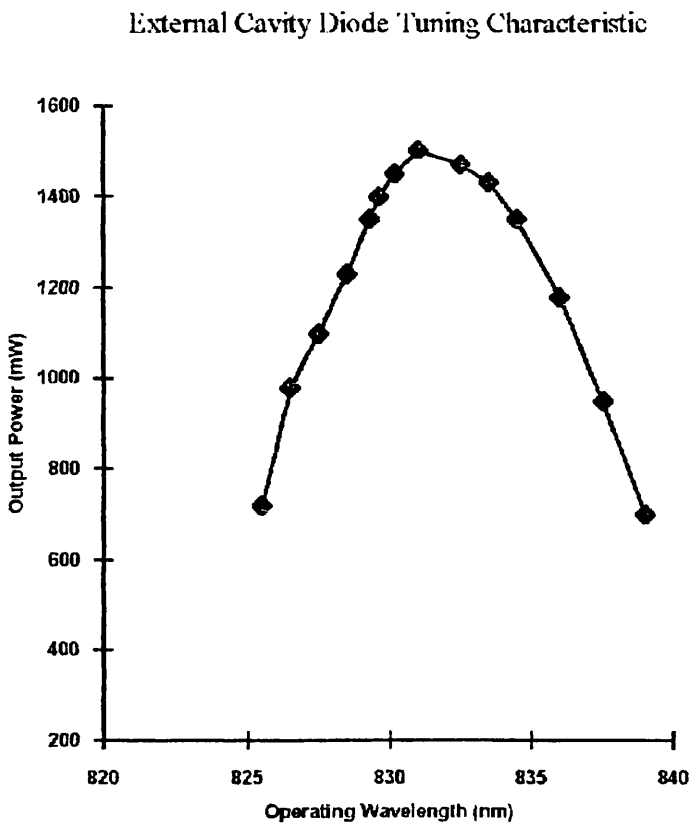

Figure 5.11 Tuning Characteristics of External Cavity Laser Diode Module

and since the only geometrical change was a change in length the overall reduction factor is $1/L^2$.

Concommitant with this reduction in linewidth there is a large reduction in the modulation sensitivity of the laser. This is as a result of the reduced effect that changes in the length of the active region of the semiconductor have in altering the frequency of the new laser module. The effect of fractional changes in the optical length of the semiconductor upon the frequency of the module are reduced by

$$\frac{nl}{nl + L} \qquad L>>nl \qquad 5.3.6$$

When the laser is operating in the external cavity its frequency stability depends upon the mechanical stability of the external resonator. The frequency of the laser changes whenever the length of the cavity changes according to

$$\Delta\nu = -\frac{\nu}{L}\Delta L \qquad 5.3.7$$

where $\Delta\nu$ is the change in frequency and ΔL is the change in length of the cavity. From this equation it is easy to show that for a 12cm long external cavity the frequency will shift by 10MHz for a 3nm longitudinal movement of the grating

The modes in the external resonator are separated in frequency by

$$\Delta f = \frac{c}{2L} \qquad 5.3.8$$

For a 12cm cavity Δf is around 1.2GHz.

5.3.6 EXPERIMENTS ON AND OBSERVATIONS OF OPERATION OF THE EXTERNAL CAVITY MODULE

5.3.6a LINEWIDTH

The linewidth was measured using the self homodyne technique with

2.5km of fibre delay. As this experiment only has a resolution of 100kHz one can only say that the linewidth was below this value. However, using the graph in Figure 4.14 it can be said that the linewidth of these modules was less than 50kHz. Figure 5.12 shows some results from the self homodyne experiment. These results were confirmed in later experiments where two laser modules were heterodyned, see chapter 6.

5.3.6b FREQUENCY MODULATION CHARACTERISTICS

The modulation characteristics of the external cavity module are drastically different from those of a free running diode. The frequency deviation for a given change in diode current is reduced by the factor nl/(nl + L) and this effect has been confirmed experimentaly.

5.3.6c POWER VS CURRENT

When the module is operated under feedback the laser threshold current can be reduced to the previous threshold current if enough light can be coupled back into the diode. Figure 5.13 shows the power vs current characteristic both before coating and also when the laser is operated under feedback from a blazed grating. The grating was blazed for optimum operation at 780nm.

5.3.6d STABILITY

Although this module was susceptible to low frequency vibrations it operated much better than the compound cavity structure. This module did not have the same tendency to mode hop but rather the vibrations only caused the frequecy of the module to change continuously. Figure 5.14 demonstrates the instability of the laser. This trace was taken from a FPI in non−scanning mode. This experiment is described in section 5.2.3d.

The laser of course did mode hop from time to time. The size of the mode hop was dictated by the length of the external cavity.

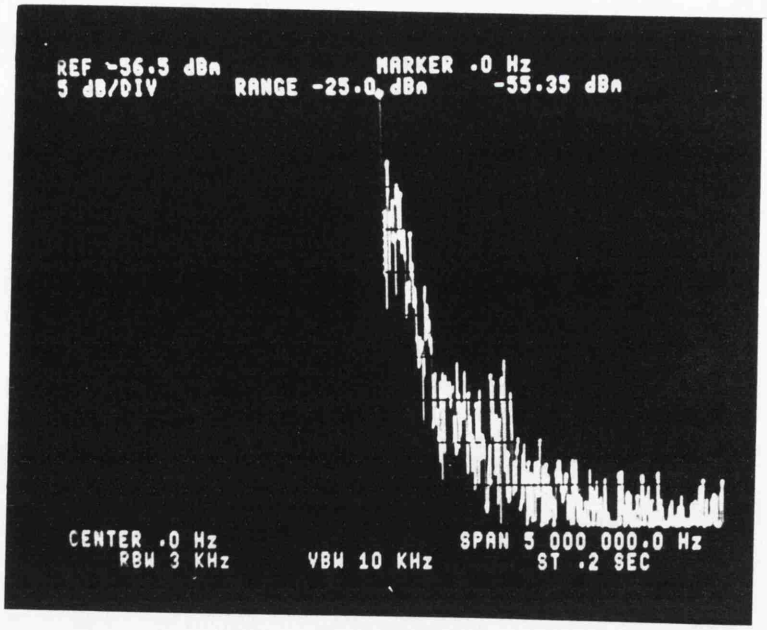

a)

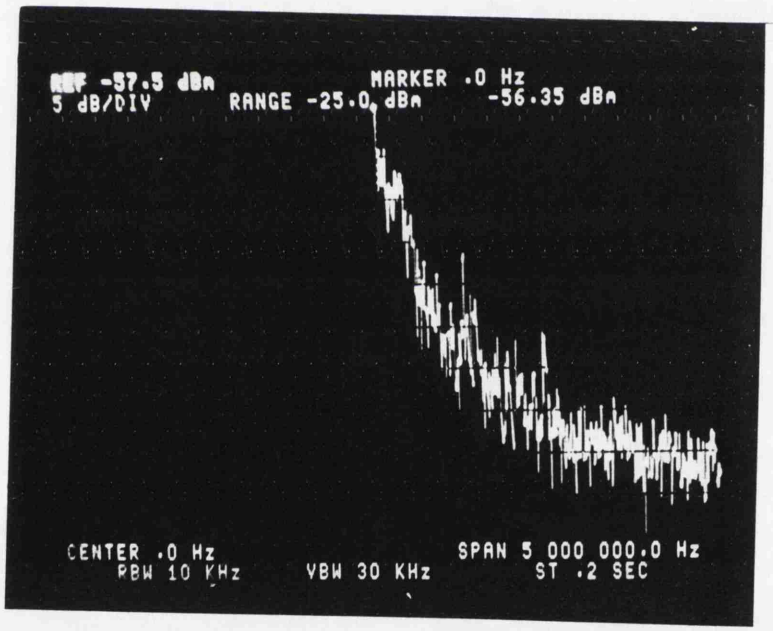

b)

Figure 5.12 Linewidth Measurement External Cavity Laser Module
a) Diode 2207 Linewidth approximately 90kHz
b) Diode 2203 Linewidth approximately 60kHz

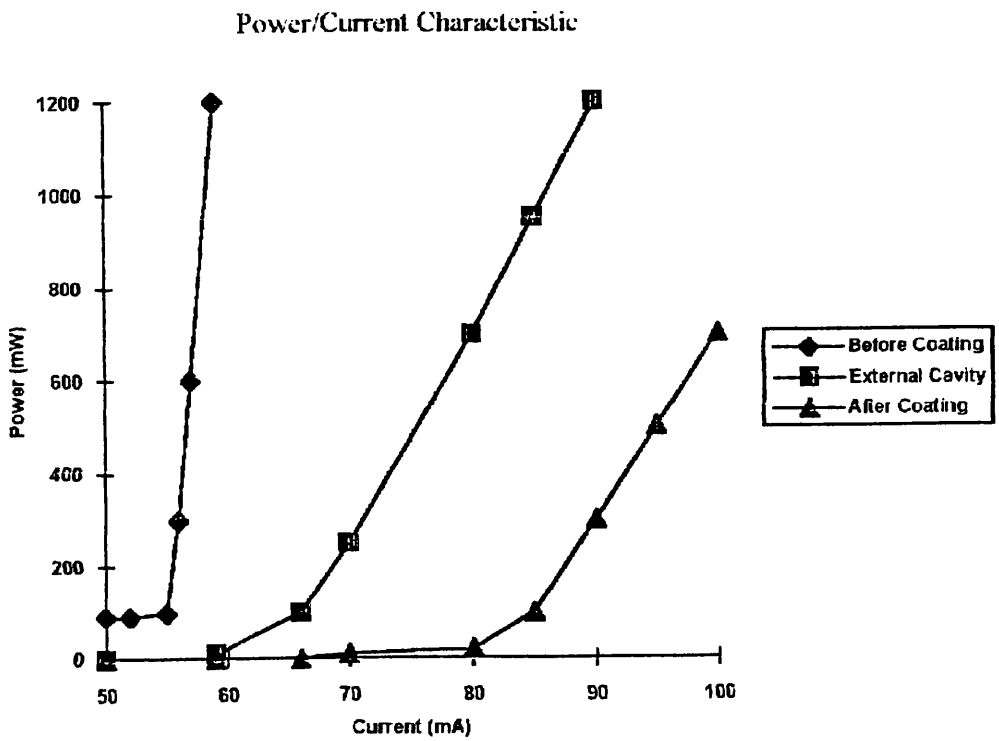

Figure 5.13 This Figure displays the Power/Current Characteristics of a HLP1400 Laser Diode before coating, after coating and also in an external cavity

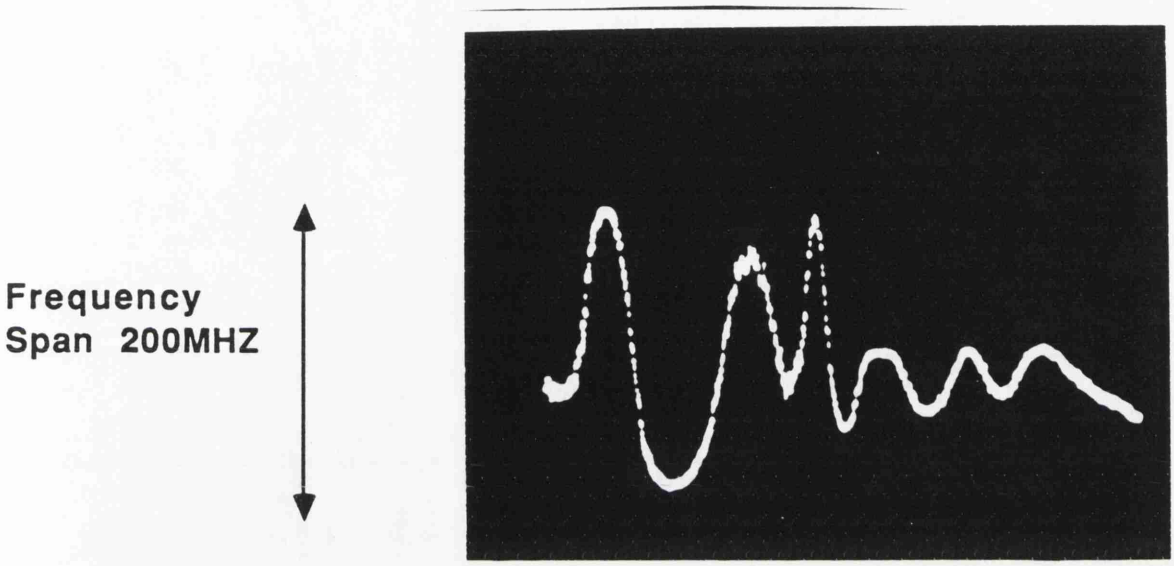

Figure 5.14

Laser Diode Frequency Fluctuations observed on Fabry Perot Interferometer in Non Scanning Mode.

5.3.6e FREQUENCY STABILISATION CONTROL LOOP

If a laser module is to be used as a source for coherent communications then it is essential that the laser frequency be relatively stable. The frequency must not drift by amounts greater than the bandwidth of the front–end receiver, which will typically be less than 1GHz.

The major problem with the use of external reflectors, whether in a compound cavity or external cavity module, to reduce the linewidth of semiconductor lasers is that the laser frequency becomes dependent upon the stability of the reflector relative to the diode. Fluctuations of as little as a few nanometers can result in frequency changes of 10's of MHz. It is therefore of paramount importance that the external reflector be extremely well stabilised and that the length of the cavity be well controlled.

Figure 5.15 shows a diagram of the servo control loop used to stabilise the frequency of the laser module by stabilising the external reflector.

Part of the laser beam was directed into a SFPI which was operating in non–scanning mode. The FP was aligned for maximum transmission of the laser signal. Figure 16 shows a trace of the transmission characteristics of the FP. A small dither signal of a frequency of 5kHz was applied to the piezo drive of the FP. The output of the FP was then mixed with the dither signal. The output of the mixer was then processed through a low pass filter and a three term controller before being fed back to the longitudinal control of the external reflector.

Figure 17 shows a photograph of the detected output of the FP when the dither signal was applied. The dither signal is also shown in this photograph.

RESULTS

The control loop worked partially. The loop held the laser signal

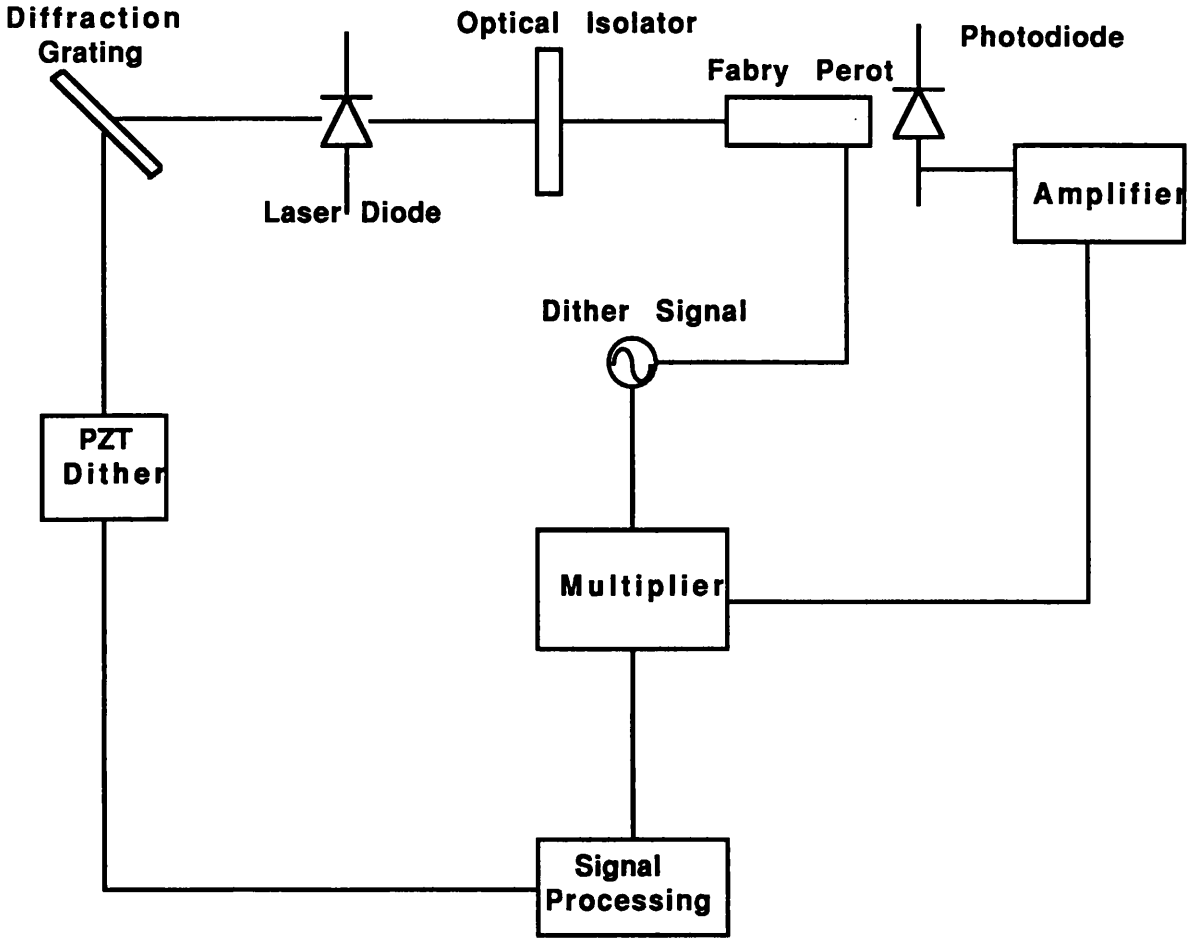

Figure 5.15

Schematic of Fabry Perot Stabilisation Circuitry

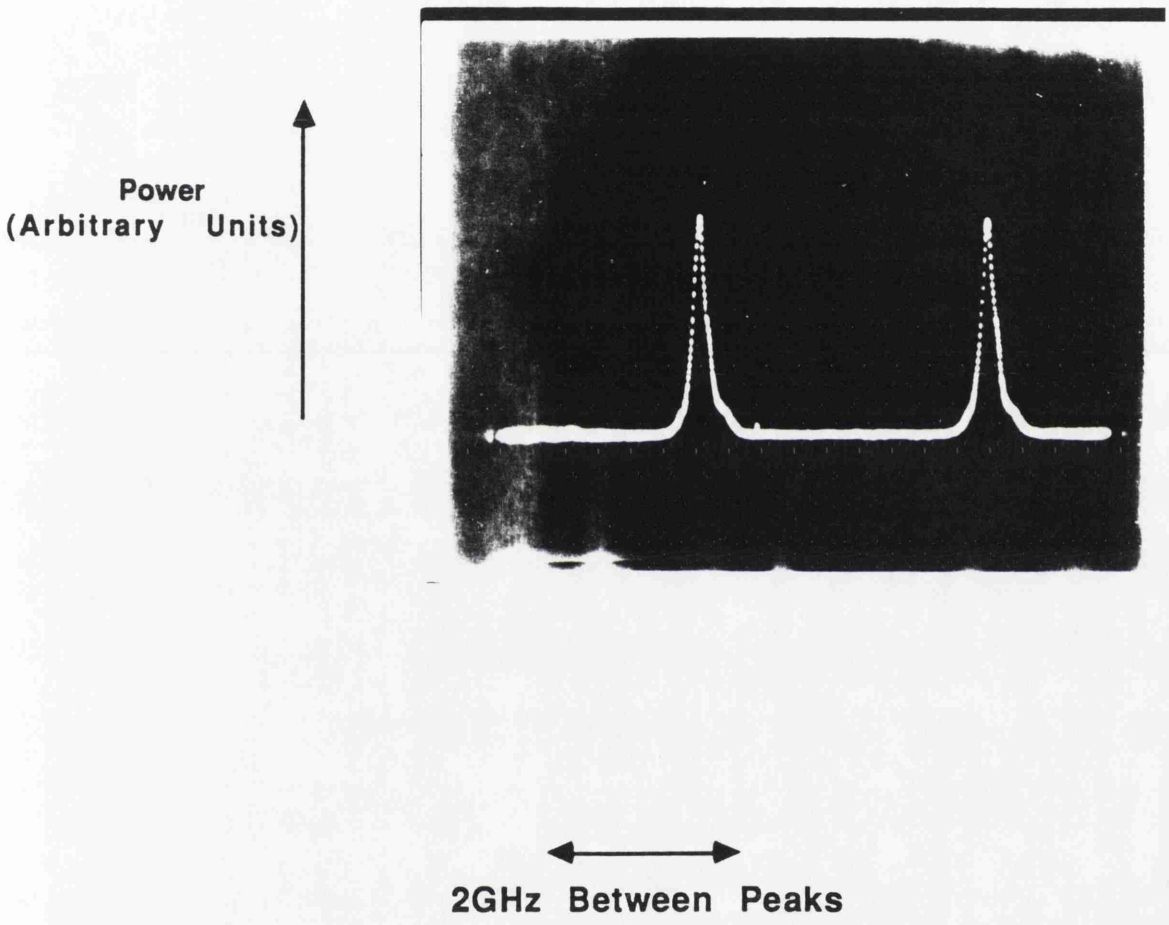

Figure 5.16

Fabry Perot Transmission Characteristic
2GHz Free Spectral Range

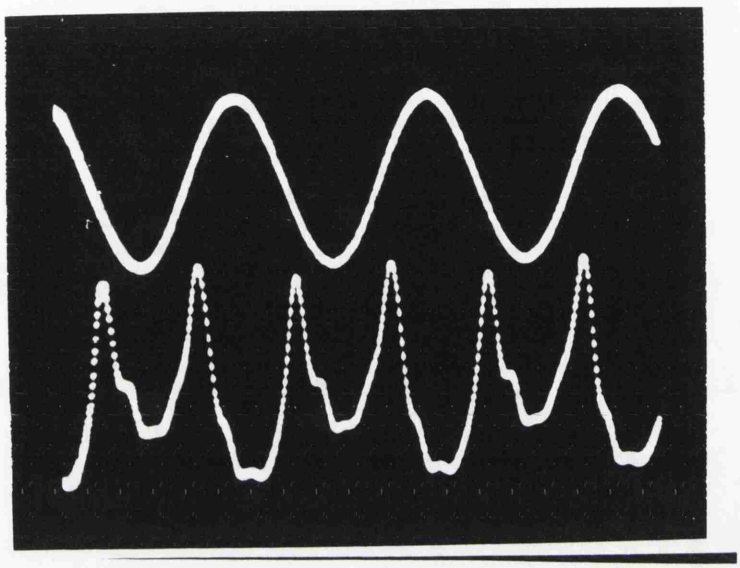

Figure 5.17

Dither Signal and corresponding Error Signal From Fabry Perot Stabilisation Control Loop

within the bandwidth (80MHz) of the FP transmission characteristic until the laser mount expanded more than .5μm (.5μm was the maximum expansion of the piezo controller). The control loop did not, however, compensate satisfactorily for small vibrations. With hindsight this would appear to have been the result of two problems. Firstly it is most probable that the power supply for the piezo driver did not have a fast enough frequency response to cope with the vibrations. Secondly the mechanical design of the laser module, not wholly under the author's control, should be improved upon. The optical axis was some 22 cm above the optical bench. Many of the components including the laser, the lenses and the grating were only secured at their bases leaving them to oscillate like tuning forks.

5.3.7. PRACTICAL DESIGN CONSIDERATIONS FOR FUTURE

1) The external cavity mount should be made from Super Invar[10] which has a very low thermal expansion coefficient, $\alpha_{\text{super invar}} = 3.6 * 10^{-7}K^{-1}m^{-1}$ and $\alpha_{AL} = 2.5 * 10^{-5}K^{-1}m^{-1}$.

2) The diodes used in this project were 300μm long which corresponds to a 0.3nm mode spacing. It would be better if the diode cavity was shorter so that the residual modes would be further apart. This would of course place more stringent requirements on other aspects of the laser operation.

3) The grating should be mounted with its lines parallel to the active region. This allows more lines to be covered, as the angular spread of the beam coming from the diode is greater in the perpendicular direction, and allows the resolution to be increased.

4)Shorter cavity lengths should be used so that the side-mode suppression ratio may be increased. Alternatively, an intra-cavity etalon could be used. This will also improve the modal stability as the cavity modes will be further apart and so the frequency will have to change by a larger amount before hopping can take place.

5) The mechanical design of the laser module should be completely overhauled. Firstly the grating should be mounted directly onto a

piezo– electric stack. The diode and all optics should all be mounted as close as possible to the baseplate and the component stands should be secured both above and below the optical axis. The overall dimensions of the external cavity should also be reduced and all components should be contained within a sealed container. The optics should be secured in place using UV curing glues and the only mobile component should be the piezoelectrically controlled grating.

Ideally a mount should be machined, to which the laser and optics are glued.

6) It could be beneficial to use an intra cavity phase modulator to tune the module. This would be most useful in a frequency stabilisation loop.

5.4 ALTERNATIVE LASER STRUCTURES

The previous two approaches to changing the operating characteristics have involved external reflectors which introduce mechanical stabilisation problems. An alternative approach is to alter the design of the laser structure at the fabrication stage. There are already several different kinds of semiconductor laser structure which have been grown and are currently under investigation as possible sources for coherent communication. This section will describe some of these alternative structures and give some details of their operating characteristics.

5.4.1 DISTRIBUTED FEEDBACK LASER

The laser structure upon which most hope is placed as a future source for coherent optical communications is the distributed feedback, DFB, laser diode. A simplified structure of one such device is shown in figure 5.18. Unlike the Fabry Perot laser structure the optical feedback mechanism in a DFB comes from a periodic perturbation of one of the cladding layers and not from two cleaved mirrors at either end of the cavity. The end facets should also be AR coated so that there is as little FP modulation as possible. The grating which produces the feedback gives the laser different characteristics such as guaranteed monomode operation, see below.

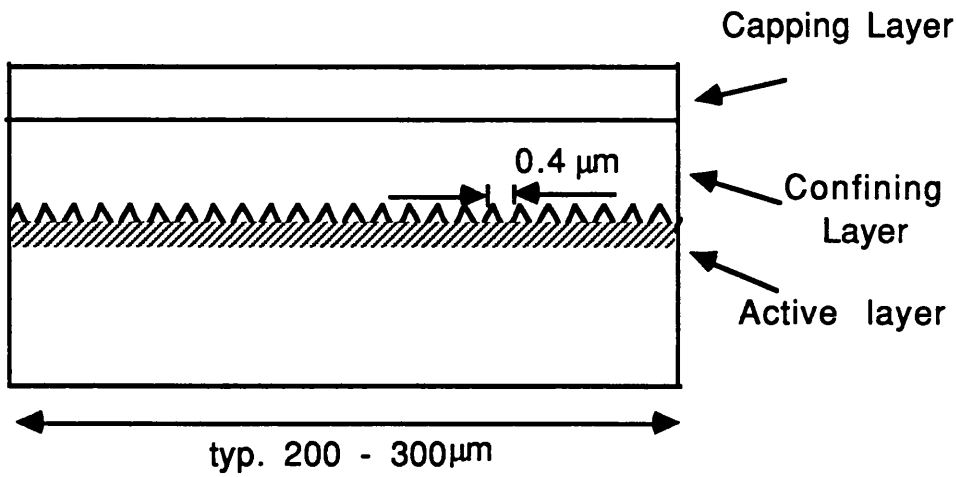

Figure 5.18 DFB Laser Diode

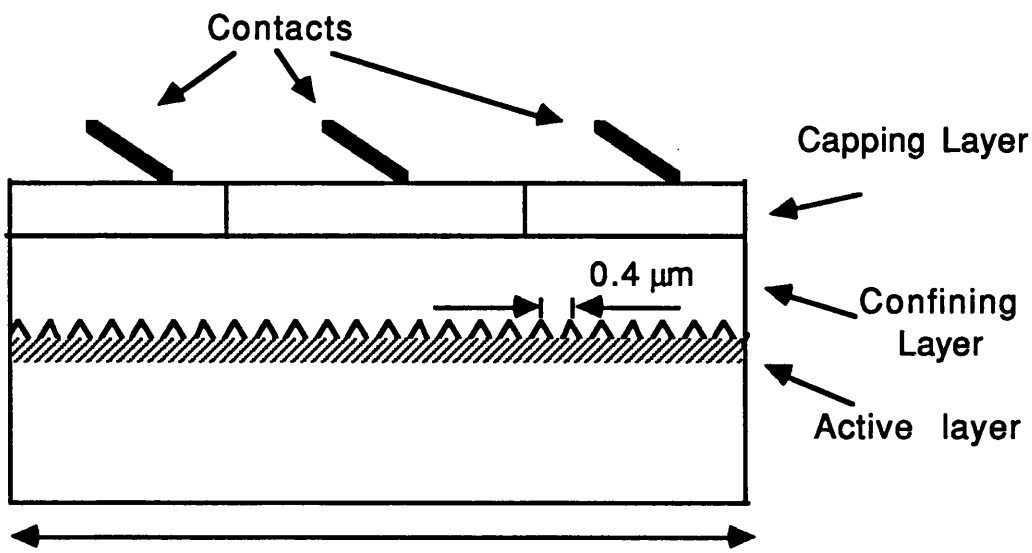

Figure 5.18a Multi-section DFB Laser Diode

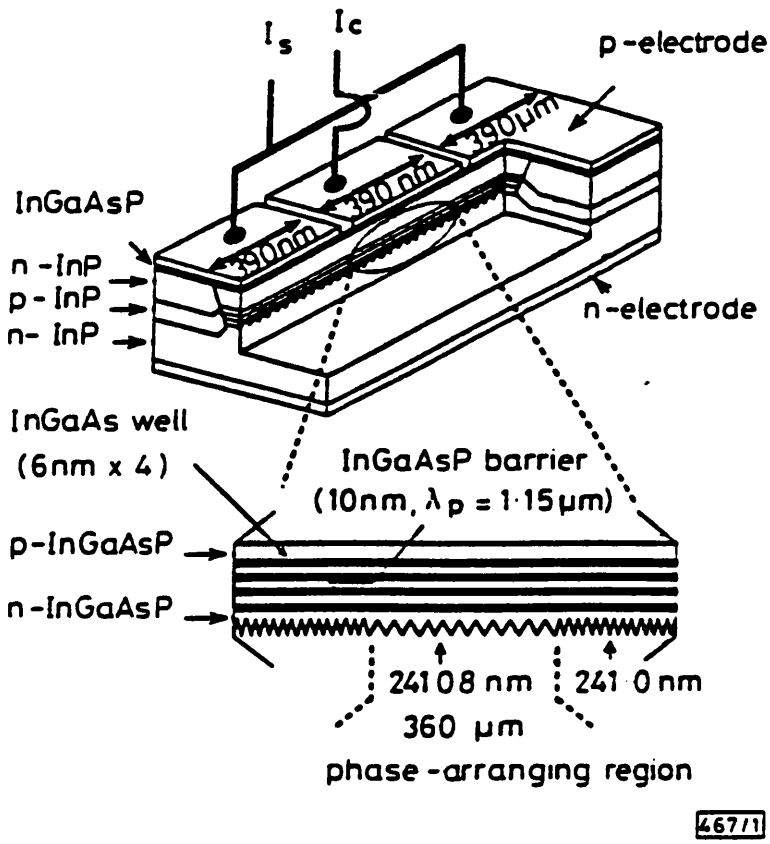

Figure 5.18c Schematic structure of three section corrugation pitch modulated multi quantum well DFB laser [30]

In recent years multiterminal DFB lasers have been designed and manufactured. These devices allow the user to supply different sections of the active region with different biassing. A schematic diagram is shown in figure 5.18b. In even more complex structures different pitches of grating are used to enable better wavelength selection and narrower linewidth lasers. A schematic of such a device is shown in figure 5.18c[30]. Multiple Qauntum Well designs have also reduced the linewidth of the laser by reducing the α, linewidth enhancement factor.

5.4.1a MODAL CHARACTERISTICS

As a result of the frequency selectivity of a dispersive element, ie the grating, the DFB laser can be made monomode. To ensure monomode oscillation a phase shift must be included in the grating. Otherwise two anti–resonant modes may oscillate.

The side mode suppression ratio can typically be greater than 35dB. The mode is also more stable as the frequency of the laser depends more on the grating than on the optical length of the cavity.

DFBs are extremely sensitive to uncontrolled feedback[25,27,28].

5.4.1b LINEWIDTH

In general the linewidth of these devices is still too large for coherent optical communication schemes. Linewidths of single section DFB are typically in the range of 10 – 100 MHz. The overall trend, however, is downward[17,18].

Recently devices have been manufactured with a minimum linewidth of 70kHz[19]. This device was 1450μm long and had a linewidth power product of around 0.2MHz mw^{-1}. The laser was a strained MQW DFB. The reduction in linewidth was as a result of a reduced α factor and the length of the diode, 1450μm. More recently a three section corrugation pitch modulated device has operated cw over a tuning range of 1.3nm with a wavelength of less than 100kHz[30].

5.4.1c OUTPUT POWER

DFB lasers have been built to give output powers equivalent to that of FP devices. DFB laser diodes have been produced which emit 10's of milliwatts.

5.4.1d MODULATION and TUNING

One major drawback of single section DFB laser diodes is that they have very narrow tuning ranges, typically less than 2nm but often as low as 0.1nm. This is as a result of the laser wavelength being largely dependent upon the grating. Single section DFBs also have non– linear modulation characteristics and are not ideally suited to direct current modulation. This however, has been overcome by fabricating multisection– multicontact devices with corrugation pitch modulation. These devices offer many improvements in terms of tunability and modulation. They are, however, expensive as they are difficult to manufacture. Recently a device has been manufactured with a 7nm tuning range with a minimum linewidth of 3MHz[20].

5.4.1e OBSERVATIONS ON SUITABILITY FOR COHERENT COMMUNICATIONS

On the negative side DFB lasers are extremely sensitive to the effects of uncontrolled reflections[25] and in general have narrow tuning ranges. They also require lithographic techniques which makes their manufacture more expensive than Fabry Perot Devices[17,18,27,28].

The major attractions of DFB lasers are that they can be integrated far more easily than FP structures and that they can be guaranteed to operate monomode. With multicontact designs they also offer controlled modulation and scope for extended tuning ranges of greater than 2nm..

5.4.2 DISTRIBUTED BRAGG REFLECTOR

The structure of the DBR laser diode is shown in figure 5.19. This is a more complicated structure than that of the DFB laser in that it

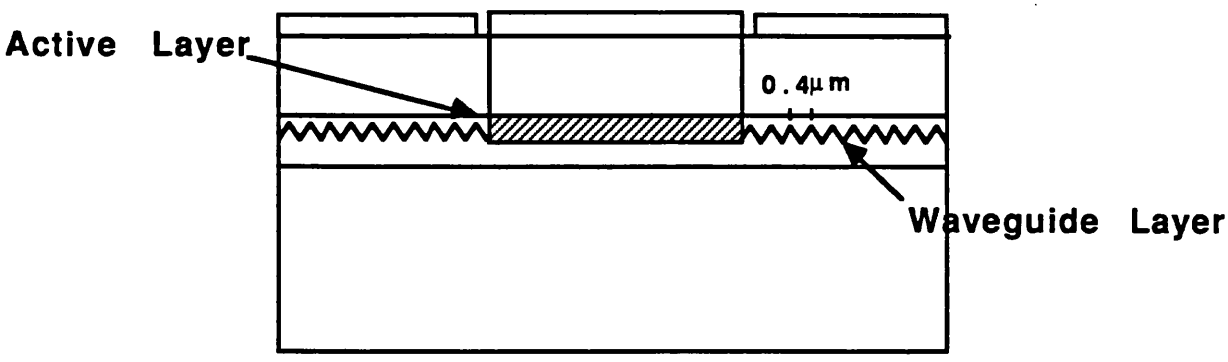

Figure 5.19a Schematic Diagram of a DBR Laser Diode

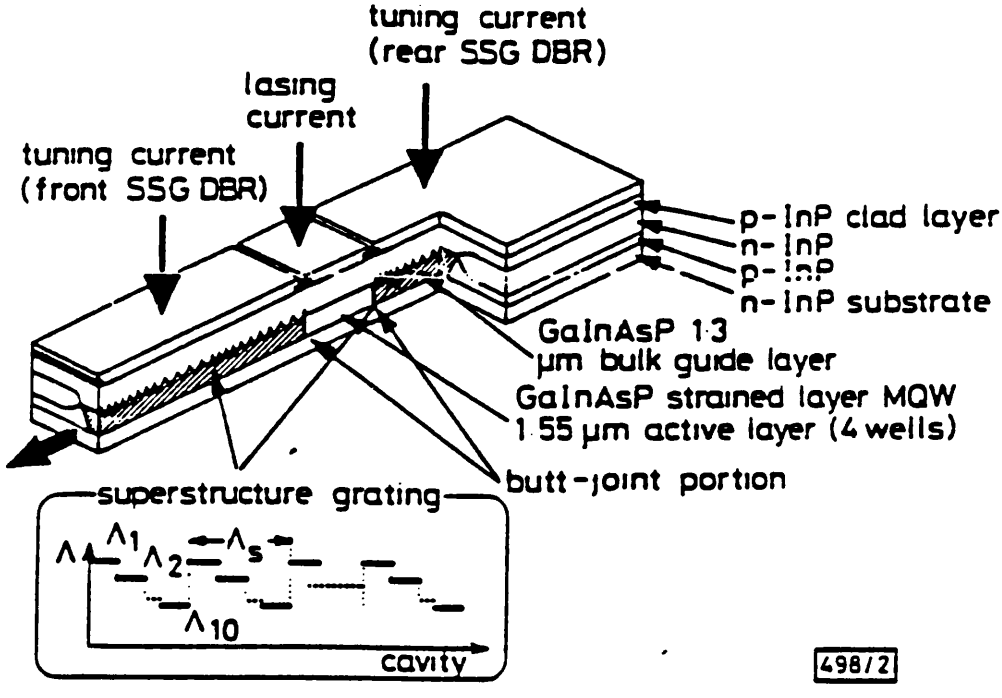

Figure 5.19b Schematic structure of 1.55 micron wavelength tunable butt-joint DBR laser with superstructure grating reflectors

has separate gain and tuning regions.

5.4.2a LINEWIDTH AND MODAL CHARACTERISTICS

The linewidth of a DBR laser diode is comparable with that of a DFB laser, typically 10 – 100MHz. DBR lasers are similar to the DFB lasers because they too are monomode devices. The linewidth will be driven down by using MQW technology, resulting in improvements of as much as a factor of 5 or more.

5.4.2b MODULATION AND TUNING

DBR lasers have wider tuning ranges than DFB lasers as the grating region is normally operated below threshold, thus allowing for larger changes in carrier concentration. Unfortunately, many of these devices suffer from mode hopping as a result of FP modulation of the active cavity.

DBRs have recently been manufactured with tuning ranges approaching 100nm. These devices use a complicated modulation of the external grating to allow for a frequency selective feedback which is controlled by the refractive index of the grating region. The refractive index is controlled by the bias current applied to that region. The structure of such a device is shown in figure 5.19b[31].

5.4.4 CLEAVED COUPLED CAVITY LASER

Cleaved coupled cavity laser structures, C^3 lasers, are another alternative to the standard FP laser diode. Figure 5.20 shows a schematic representation of such a device. The device is just a laser diode with an air gap in the middle. Current bias has to be applied to both sides of the device and by varying the bias of one part relative to the other, the properties of the C^3 laser can be made to vary[22].

Although these devices have shown promising results their operating characteristics are critically dependent upon the size of the air gap, which in practice, is extremely difficult to control. Over recent years

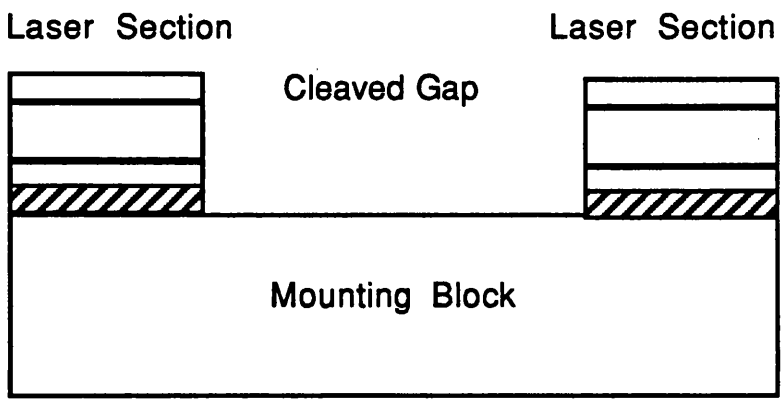

Figure 5.20 Cleaved Couple Cavity Laser (C^3)

interest in these devices has waned.

5.4.4a LINEWIDTH

The linewidth of these diodes has been measured to be as low as 250kHz at 10mw output power. This was achieved using a variable air gap to optimise operation. In typical fixed airgap devices the linewidth*power product is of the order of 30MHzmw.

5.4.4b MODAL STRUCTURE

Under optimum conditions these device have been measured as having side mode suppression ratios of around 34dB.

5.4.5 INTEGRATED PASSIVE CAVITY LASER

This laser structure is shown in figure 5.21. This laser has a line narrowed spectrum obtained by using the same principle as the external cavity, i.e. by increasing the photon lifetime. The advantage of this system over the external cavity is that there is no mechanical vibration problem.

The linewidth of such a device has been measured to be less than 1MHz. The disadvantage of this device when compared to the external cavity described previously is that this device only has a small tuning range[23].

5.4.6 LINEWIDTH REDUCTION AND FREQUENCY STABILISATION USING ELECTRICAL FEEDBACK.

It is possible to reduce the linewidth of a semiconductor laser by using negative electrical feedback[24]. Figure 5.22 shows a diagram of the experimental technique. A Fabry Perot interferometer is used as a frequency discriminator for the FM noise detection, and the output signal from the detector is negatively fed back to the laser.

Using this technique the linewidth of a laser has been reduced from 5MHz to 330kHz. The stability of the laser is also improved as a

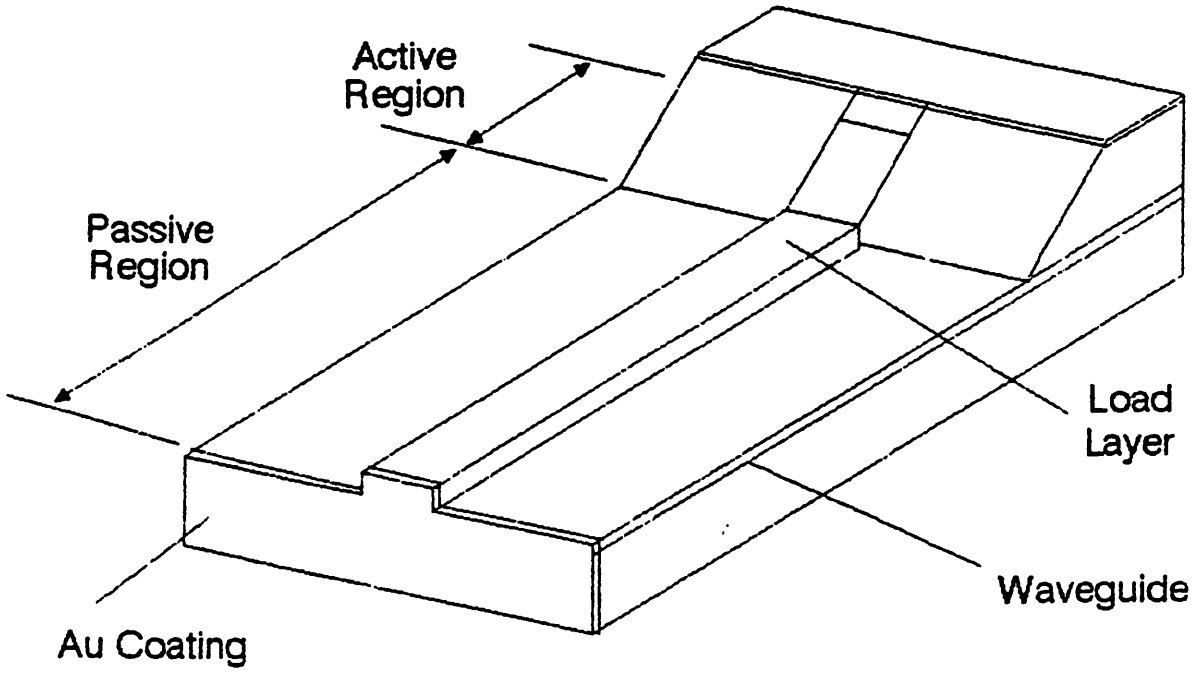

Figure 5.21 Passive Cavity Laser Diode

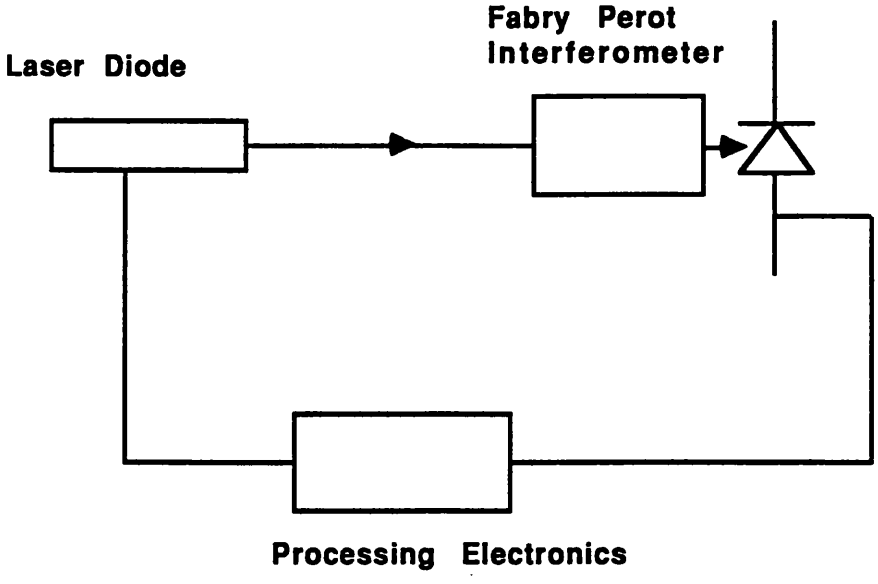

Figure 5.22 Schematic Diagram of system to reduce the laser linewidth using negative electrical feedback

result of the diode being locked in frequency onto the side of a FP transmission curve. The major advantage of this scheme is that provided one modulates at rates greater than the bandwidth of the feedback loop the modulation characteristics of the laser are unaffected.

The limitations of this scheme are dependent upon the processing time and in the added system complexity. Wholly integrated negative feedback loops may be possible in the future.

5.5 CONCLUSIONS

An ideal optical source for coherent communications would be monomode, tunable over the bandwidth of the low loss window in optical fibre, 50,000GHz, be stable in frequency but be capable of modulation at rates upto a few GHz. The source would also have a narrow linewidth and should not mode hop. The device should also be insensitive to optical feedback and emit several milliwatts of power.

From the properties of the laser modules and alternative laser structures described earlier it is clear that no individual device scores well on all of these fronts. Immediately one can reject the compound cavity module as it is extremely sensitive to changes in any of its parameters. It also has poor tuning characteristics. The C^3 laser can also be rejected for, although it has many of the desired properties such as narrow linewidth, monomode operation with the potential for modulation, it is extremely difficult to optimise the properties of the laser. In addition it has so far proven difficult if not impossible to manufacture, in bulk, many devices with similar operating characteristics, as the properties of the device are governed by the size of the air gap. Recently not much has been reported on C^3 devices.

The external cavity module has a narrow linewidth (less than100kHz), monomode operation and a large tuning range well in excess of 10nm. It may even be possible to compensate for mechanical vibrations of the cavity by building a servo–control loop, see section 5.3.6e. This type of stabilisation may work well if the feedback loop ends on an

intra–cavity phase modulator rather than on a piezo–electrically controlled mirror mount. B.T. have developed a packaged device which has performed well in field trials. Currently these devices outperform free running lasers in terms of tunability, stability and spectral purity. In addition they are useful laboratory tools and should therefore be further developed.

The long term future for coherent optical communications, however, probably lies in building wholly integrated receivers. This will reduce the propagation delay in the loop and will thus reduce the overall linewidth requirement. With this in mind the most promising devices for the long term are probably MQW multi–contact DFB laser diodes and multi–contact DBR laser diodes incorporating corrugation pitch modulation. Much research and development, however, is still required. In particular the sensitivity of DFBs to reflections has to be resolved and narrow linewidths have to be guaranteed.

The integrated passive cavity gives the small laser chip the required linewidth for coherent systems while removing the mechanical instabilities of an external resonator. Since the major problems with the DFB are that it has a large linewidth and that it is sensitive to uncontrolled feedback a possible solution may be to add an integrated passive cavity.

REFERENCES

1. R.P. Salathe "Diode lasers coupled to External Resonators" Applied Physics vol 20, pp 1 – 18, 1979.

2. O. Nilsson, S. Saito and Y. Yamamoto "Oscillation Frequency, Linewidth Reduction and Frequency Modulation Characteristics for a Diode Laser with External Grating Feedback" Elect. Lett. vol 17(17) 1981 pp589 – 591.

3. R. Lang and K. Kobayashi "External Optical Feedback Effects on Semiconductor Injection Laser Properties" IEEE J. Quant. Elact. vol QE–16(3) 1980 pp347 –355.

4. F. Favre. D. Le Guen and J.C. Simon "Optical Feedback Effects upon Laser Diode Oscillation Field Spectrum" IEEE J. Quant. Elect. vol QE–18(10) 11982 pp1712 – 1717.

5. K. Kikuchi and T. Okoshi "Simple Formula giving Spectrum–Narrowing Ratio of Semiconductor Laser Output Obtained by Optical Feedback" Elect. Lett. vol18(1) 1982 pp10 –11.

6. L. Goldberg, H.F. Taylor, A. Dandridge, J. Weller and R.O. Miles "Spectral Characteristics of Semiconductor Lasers with Optical Feedback" IEEE J. Quant. Elect. vol QE–18(4) 1982 pp555 – 564

7. E. Patzak, H. Olesen, A. Sugimura, S. Saito and T. Mukai "Spectral Linewidth Reduction in Semiconductor Lasers by an External Cavity with Weak Optical Feedback" Elect. Lett. vol 19 1983 pp 938 – 940.

8. G. P. Agrawal "Line Narrowing in a Single Mode Injection Laser Due to External Optical Feedback" IEEE J. Quant. Elect. vol QE–20(5) 1984 pp468 – 471.

9. I.P. Kaminow, G. Eisenstein and L.W. Sulz " Measurement of the Modal Reflectivity of an Antireflection Coating on a Superluminescent Diode" IEEE J. Quant. Elect. vol QE−19(4) 1983 pp493 −495.

10. M. W. Fleming and A. Mooradian " Spectral Characteristics of External Cavity Controlled Semiconductor Lasers" IEEE J. Quant. Elect. vol QE−17(1) 1981 pp44 −59.

11. R. Wyatt and W. J. Devlin " 10 kHz Linewidth 1.5μm InGaAsP External Cavity Laser with 55nm Tuning Range" Elect. Lett. vol 19(3) 1983 pp 110 − 112.

12. R. Wyatt, K.H. Cameron and M.R. Matthews "Tunable Narrow Line External Cavity Lasers for Coherent Optical Systems" British Telecom Technology vol 3(4) 1985 pp5 − 11.

13. M.R. Matthews, K.H. Cameron, R. Wyatt and J. Devlin "Packaged Frequency−Stable Tunable 20kHz linewidth 1.5μm InGaAsP External Cavity Laser" Elect. Lett. vol 21(3) 1985 pp113 − 115.

14. C.Y. Kuo and J.P. van der Ziel "Linewidth Reduction of 1.5μm Grating Loaded External Cavity Semiconductor Laser by Geometric Reconfiguration" Appl. Phys. Lett. vol 48(14) 1986 pp885 − 887.

15. H. Sato and J. Ohya "Theory of Spectral Linewidth of External cavity Semiconductor lasers" IEEE J. Quant. Elect. vol QE−22(7) 1986 pp1060 − 1063.

16. K. Kikuchi and T.P. Lee "Spectral Stability Analysis of Weakly Coupled External Cavity Semiconductor Lasers" J. Lightwave Tech. vol LT−5(9) 1987 pp1269 − 1272.

17. K. Kobayashi and I. Mito "Single Frequency and Tunable Laser Diodes" J. Lightwave Tech. vol 6(11) 1988 pp1623 − 1633.

18. T.L. Koch and U. Koren "Semiconductor Lasers for Coherent Optical Fiber Communications" J. Lightwave Tech. vol 8(3) 1990 pp274 – 293.

19. H. Bissessuk, C.Stark, J.Y. Emery and F. Pommereau et al. "Very Narrow Linewidth(70kHz) 1.55μm Strained MQW DFB Lasers" Electronics Letters Vol. 28(11) 21 May 1992

20. D.V. Eddolls, S.J. Vass, R.M. Ash and C.A. Park "Two Segment MQW lasers with 7nm tuning range and narrow linewidth" Electronics Letters Vol. 28(11) 21 May 1992

21. F.S. Choa et al "Very High Side Mode Suppression Ratio – DBR Lasers Grown by Chemical Beam Epitaxy" Electronics Letters Vol. 28(11) 21 May 1992

22. T.P. Lee, C.A. Burrus and D.P. Wilt "Measured Spectral Linewidth of Variable Gap Cleaved Coupled Cavity Lasers" Elect. Lett. vol 21(2) 1985 pp53 – 54.

23. T. Fujita, J. Ohya, K. Matsuda, M. Ishino, H. Sato and H. Serizawa "Narrow Spectral Linewidth Characteristics of Monolithic Integrated Passive Cavity InGaAsP/InP Semiconductor Lasers. Elect. Lett. vol 21(9) 1985 pp374 – 376

24. M. Ohtsu, S. Kotajima "Linewidth Reduction of a Semiconductor Laser by Electrical Feedback" IEEE Journal of Quantum Electronics QE–21 No. 12 Dec. 1985

25. G. Wenke and S Saito "Stabilised PSK Transmitter with Negative Electrical Feedback to a Semiconductor Laser" Elect Lett vol 21(15) 1985 pp653 – 655.

26. R.W. Tkach, A.R. Chrapylyvy "Regimes of Feedback Effects in 1.5μm Distributed Feedback Lasers" Journal of Lightwave technology vol. LT4(11) 1986

27. T. Kimura"Coherent Optical Fiber Transmission" J. Lightwave Technology vol LT− 5(4) 1987 pp414 − 428

28. R. Linke and A. Gnauck"High Capacity Coherent Lightwave Systems" J. Lightwave Technology vol 6(11) 1988 pp1730 − 1769

29. M.C. Brain, et al"Progress Towards the Field Deployment of Coherent Optical Fibre Systems" Journal of Lightwave Technology Vol. 8(3) 1990

30. M. Okai and T. Tsuchiya "Tunable DFB Lasers with Ultra− Narrow Spectral Linewidth" Electronics Letters 18 Feb. 1993 Vol. 29(4) PP 349 − 350

31. Y. Tohmori et al. "Over 100nm Wavelength Tuning in Superstructure Grating (SSG) DBR Lasers" Electronics Letters 18 Feb. 1993 Vol. 29(4) PP 352 − 354

CHAPTER 6

6.1 INTRODUCTION

The main purpose of this chapter is to report upon and discuss the results of the experiments which were performed during the course of this project, the primary object of which was to phase–lock two independent semiconductor laser modules.

The chapter begins by describing the basic experimental system which was used throughout the course of the project, a heterodyne phase–lock loop. This is followed by a section, which discusses the experimental programme which was carried out before theoretical work showing fully the effects of propagation delay had been carried out. This section deals with attempts to build a wide bandwidth loop using free running lasers, that is without any form of optical feedback. This work was followed by an attempt to build a wide bandwidth loop using compound–cavity lasers. A detailed report on the experimental programme on building a narrow bandwidth loop using line–narrowed external–cavity semiconductor laser modules is then presented. This is followed by presenting some results on laser spectral degradation, which caused the experimental programme to be terminated. The chapter conludes by comparing the experimental work presented in this thesis with that of other groups and by reporting on advancements in the years between the termination of the experimental programme and the writing of the thesis.

The chapter is presented almost chronologically to enable the reader to fully understand both how and why the experimental programme evolved and how the theory incorporating the effect of time delay arose.

6.2 HETERODYNE OPTICAL PHASE LOCK LOOP

It was decided at the very outset of the project that the experimental programme should focus on building a heterodyne as opposed to a homodyne optical phase lock loop. The first and perhaps most strongly influencing factor in making this decision was that a previous worker,

R.C. Steele, had succesfully locked a heterodyne loop. Secondly the receiver electronics are very much simpler in a heterodyne loop. Specifically, the need to build a balanced receiver is removed, as is the need for a wide bandwidth d.c. coupled amplifier. A.C.– coupled amplifiers are, generally speaking, much easier to build.

Figure 6.1 shows a schematic diagram of the basic experimental system which was used throughout the project. One semiconductor laser module was used as a transmitter while the other was used as a local oscillator. Each laser was optically isolated from unwanted reflections by using a polarizing filter and quarter–wave plate combination, as discussed in section 4.4, and by using slight optical misalignment. To confirm that the lasers were not suffering from the effects of uncontrolled reflections each laser was continuously monitored on a scanning Fabry Perot Interferometer of 2GHz free spectral range. The beams from each laser were spatially combined using a high quality 50/50 beamsplitter. One of the combined beams provided by the beamsplitter was then directed into a Rank Hilger monochromator to monitor the wavelength separation between the two lasers, while the other beam was focused down onto an avalanche photodiode which formed the front end of the receiver electronics. The signal from the photodiode was then amplified and mixed with a reference RF signal in a double balanced mixer before being filtered and fed back to the local oscillator. The signal from the front end receiver was monitored on a Tektronix Spectrum Analyser. During the course of the project different amplifiers, photodiodes, filters and laser modules were used but the system remained basically the same.

6.3 TECHNIQUES FOR OBTAINING A BEAT BETWEEN TWO LASER MODULES.

Before discussing the attempts that were made to phase lock two lasers together, it is important, from an experimental point of view, to explain one of the main problems which has to be overcome if FP semiconductor lasers are ever to be used in coherent systems without having to be very carefully customised. The problem of mode hopping has to be overcome, because otherwise it will prove impractical even to obtain beat signals between two devices.

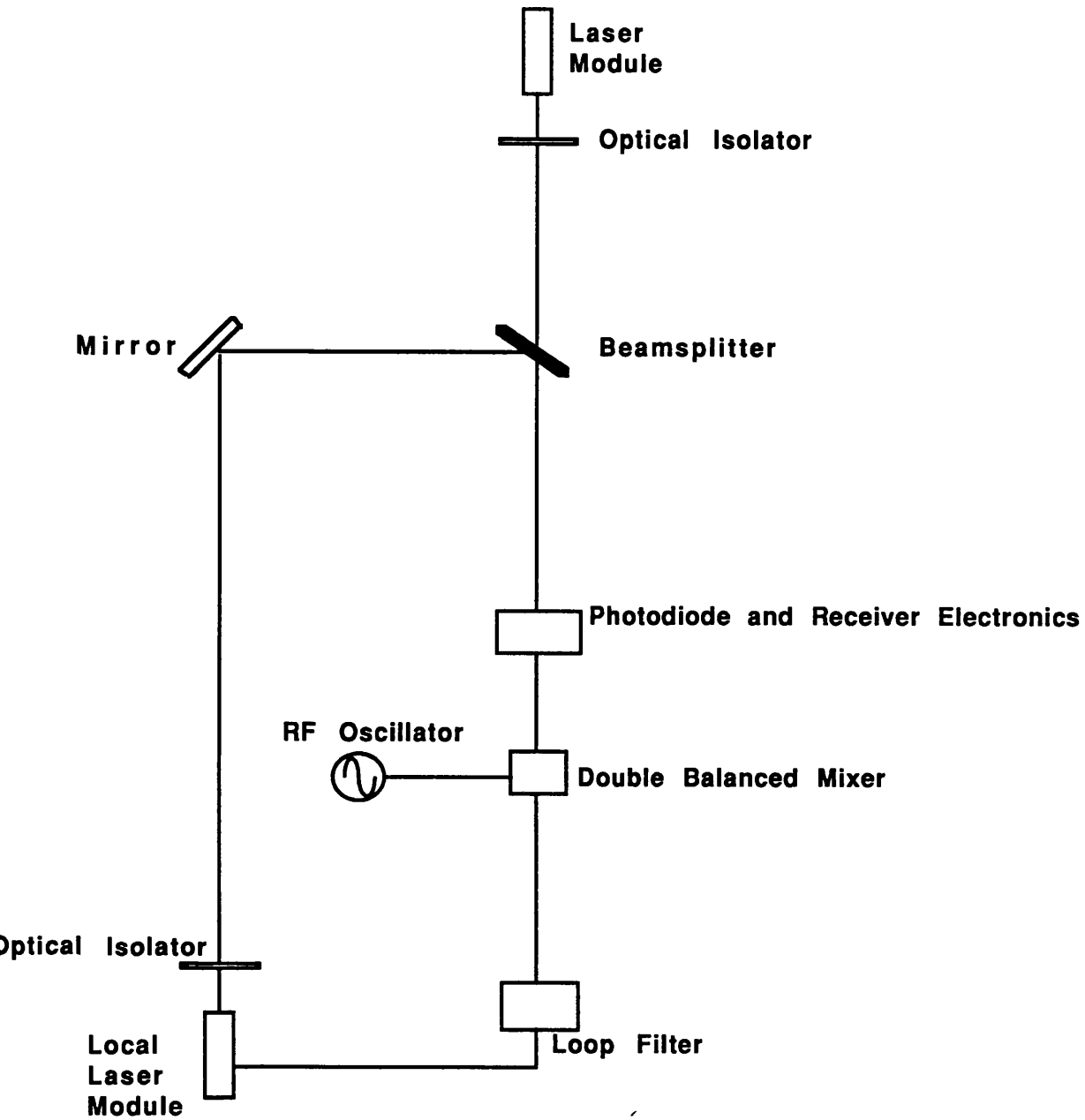

Figure 6.1 Schematic of Heterodyne Optical Phase Lock Loop

At first thought it may seem a trivial problem to obtain a beat signal between two semiconductor laser modules. It is only when the stability of the lasers is considered, see section 4.4, that the difficulty of controlling two lasers to within, say, 1GHz of each other is fully appreciated.

The technique which was used throughout the project, consists of a series of steps. This should not be as difficult with multicontact DFB and DBR laser diodes.

1) The lasers which are used should be matched in wavelength to within two or three nanometer while operating under standard conditions, ie 30mA above threshold at 25°C. This is no longer quite as severe a problem. Closer matches can be achieved quite easily.

2) Look at plots of wavelength against current, at several different temperatures, for each laser. This enables points where the two lasers have similar frequencies to be identified. Ideally one or both of the lasers will have operating regions where they can be continuously tuned. In practice it is a matter of chance whether two lasers can be found with stable, tunable and overlapping modes. (In this project the author used sixteen HLP1400 laser diodes which were all nominally matched to within 3nm when operated at 25°C. At 25°C , however no two lasers had suitable modal characteristics for obtaining a beat.)

3) Once these operating regions have been identified the individual lasers are set at the appropriate temperature and bias current. The wavelength of each laser is then monitored using the monochromator. This has a resolution of 1 Angstrom, which is equivalent to 42GHz at 850nm.

4)One of the lasers is then tuned towards the other by changing the bias current. If the lasers never mode hopped, such tuning, would be a relatively simple procedure. In practice much trial and error is involved before a beat signal is obtained. In some instances it can take several hours to find suitable operating points for both lasers and occasionally one of the lasers has to be replaced.

Reference Level

Marker Frequency

Horiz. Scale MHz/div

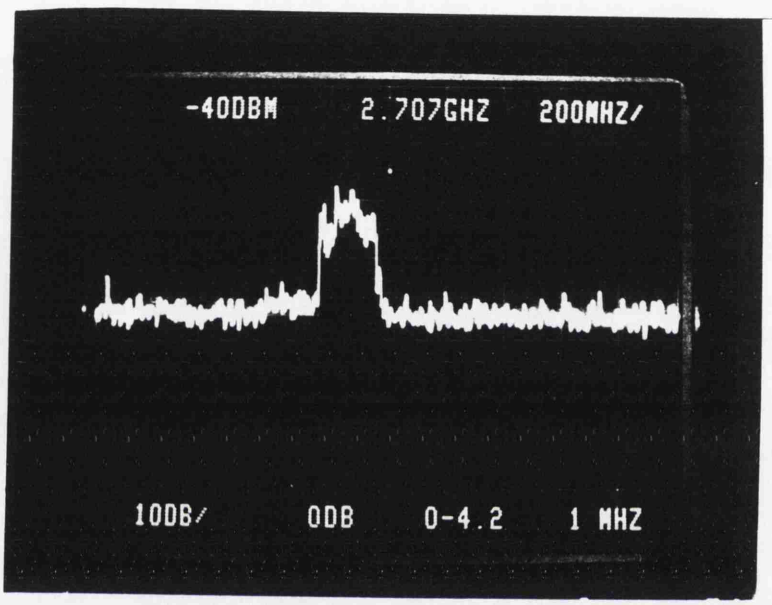

Vertical Scale dB / Div

Input Attenuation

Freq. Span GHz

Resolution Bandwidth

Figure 6.2

Free Running Laser Diode Beat Spectrum Linewidth Approximately 100MHz

5) Once two lasers are found which have overlapping modes it is relatively simple both to obtain and to maintain a beat signal providing the temperature and current control is adequate.

Figure 6.2 displays a typical beat spectrum obtained using two free running laser diodes. The most notable feature of this spectrum is that it is neither Lorentzian nor is it of the expected linewidth of around 15 MHz. The reason for the spectrum actually observed is that the beat signal is drifting while the spectrum analyser is scanning, due to low frequency fluctuations in the laser temperature.

6.4 WIDE BANDWIDTH LOOP

Initially, before the theory incorporating the effect of time delay into the system had been properly developed, it was thought that it would be possible to obtain phase–lock between two free running HLP1400 laser diodes. Many attempts were made at phase–locking using a variety of different filter designs and by increasing and decreasing the loop gain and hence the bandwidth. It was only after several months of experimenting with good beat signals that it was concluded that there was something more fundamental than inadequate temperature control preventing the loop from locking.

When the effect of time delay was incorporated into the theory it was immediately apparent that the loops which had been designed were all either inherently unstable, because their $\omega_n T_d$ product was too high, or that they were operating too far away from the optimum bandwidth for the loop to have any chance of locking. These points have been covered in chapter 3.

In designing the initial experiments the effect of loop propagation delay was never considered other than from the point of view that no excess delays should be present in the system. This was largely due to the fact that no analysis of optical systems behaviour that was known at that time mentioned the problem. Moreover R.C. Steele, who succesfully locked a heterodyne loop, had designed his loop to be wideband, although when it was built up it was in fact narrowband. This came to light only recently[6] when R.C. Steele's loop was

analysed taking the effect of time delay into account. Other workers who had built successful loops using CO_2 lasers also did not mention the problem.

A description of the wideband system that was used in this project is now given. The time that was spent experimenting with it was not wasted, as the laser temperature control, drive circuitry and loop electronics were all improved in the course of the experimental work.

Whether the loop being designed is of wide or of narrow bandwidth, the front end receiver should have a wide bandwidth. This is for two reasons. Firstly, the wider the bandwidth the easier it is to find a beat signal and secondly, in order that the loop performance is not unduly degraded, the bandwidth of the front end electronics should be at least six times the loop bandwidth[6].

The initial front end receiver configuration was built around a hybrid UHF amplifier from RS Components Ltd., device number OM361 (Technical Specification 40 − 860MHz bandwidth and 28db of gain) and a Telefunken avalanche photodiode BPW26. The module was tested with by scanning a beat signal across the bandwidth. These experiments showed the device to have a bandwidth of around 1150MHz, with a low frequency cut off of 1MHz and a gain of 20dB.

The output of the amplifier was coupled into a wide bandwith double balanced mixer (DBM), Mini Circuits ZFM−54, where it was multiplied with an RF signal from a HP Oscillator. The insertion loss of the mixer at a maximum drive level of 7dBm was −7dB. The insertion loss increased as the RF power was reduced. At a drive level of −20dBm the loss was −50dB. It should be noted that the loop gain could be controlled by varying the RF power into the double balanced mixer. This had the effect of amplifying the beat signal in the same way as the local oscillator is used to amplify the transmitted signal.

Various attempts were made to lock the loop using different filters and by altering the gain of the loop through control of the received

power and the RF drive power, but these changes were all to no avail. Much thought was given to why the loop was not locking. One reason was thought to be that there was too much phase noise in the system and that our understanding of the laser phase noise was not complete. Another possible reason related to acquisition of the locked condition. It was thought that the rate of frequency drift of the beat signal was too high for the loop to lock. Other suggestions included poor control over the damping factor, which would lead to instability.

Each of these suggestions was systematically examined, either experimentally or analyticaly, and the loop components and the control over the loop parameters were improved. The laser temperature control was redesigned to improve the laser stability. Various different forms of laser mount and collimating lenses were tried, to improve the overall stability of the system. The loop electronics were constantly under review and the whole system was overhauled regularly, but all to no avail. The clue which pointed to propagation delay as a key factor was when the same experiments were carried out using compound cavity laser modules.

Although these lasers were extremely unstable, it was possible on occasion, with very low levels of feedback, to obtain relatively stable beat signals. The RF signal was then tuned to the beat, but still the loop never looked likely to lock. Only after months of investigation did the effect of time delay receive proper consideration.

As soon as the effect of time delay was fully understood it was obvious why the loops had never locked, even when the compound cavity lasers were used. The loops had either been unstable or were operating at spurious bandwidths.

The more complete theory predicted that it would be impossible to build a bulk optics phase lock loop using free running semiconductor lasers, as the $\omega_n T_d$ stability criterion makes T_d too small. It also laid down a new set of design criteria which indicated that the most sensible approach would be to build a narrow bandwidth loop with line narrowed laser modules.

Reference Level | **Marker Frequency** | **Horiz. Scale MHz/div**

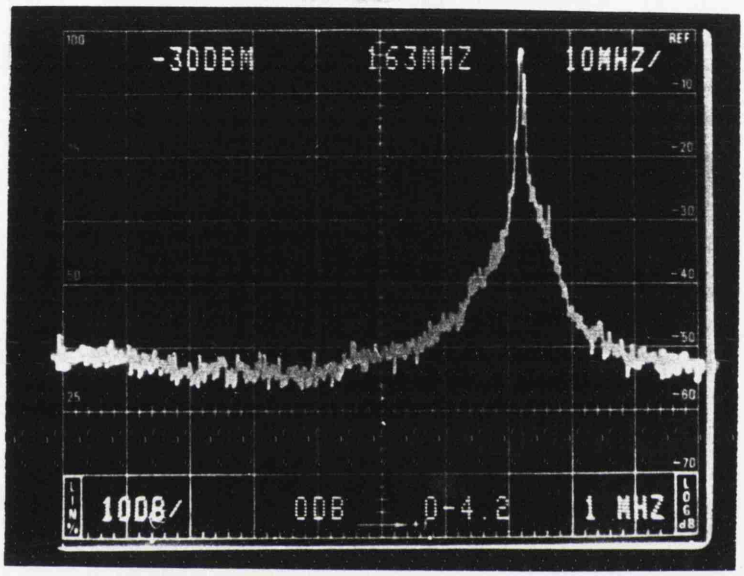

Vertical Scale dB / Div | Input Attenuation | Freq. Span GHz | Resolution Bandwidth

Figure 6.3a

Compound Cavity Beat Spectrum
Individual Linewidth 400kHz

Reference Level

Marker Frequency

Horiz. Scale MHz/div

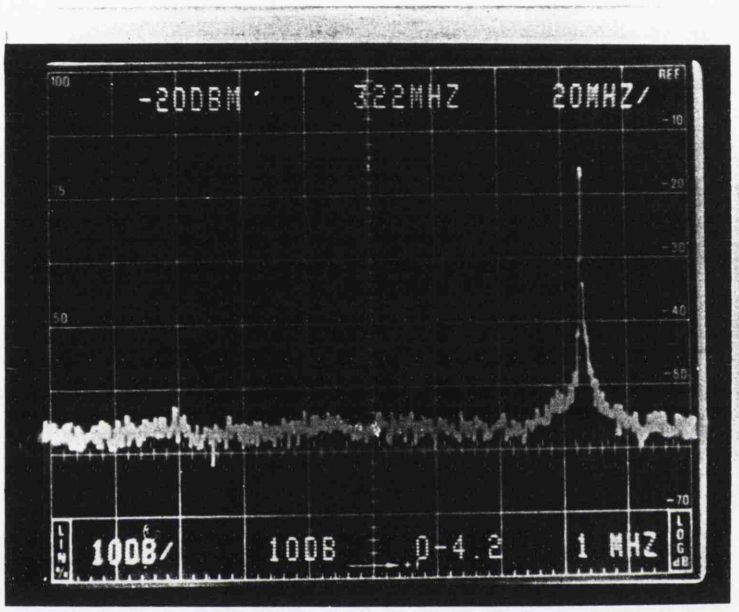

Vertical Scale dB / Div

Input Attenuation

Freq. Span GHz

Resolution Bandwidth

Figure 6.3b

Compound Cavity Beat Spectrum
Individual Linewidth 100kHz

6.5 NARROW BANDWIDTH LOOP

The new loop parameters were selected in line with the design criteria described in chapter 3. The variables which dictate the loop gain and loop time constants are the linewidths of the two lasers, the total received optical power and the total time delay around the loop. These are all readily measured.

The lasers which were used in this series of experiments were true external cavity laser diodes. The operating characteristics of these devices have been described in detail in chapter 5. Figure 6.4 displays beat signals between two such laser modules. The estimated linewidth, from these photographs, of each laser is of the order of 10 to 100kHz. Figure 6.5 shows a time domain version of the beat signal.

The received optical power was very dependent upon the optical alignment of the system. It was, however, possible to control this parameter by using an optical attenuator in front of the photodiode receiver. In this way the loop gain could be controlled. The received optical power was in the range from -30 to -60dBm.

The third variable mentioned above was the propagation delay around the loop. This was calculated as follows: the total free—space optical transit delay was measured in distance and the corresponding time delay was calculated using the speed of light. This delay was estimated to be between 3 and 4 nanoseconds corresponding to 90 to 120cm.. In a fibre or integrated system this delay could be substantially reduced. The delay introduced by the front end receiver was measured to be 2.1ns by comparing the time it took a sinusoidal signal to travel through a piece of coaxial cable and the loop electronics to the the time taken by the signal with the electronics missing. The comparison was made using a Tektronix 1100 oscilloscope which had a resolution of around 1ns. The time taken for the double balanced mixer to process the two incoming signals and produce an output was estimated to be 1 or 2 ns. The local oscillator also had a response time in excess of 1ns as a result of the external cavity length of around 15cm. The total loop delay was therefore in the region of 5 to 10 ns.

Reference Level

Marker Frequency

Horiz. Scale MHz/div

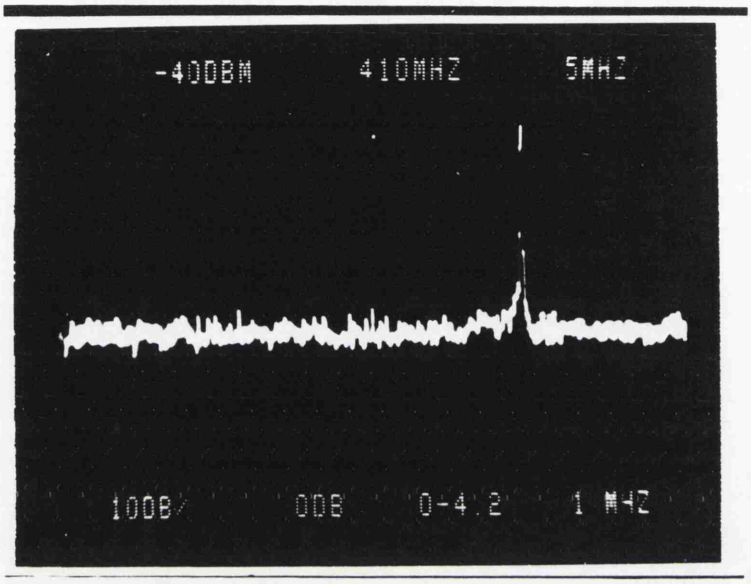

Vertical Scale dB / Div

Input Attenuation

Freq. Span GHz

Resolution Bandwidth

Figure 6.4a

External Cavity Beat Spectrum
Individual Linewidth 50kHz

Reference Level | **Marker Frequency** | **Horiz. Scale MHz/div**

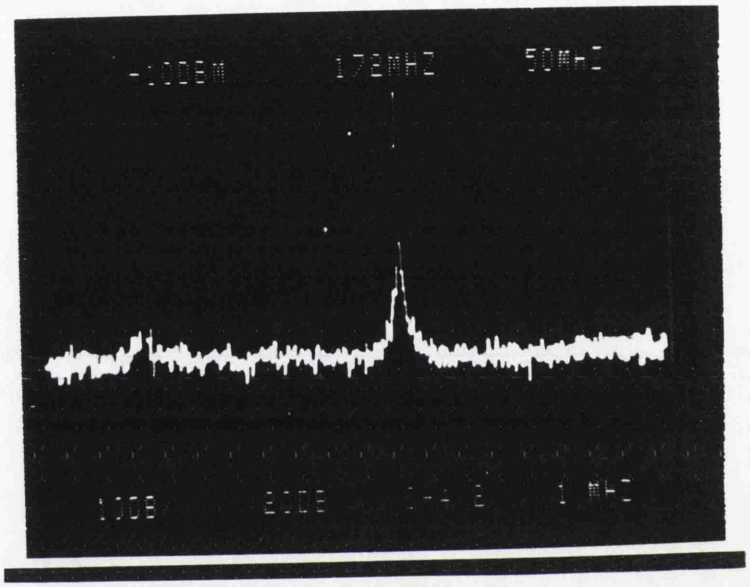

Vertical Scale dB / Div | Input Attenuation | Freq. Span GHz | Resolution Bandwidth

Figure 6.4b

External Cavity Beat Spectrum
Individual Linewidth 50kHz

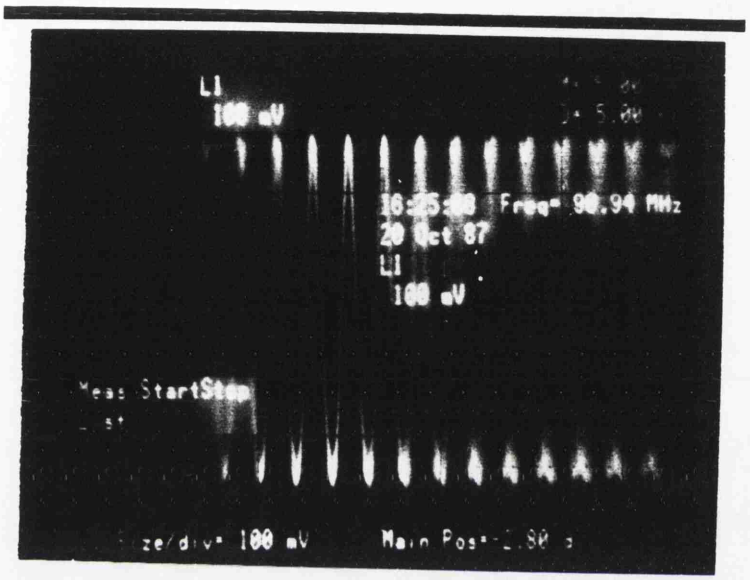

Figure 6.5

Heterodyne Beat Note in Time Domain

In chapter 3 it was shown that $\omega_n T_d$ products greater than 0.2 seriously degrade the performance of the loop. Therefore a time delay of this magnitude coupled with a beat signal of linewidth less than 100kHz suggests that loop natural frequencies of the order of 10 to 30Mrad/s will retain stability and satisfactory performance. Smaller bandwidths could be used but the problem of acquisition and tracking have always to be borne in mind. The larger the bandwidth the better the tracking and acquisition characteristics of the loop.

The loop filter which was chosen for the system is shown in figure 5. The resistors and the capacitor were selected using the above information together with the loop gain. The operational amplifier used in this project was a wide bandwidth Burr Brown device, 3551 series. These have slew rates on the order of 250V per micro second. This device will allow a signal of amplitude greater than 1volt and frequency 5MHz(30Mrads/sec) to be processed. For a loop with maximum bandwidth of upto 30Mrads/sec and a local oscillator of gain greater than 10MHz/mA this was sufficient as the feedback signal to the local oscillator was connected via a 50Ω resistor, ie it will allow a signal of 20mA at a frequency of 5MHz to modulate the local laser. In practice the beat signal was seen to vary at sub kHz frequencies.

The gain of the loop was dependent upon the gain of the front end receiver, the gain of the local oscillator, the efficiency of the mixer and the received opticcal power. R_1 as shown in figure 6 was chosen arbitrarily as 1kΩ. The gain of the front end receiver had to be increased from the previous loop experiments to compensate for the reduction in the gain of the local oscillator which was caused by the inclusion of the line–narrowing external cavity. The new front end receiver consisted of three Watkins and Johnson wideband amplifiers in cascade. The new arrangement had a gain of 55dB and a bandwidth of 900MHz. The filter capacitance was then calculated by rearranging equation 3.2.18 to give

$$C = \frac{2R_{esp} \cdot K_{amp} \cdot K_{LO} \cdot K_m (P_t P_{LO})^{1/2}}{R_1 \omega_n^2} \qquad 6.5.1$$

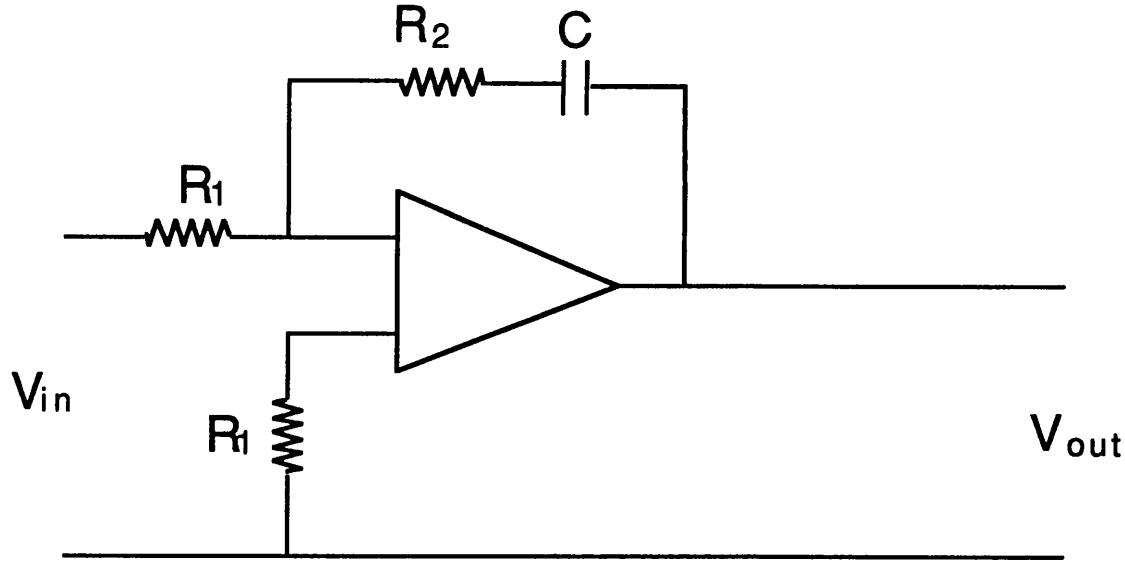

$$F = \frac{1 + S\,\tau_2}{S\,\tau_1}$$

$$\tau_1 = (R_1 + R_2)C$$

$$\tau_2 = R_2\,C$$

Figure 6.6 An Active First Order Filter

where R_{esp} is the responsivity of the photodiode, K_{amp} is the gain of the front end reciever amplifier, K_{LO} is the gain of the laser Hz/A, K_m is the mixer gain, P_t and P_{LO} are the recieved and local oscillator powers, R_1 is the value of the loop filter restance and ω_n is the loops natural frequency. C was chosen to be in the region of 6.4μF to 6.4nF depending upon the received optical power.

Using the external cavity laser modules it was a simple task to obtain a beat signal of suitable linewidth and power for a loop, as described previously, to lock. However, whenever the loop was closed, lock was never observed even after much experimentation with the loop gain and the filter time constants.

It is conceivable that the loop did lock momentarily but that this was never observed. This possibility is due to the fact that no phase noise reduction would have been observed, as the linewidth of the beat was so narrow.

The main reason why the loop did not lock was considered to be frequency instability resulting from mechanical vibration of the laser cavities. Such vibrations cause low frequency oscillations, but these can be of large magnitude. In section 5.3.5 it is shown that an increase in the length of either laser cavity of 1nm results in a change in the frequency of the laser of 3MHz. The instabilities being observed must have been greater in size than this or the loop should have locked.

Another problem which was encountered was hysteresis. The piezo controllers, combined with the mechanical mount, suffered from hysterisis. The structure also suffered from backlash. Each of these problems contributed to the laser instabilities.

At this stage in the project a choice had to be made regarding the way forward. The whole laser mounts could have been re-designed in line with the recommendations made in section 5.3.6 and 5.3.7. Alternatively an attempt could be made to solve the problem by using a control loop and the existing mounts. The decision was made after discussing time scales with the departmental workshop and with component manufacturers /suppliers. A new mount complete with the

type of piezo control necessary would have taken several months to manufacture. Furthermore, it was thought that the problem could be overcome electronically.

6.6 INTERMEDIATE FREQUENCY CONTROL LOOP

An intermediate–frequency control–loop was designed and built both to measure and control these instabilities to within the PLL acquisition range. The IF control loop, which was designed to work in parallel with the PLL, is shown in Fig 6.7. It consisted of a frequency discriminator with a bandwidth of around 70MHz, which was used to monitor the beat signal between the two lasers. The discriminator consisted of a double–balanced–mixer and a delay line. The output of the mixer was amplified and level–shifted to produce a voltage swing of +15v to −15v across its bandwidth. Figure 6.8 shows the discriminator characteristic. This output was then processed through a PID controller before being amplified and level shifted again en route to being fed back to a piezo–drive on the longitudinal axis of the local laser module.

Figure 6.9 displays the output of the discriminator with the loop open. It can be seen from this that the laser modulation oscillations are in the audio frequency range up to around 500Hz. The frequency deviations can also be seen at times to be greater than 80MHz. This would indicate that the mechanical oscillations are of the order of 10 to 20nm in magnitude in each laser cavity. The magnitude of these vibrations and the associated problems of controlling them are largely a result of inadequate mechanical design.

Figure 6.10 displays the output of the discriminator while the loop was working. It can be seen from this that the loop held the beat signal to within 10MHz of the desired value. The loop operated in this way for many, several minutes at a time until the control loop integrator saturated. The saturation effect was a result of long–term temperature–drift causing the cavity as a whole to expand. This happened continuously throughout the day while the laboratory was heating up. The temperature of the laser diode was controlled but not the temperature of the whole laser mount. This was thought to be

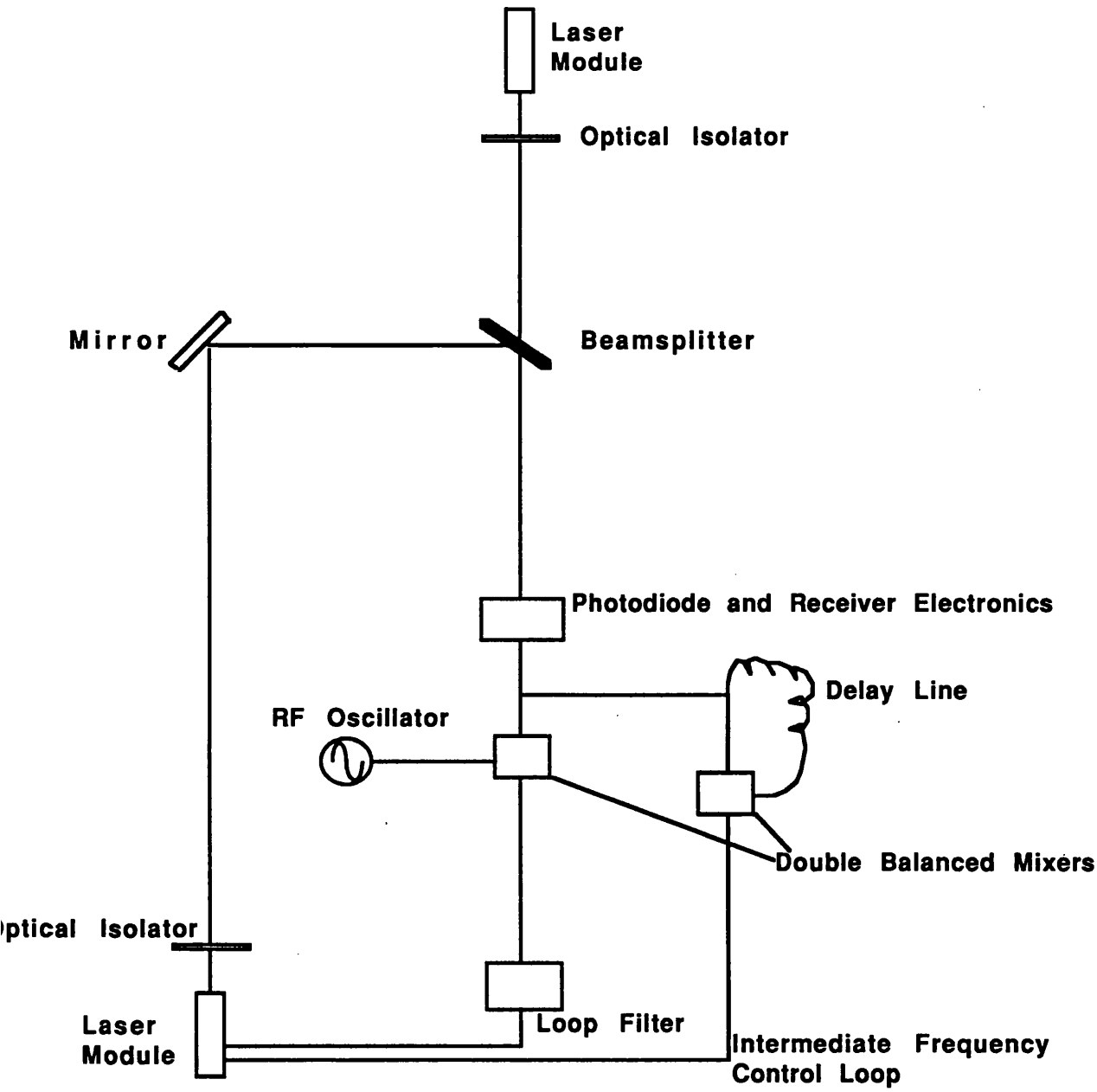

Figure 6.7 Systems Experiment Incorporating IF Control Loop

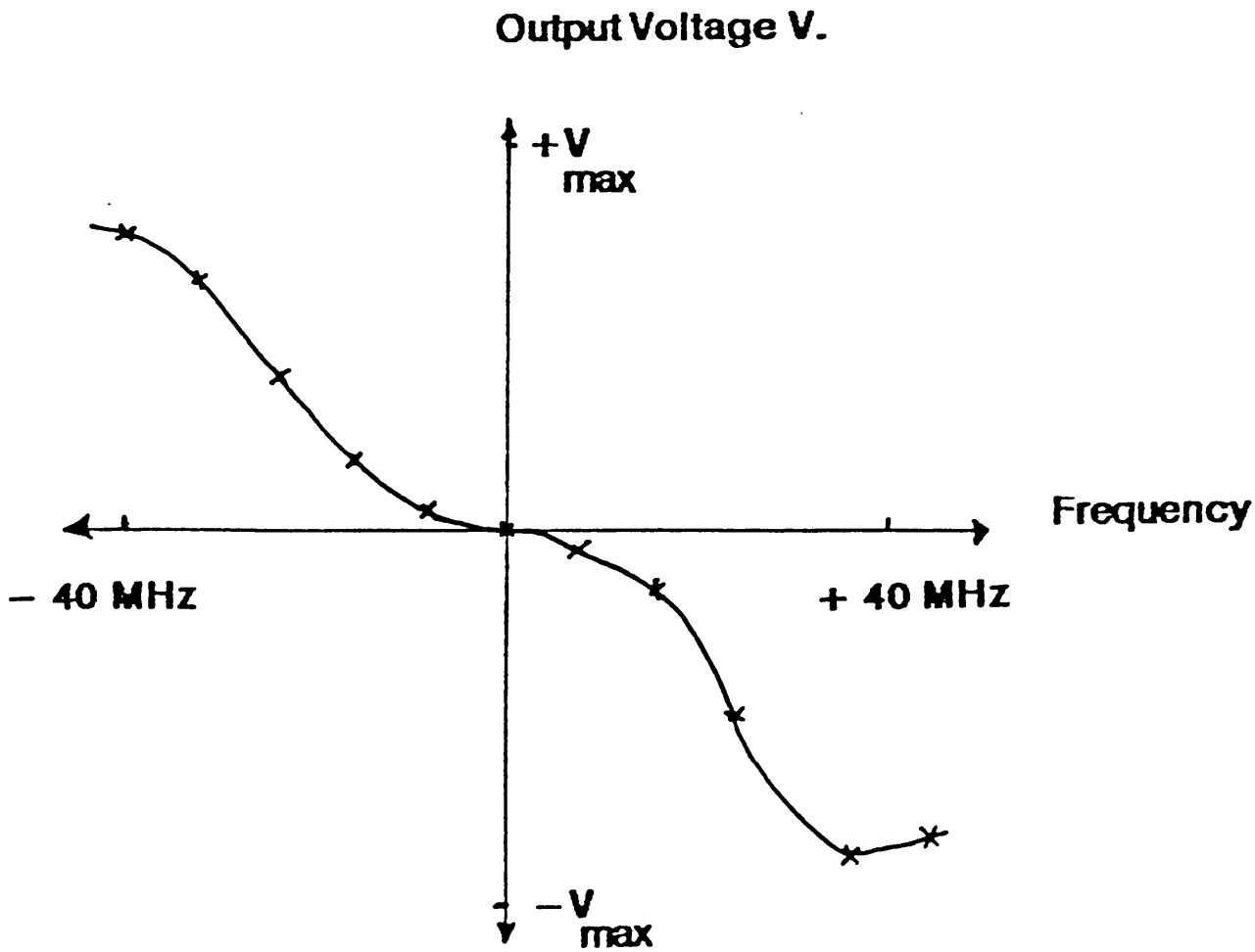

Figure 6.8 Discriminator Characteristic

Frequency
20 MHz/cm

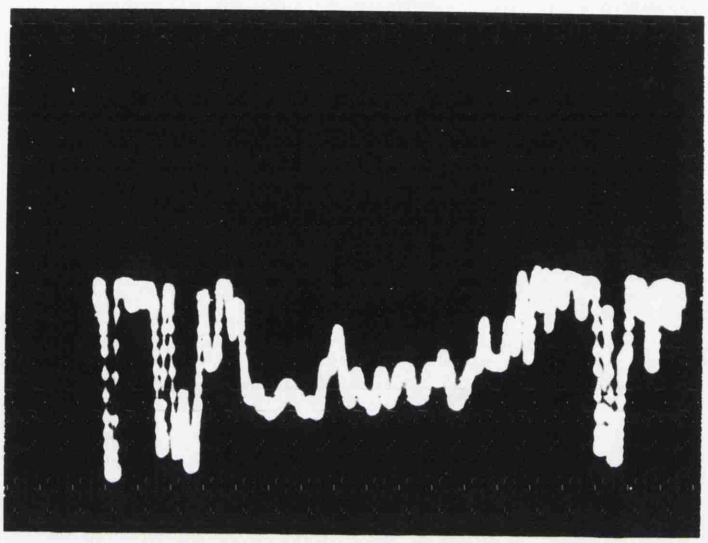

Time 10ms/cm

Figure 6.9

IF Discriminator Output: Open Loop Configuration

Frequency
10 MHz/cm

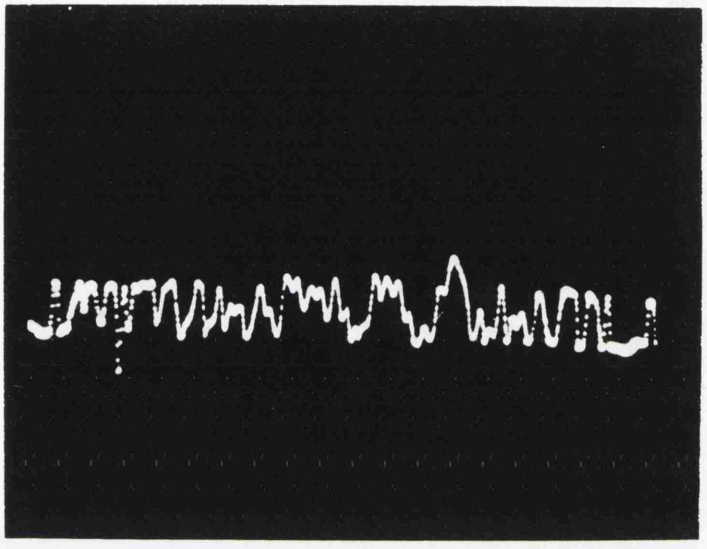

Time 10ms/cm

Figure 6.10

IF Discriminator Output: Closed Loop Configuration

impractical. The maximum range of the piezo–spacer was .5μm. The thermal expansion coefficient for aluminium is $25*10^{-6}K^{-1}m^{-1}$. Therefore a change in temperature of 0.03K was enough to saturate the controller. The temperature of the lab changed by several degrees over the course of the day.

With hindsight it would appear that the control loop coped well with the dc temperature drift until saturation set in but that it had real difficulty in coping with higher frequency ac terms. With hindsight it may be that the reason for this was that the driver to the piezo spacer was unable to deliver enough charge quickly enough.

It should also be noted that even when the loop was operating it was noticeable that there were still discrete jumps in frequency rather than smooth variations. This appeared to be due to hysteresis in the piezo–spacer or in the mechanical mounting or in both.

6.7 TERMINATION OF THE EXPERIMENTAL PROGRAMME

The experimental programme was terminated when it was noticed that the laser spectra were deteriorating, as was also the stability of the individual lasers.

Over the course of several months many attempts were made to lock two independent laser modules using a combination of the frequency control loop and the phase–lock control loop. It appeared from all the results that were obtained that the theory was understood and that the only problems to be overcome were directly related to the mechanical stability of the laser cavity and to the hysterisis in the piezo–controllers. These problems could possibly have been overcome using a combination of redesign of the laser mount/cavity and improvements to the control loop.

Unfortunately another more serious problem apppeared. The laser modules started to exhibit drastically degraded spectral purity and decreased stability. The lasers started to mode hop more often than previously. It was also noticeable that they were more difficult to align to obtain monomode operation. Overall they became more to difficult

Intensity
(Arbitrary Units)

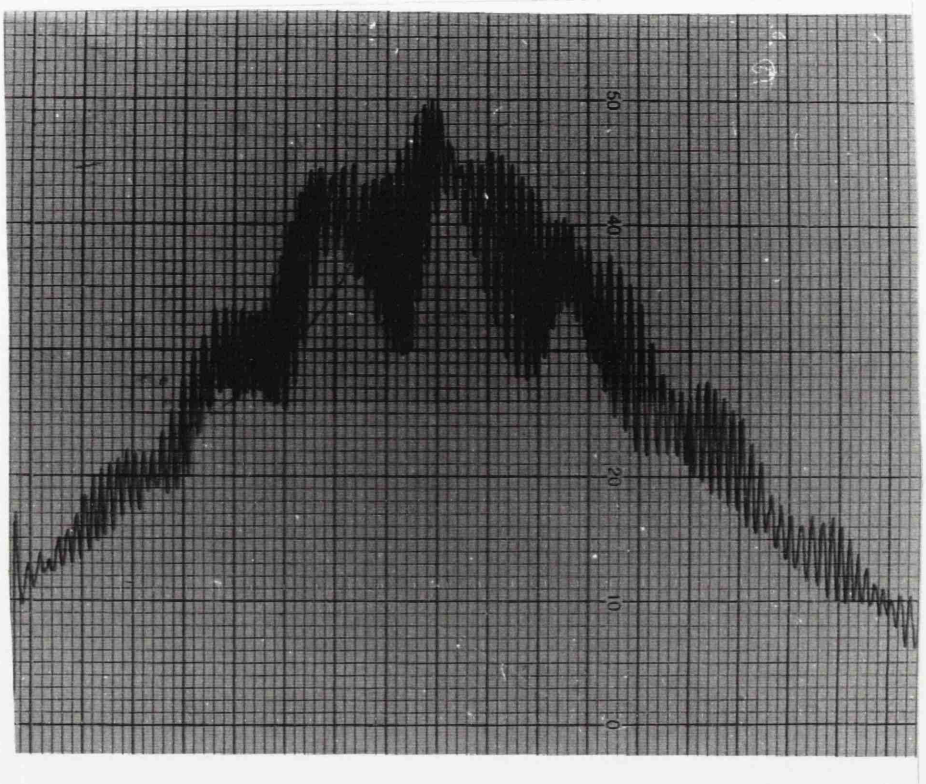

Wavelength Scan 820 - 850 nm
Peak in Profile 834 nm

Figure 6.11

Spontaneous Emission Profile of Laser 2203
Measurement made after 3 months of experimental use

to work with.

To find out what was causing the problems, laser spectra were taken using the monochromator. The laser spectra were taken free–running at the threshold levels measured before coating had been carried out. They were taken at these currents, as comparisons could be made with previously obtained spectra. The spectra obtained are shown in Fig 6.11. As can be seen from the traces, a modulation has been superimposed upon the original spectra shown in chapter 5. The source of this modulation is unclear, although it corresponds to a cavity length of 30 μm. As there were no external optics so close to the cavity, the effect must have been due either to some internal defect or to a periodicity in the laser AR coating. It was felt that it was unlikely to be a problem with the coating and that the most likely cause was some form of defect in the laser structure itself, such as darkline defects.

6.8 CONCLUSIONS AND COMPARISON WITH OTHER WORK

At the end of the systems experimental programme the key results could be summarised as :

1. Good line–narrowed beat spectra, less than 100kHz, were obtained on a repeatable basis.

2. A frequency control loop was built which held the line–narrowed beat spectra within a 5MHz bandwidth. The control loop only failed as a result of long term temperature drift.

3. The requirements placed upon the loop propagation delay make it impractical to build a bulk–optics phase–lock loop for free running Hitachi HLP1400 laser diodes.

4. Low frequency acoustic vibrations would appear to be the main obstacle to be overcome when using external cavity laser modules.

5. HLP 1400 laser diodes exhibit severe spectral degradation when operated in an external cavity over a sustained period, around 200 or

300hrs.

6. Hitachi HLP1400 laser diodes are difficult to work with since they are extremely sensitive tochanges in their environment. They were however at the time of this project the best commercially avaialable lasers operating at 850nm.

The results of the experimental programme described are similar to those obtained by other workers, in terms of measured linewidths of beat signals and stability of beat signals. At the termination of the experimental work in January 1988 no group worldwide was claiming to have successfully built a working phase locked loop using two free running laser diodes. Workers at British Telecom had, however, successfully built an OPLL using one external cavity module and a HeNe laser operating at 1.55μm.

Since then major developments have taken place, both in the improvement of the spectral quality of the laser sources and in the design and construction of phase lock loops themselves. Miniaturised external cavity modules have been built and so too have complex multisection DFB and DBR devices. These are covered in chapter 5. Workers in Germany[10] and Japan[14] have successfully constructed loops which use external cavity structures to improve the spectral quality of the lasers. Kourogi et al[13] have also locked a free running laser onto a laser which had previously been line narrowed using electrical feedback. This loop had bandwidth of 134MHz and a time delay of around 1ns. Gliese[11,12] et al has demonstrated a system operating at 1.5μm. and Ramos and Seeds[15] successfully phase locked a loop using two free running double quantum well laser diodes. All of these loops took into account the design criteria presented in chapter three of this thesis. All of the loops had very short propogation delays. These groups are all continuing to develop the theory and experimental development of coherent systems. Reference 16 and 17 present good overview of the foundations and developments in coherent systems and reference 11 indicates some of additional design requirements for future applications.

References

1. R.C. Steele, "Ph.D. Thesis." University of Glasgow 1983.

2. R.C. Steele, "Optical Phase–Locked Loop using Semiconductor Laser Diodes" Electronics Letters vol 19(2) Jan. 1983

3. F.M. Gardner "Phaselock Techniques" New York: Wiley, 1979.

4. A. Blanchard "Phase–Locked Loops. Application to Coherent Reciever Design" New York: Wiley, 1976

5. M.A. Grant, W.C. Michie and M.J. Fletcher "The Performance of Optical Phase–Locked Loops in the Prescence of Non Negligible Loop Propagation Delay." Journal of Lightwave Technology vol LT–5(4) 1987

6. W.C. Michie "Ph.D. Thesis: Carrier Phase Recovery for Coherent Optical Transmission Systems" University of Glasgow, 1989

7. S. Saito, O. Nilsson and Y. Yammamoto, "Frequency Modulation Noise and Linewidth Reduction in a Semiconductor Laser by means of Negative Frequency Feedback Technique" Appl. Phys. Lett. 46(1) Jan. 1985

8. G. Wenke, S. Saito "Stabilised PSK Transmitter with Negative Electrical Feedback to a Semiconductor Laser" Electronics Letters Vol.21(15) 1985

9. D.J. Malyon, D.W. Smith, R.Wyatt "Semiconductor Laser Homodyne Optical Phase–Locked Loop" Electronics Letters vol.22(8) 1986

10. H.R. Telle, H.Li "Phase Locking of Laser Diodes" Electronics Letters vol.26(13) 1990

11. U.Gliese, E.L. Christensen and K.E. Stubkjaer "Laser Linewidth Requirements and Improvements for Coherent Optical Beam Forming

Networks in Satellites" Journal of Lightwave Technology Vol.9(6) 1991 pp779 – 790

12. U. Gliese et al " A Wideband Heterodyne Optical Phase–Locked Loop for Generation of 3 – 18GHz Microwave Carriers" IEEE Photonics Technology Letters Vol.4(8) Aug. 1992 pp936 – 940

13. M. Kourogi, C.H. Shin and M. Ohtsu "A 134MHz Bandwidth Homodyne Optical Phase–Locked Loop of Semiconductor Laser Diodes" IEEE Photonics Technology LettersVol.3(3) March 1991 pp 270 – 272

14. C.H. Shin, M. Ohtsu "Homodyne Optical Phase Locking of Resonant Cavity Coupled Semiconductor Lasers" IEEE Journal of Quantum Electronics Vol.29(2) Feb. 1993 pp 374 – 385

15. R.T. Ramos, A.J. Seeds "Fast Heterodyne Optical Phase–Lock Loop Using Double Quantum Well Laser Diodes" Electronics Letters vol. 28(1) 1992

16. R.A. Linke, A.H. Gnauck "High Capacity Coherent Lightwave Systems" Journal of Lightwave Technology vol.6(11) 1988

17. M.C. Brain, et al. "Progress Towards the Field Deployment of Coherent Optical Fibre Systems" Journal of Lightwave Technology vol. 8(3) 1990

CHAPTER 7. CONCLUSIONS AND SUGGESTIONS FOR FURTHER RESEARCH

7.1 CONCLUSIONS

The work presented in this thesis was carried out as part of a project to build a bulk optics phase–locked loop (OPLL) using semiconductor lasers. Along the way several goals were realised, although the major objective was never achieved. In particular the understanding of the operation of such systems was advanced and design criteria drawn up which laid the foundation for other workers finally to build reliable OPLLs. In addition much work was carried out in building reliable line–narrowed (less than 100kHz), frequency tunable (greater than 10nm), laser diode modules.

At the start of the project it was already known that there were particular problems associated with building coherent optical communication systems and that most of these problems were related to the spectral purity and stability of semiconductor lasers. However it was also known that semiconductor lasers present the most attractive option for future coherent systems in terms of cost, size, reliability, tunability, lasing wavelength and ease of bulk manufacture.

In chapter 2 the reasons for carrying out this research were presented. These being that coherent systems offered the potential to fully exploit the bandwidth of optical fibre by multiplexing thousands of signals spaced one or two GHz apart. Secondly it was shown that coherent systems offered substantial improvements, upto 20dB, over practical intesity modulated direct detection (IMDD) systems in terms of receiver sensitivities.

An analysis of phase–locked loops was then presented in chapter 3. This started by explaining how such loops operate before analysing in detail the effects of shot noise and laser phase noise on the overall system performance. The first part of this analysis led to various design criteria fo ensuring optimal loop performance. It was found that for narrow linewidth lasers (less than 100kHz), near quantum–limited detection was possible and that as the linewidth of

the lasers increased so the overall system performance degraded and the engineering requirements increased to the point where phase–locking became impossible. This analysis, however, did predict that, although two lasers with linewidths of the order of one or two MHz could be phase–locked, it is nearly impossible to phase–lock lasers with linewidths in excess of 10MHz.

Experimental work which was presented in chapter 6 indicated that the analysis given at the start of chapter 3 was inaccurate in that phase lock was not achieved when expected. For many months systems experiments were carried out which met the initial criteria in terms of received power, receiver banwidth and laser linewidths but all to no avail. As a result of this failure the theory was re–examined and the effect of propagation time delay on loop operation was evaluated. The new theory showed quite clearly that in order for a loop to lock, there was a severe trade–off between receiver bandwidth and time delay. The limitation on loop stability was calculated to be given by:

$$\omega_n T_d \leq 0.736$$

where ω_n is the natural frequency of the OPLL and T_d is loop propagation time.

In practice $\omega_n T_d$ should not go much above 0.3. The effect of propagation delay also meant that what were previously thought to be optimal receiver bandwidths were far from optimal and possibly unstable.

This new theory indicated that the experimental programme should concentrate on building OPLLs with line–narrowed semiconductor laser modules, as the time delay in the bulk system being used in this project, around 5 to 10ns, meant that the bandwidth of the OPLL should be around 10 to 30Mrads/s.

In chapter 3 it is shown that an OPLL with a bandwidth of this order will only lock if the linewidth of the beat signal is of the order of a few hundred kilohertz or less. This is because of the excess phase noise inherent in semiconductor lasers. This phase–noise is why it was only practical to phase lock two line–narrowed laser modules using the bulk system described in chapter six.

The origins and manifestations of laser phase–noise were described in chapter 4 alongside a fairly detailed examination of the operating characteristics of the Hitachi HLP1400 laser diode. This chapter pointed out that although semiconductor lasers have many points in their favour regarding their suitability as a source for future coherent systems they have their drawbacks too. The key positive points are that they are cheap, reliable, small, have low power consumptions, are manufactured using fairly mature technologies, that they are tunable and, perhaps most important of all, they have the potential to form part of a wholly integrated receiver. On the negative side they are extremely sensitive to changes in temperature and or current, they are sensitive to reflections of light and as they stand at this point in time they are too noisy, typical linewidths in excess of 5MHz.

The theory behind reducing the phase noise of semiconductor lasers and some experimental attempts at doing so were presented in chapter 5. The chapter investigated two possible approaches to reducing the linewidth of a semiconductor laser. Either the finished article can be used to form the active part of a larger laser module or alternatives to the Fabry Perot structure can be manufactured. In this project only the former was attempted, although some theory and results regarding alternative laser structures such as Distributed Fedback, Distributed Bragg, Cleaved Coupled Cavity and Integrated Passive Cavity laser devices have been presented.

The two techniques used to improve the spectral properties of the semiconductor laser involved reflecting some of the laser output back into the active layer. The first approach was to build a compound cavity where weak feedback dramatically altered the linewidth of the laser. Unfortunately this technique is far from ideal as the module is extremely sensitive to changes in current, temperature and movement of the reflector. The module is difficult to tune and it mode–hops regularly. The second and much better technique is to reduce the reflectivity of one of the semiconductor laser facets and then to use strong optical feedback to form a bigger laser with a small active section. This technique has shown itself to be very successful in reducing the linewidth, in extending its tuning range to greater than 10nm and in improving the overall stability of the device. The main

problem with this type of module however is in controlling the mechanical stability of the external reflector. Movements of as little as a few nanometers can cause frequency shifts of several MHz. These vibrations are at frequencies in the 0 to 100 Hz range. I bilieve that it was these low frequency vibrations of the laser cavities which stopped the successful construction of an optical phase–locked loop.

In reviewing alternative laser structures it was recommended that the way forward would be to manufacture and investigate some form of hybrid DFB/passive cavity type device. It was also mentioned that quantum well structures offer much hope for the future. Unfortunately, no single device would appear to meet all the desired criteria for an ideal optical source, namely that it should be tunable, monomode, have narrow linewidth and not be succeptible to mode hopping. It should also have a low electrical power consumption, be reliable and be insensitive to external reflections.

In chapter six, a range of experiments which had been carried out during the course of the project were reported upon. Many attempts were made at phase–locking two laser modules. The problems always came down to inadequate control of laser noise, whether this was phase–noise when using free running lasers or low frequency fluctuations of the signal from an external cavity laser, lock was never confirmed. Attempts were made to stabilise the external reflector using piezoelectric transducers and by locking the laser onto a Fabry Perot interferometer. Although these attempts were partially successful, the design of the external cavity was found wanting. Chapter five gives some recommendations regarding the design of such devices. An alternative design would not guarantee success, as the first successful loops used one semiconductor laser and one HeNe laser.

RECOMMENDATIONS FOR FUTURE WORK

There are four main areas of activity which should be pursued over the next five years. Indeed research is on going in all of them.

The first area is perhaps the simplest and most obvious. Work should continue on weakly coherent systems. It is not crucial to the future of

optical communications that phase locked loops be built using semiconductor lasers. Many researchers have demonstrated wavelength multiplexed systems using frequency shift keying. More work is required to take these systems from the laboratory through field trials into everyday use. This area allows users to exploit the bandwidth of optical fibre by spacing many signals several gigahertz apart. Indeed if multi level FSK is used similar power performance can be achieved when compared to binary PSK.

Following on from the work presented in chapters four, five and six it is crucial that research should continue on improving the operating characteristics of semiconductor laser diodes. Multiple quantum well devices using multi–contact DFB and DBR structures are continually improving the performance of these devices. One area of particular importance is that of de sensitising the laser diodes to the effects of unwanted and uncontrolled reflections. This may be addressed in the future by using some form of integrated isolator. Research should also continue on building small packaged external cavity devices as they currently outperform all free running devices with regard to tunability and linewidth.

It is also crucially important to the future use of coherent optical communications that research continue on developing active polarisation control systems or very good polarisation maintaining fibre. Although this area has not been mentioned in great detail in this thesis, largely because the experimental work used bulk optics and polarisation control was not a serious problem, it is essential that control is achieved. The reason this is so important is that all power benefits of using a local oscillator at the receiver end could be lost if good mixing is not achieved.

In the longer term the author firmly believes that the future for coherent systems technology lies in the area of wholly integrated or hybrid receivers. These are receivers which will include photodiodes, amplifiers, filters and local oscillators all on or around one chip. This will remove the need for extremely narrow linewidth lasers by reducing the propagation delay and therefore will allow for practical optical phase locked loop systems to be implemented.